UNIVERSITY OF CAPE TOWN

Department of Mechanical Engineering

Centre for Materials Engineering

Development of High Performance and Efficient Coating Repair Systems for Offshore Tropical Marine Environment

By

Francisco José Agostinho

AGSFRA001

August 2017

DEVELOPMENT OF HIGH PERFORMANCE AND EFFICIENT COATING REPAIR SYSTEMS FOR OFFSHORE TROPICAL MARINE ENVIRONMENT

A Dissertation Submitted in Partial Fulfilment of the Requirements for the Degree of Masters of Science in Engineering to the Faculty of Engineering and Built Environment of the University of Cape Town

By

Francisco José Agostinho

Centre for Materials Engineering

Department of Mechanical Engineering

University of Cape Town

2017

ABSTRACT

Rehabilitation coatings of offshore equipment rarely perform as well as the original coating, despite the high cost involved. The performance gap is probably due to high relative humidity, salt contamination and limitations on the use of abrasive blast cleaning. Thus, this research aims to deepen the understanding of surface preparation parameters that affect organic coating performance.

Carbon steel samples were subjected to a variety of surface alterations consisting of salt contamination, mechanical (wire brushing) and chemical (rust converter and remover) surface preparations followed by coating application and performance testing. The samples were first pre-corroded in a corrosion chamber to mimic degradation from service then surface preparations were performed after which a coating was applied. Coated new samples (RN) and fully corroded samples (SN) were the reference sets, while other samples were prepared to a variety of surface conditions.

Visual inspection and electrochemical impedance spectroscopy (EIS) were performed prior to exposure and periodically during accelerated cycling corrosion testing for a period of 30 days. The visual condition of the samples was used to rank the performance of the prepared samples. These results were used as benchmark to decide the optimum EIS method, either phase angle at high frequency or total impedance at low frequency, for early evaluation of the organic coating performance under the conditions studied. Furthermore, adhesion pull-off testing was performed to rank the effectiveness of the coating over various prepared coating.

The reference new samples (RN) proved to be the best surface condition and the corroded samples without preparation (SN) had the worst performance for all tests performed. In addition, it was established that salt contamination had a stronger impact on the coating performance than the amount of corrosion product remaining on the surface. Moreover, it was determined that the best preparation approach after pre-corrosion of the plates was to apply rust converter to the surface before coating. Adhesion measurement was of secondary concern on the studied coated surfaces as cohesive failure occurred on the pre-treatment layers rather than coating adhesion failure between the coating and the treated surface.

ACKNOWLEDGEMENTS

I wish to express my appreciation to all those who assisted me during the course of this research project, in particular:

Professor R.D. Knutsen, my supervisor, for his advice, guidance and support.

BP – Angola are greatly acknowledged for the provision of financial support.

Tim Evans, Angola Region Materials and Corrosion Technical Authority of BP, for presenting the real-life challenge where this research originated and his continuous support.

Simon Norton, for offering his expertise and vast experience in testing of organic coatings and corrosion to make me think deeper on the technical aspect of this work.

The workshop staff for the technical support and manufacturing of my engineering drawings. Especially Mr. Gavin Doolings is greatly acknowledged for helping me fetch seawater every week from the cold beaches of Cape Town.

Professor Pieter Levecque for his help with my early electrochemistry lab experiments and continuous support with instruments and software.

Penny Louw for ensuring all lab equipment was always handy.

Beverly Glass for the administrative support.

Gabriela Muai, my dear wife and mother of my children (Francisco, Vilmar and Aline), has my sincere thanks for encouraging me to follow my dreams and supporting me every step of the way.

DECLARATION

I, Francisco José Agostinho, know the meaning of plagiarism and declare that all the work in the document, save for that which is properly acknowledged, is my own. This thesis/dissertation has been submitted to the Turnitin module and I confirm that my supervisor has seen my report and any concerns revealed by such have been resolved with my supervisor.

Signature: Date: 02/08/2017

Signed by candidate

TABLE OF CONTENTS

ABSTRACT iii

ACKNOWLEDGEMENTS iv

DECLARATION v

LIST OF FIGURES ix

LIST OF TABLES xiii

LIST OF SYMBOLS, CODES AND ACRONYMS xiv

Samples Labelling Codes xiv

Acronyms xiv

Symbols xv

CHAPTER 1. INTRODUCTION 1

1.1. Context of Research 1

1.2. Scope and Limitations of Research 2

1.3. Aim of Research 3

CHAPTER 2. LITERATURE REVIEW: CORROSION AND ORGANIC COATINGS 4

2.1. Corrosion 4

2.2. Organic Coatings 4

2.3. Corrosion under Organic Coating 4

2.4. Adhesion of Organic Coatings 5

2.5. Coating Failures and Defects 6

CHAPTER 3. LITERATURE REVIEW: CORROSION TESTS FOR ORGANIC COATINGS 10

3.1. Accelerated Exposure Test 10

3.1.1. Effect of Temperature on Coating Deterioration 10

3.1.2. Continuous and Cycling Protocols in Accelerated tests 11

3.2. Electrochemical Impedance Spectroscopy (EIS) 11

3.2.1. Basics of EIS Technique 11

3.2.2. Impedance Data Representation 13

3.2.3. EIS Data Analysis 13

3.2.4. Phase Angle at High Frequency 14

3.2.5. Stages of Organic Coating Performance and Corresponding Phase Angle Responses at High Frequency 14

3.2.6. Total Impedance at Low Frequency 15

3.2.7. Advantages of Phase Angle at High Frequency and Total Impedance at Low Frequency over other Analysis Methods 15

CHAPTER 4. EXPERIMENTAL PROCEDURES AND MATERIALS 17

4.1. Materials 17

4.1.1. Metal Substrate 17

4.1.2. Organic Coating 18

4.1.3. Rust Converter 18

4.1.4. Rust Remover 18

4.2. Surface Conditions Studied 18

4.2.1. Reference New Samples (RN) 19

4.2.2. Samples with Salt Contamination and no Rust-Cleaning Attempt (SN) 19

4.2.3. Samples with no Salt Contamination and no Rust-Cleaning Attempt (NN) 20

4.2.4. Samples with no Salt Contamination and Chemical (Rust Converter) Surface Preparation (NC1) 20

4.2.5. Samples with no Salt Contamination and Mechanical Surface Preparation (NM) ... *21*
4.2.6. Samples with no Salt Contamination and both Mechanical and Chemical (Rust Converter) Surface Preparation (NB1) ... *22*
4.2.7. Samples with Salt Contamination and Chemical (Rust Converter) Surface Preparation (SC1) ... *22*
4.2.8. Samples with Salt Contamination and Mechanical Surface Preparation (SM)… ... *23*
4.2.9. Samples with Salt Contamination and both Mechanical and Chemical (Rust Converter) Surface Preparation (SB1) ... *23*
4.2.10. Samples with Salt Contamination and both Mechanical and Chemical (Rust Remover) Surface Preparation (SB2) ... *24*
4.3. Sample Preparation ... 25
4.3.1. Pre-Corrosion Procedure ... *25*
4.3.2. Salt Cleaning Procedure ... *25*
4.3.3. Mechanical Preparation Procedure (Wire Brushing) ... *25*
4.3.4. Chemical Surface Preparation ... *26*
4.4. Visual Inspection Criteria ... 27
4.4.1. Transition Time to Corrosion Based on Visual Inspection ... *27*
4.4.2. Criteria for Determining Transition Time to Corrosion from Visual Inspection… ... *27*
4.5. Pull-Off Adhesion Testing ... 29
4.5.1. Apparatus ... *29*
4.5.2. Specimen Preparation for Pull-Off ... *30*
4.5.3. Pull-Off Test Procedure ... *31*
4.6. Accelerated Exposure Testing ... 31
4.6.1. Apparatus ... *31*
4.6.2. Exposure Test Procedure ... *32*
4.7. Salt contamination test ... 33
4.7.1. Apparatus ... *33*
4.7.2. Salt Measurement Procedure ... *33*
4.8. Electrochemical Impedance Spectroscopy (EIS) Testing ... 34
4.8.1. Apparatus ... *34*
4.8.2. Specimen Preparation for EIS measurement ... *35*
4.8.3. Electrolyte used ... *35*
4.8.4. EIS measurement Procedure ... *35*

CHAPTER 5. RESULTS ... 36
5.1. Consistency in the Visual Inspection Results ... 36
5.3. Coating Performance Based on Visual Inspection ... 52
5.3.1. Visual Condition of the Samples at Transition Time ... *52*
5.3.2. Types of Failure Observed on the Samples ... *56*
5.3.3. Estimated Percentage Failure on Transition Period ... *58*
5.3.4. Determining Transition Time to Corrosion ... *60*
5.4. Dry Film Thickness Results ... 61
5.4.1. Dry Film Thickness of Visually Inspected Samples ... *63*
5.4.2. Dry Film Thickness of EIS Tested samples ... *65*
5.4.3. Dry Film Thickness of Adhesion Pull-Off Tested samples ... *65*
5.5. Salt Contamination Results ... 67
5.6. Pull-Off Test Results ... 68
5.6.1. Samples with Adhesive Failure ... *69*
5.6.2. Samples with Cohesive Failure ... 70
5.6.3. Samples with Mixed Failure Modes ... *74*
5.6.4. Pull-Off Strength to Failure ... *78*

5.6.5. Adhesion Strength and Coating Performance 78
5.7. Electrochemical Impedance Spectroscopy (EIS) Results 79
5.7.1. Phase Angle at High Frequency and Coating Performance 80
5.7.2. Total Impedance at Low Frequency and Coating Performance 83

CHAPTER 6. DISCUSSION 86
6.1. Coating Performance Based on Visual Inspection 86
6.1.1. Types of Failure Observed on the Samples 86
6.1.2. Estimated Percentage Failure 88
6.2. Effect of Dry Film Thickness on Coating Performance 89
6.3. Salt Contamination 89
6.4. Using EIS for Early Evaluation of Organic Coating Performance on Different Surface Condition 90
6.4.1. Sudden drop in both phase angle and total impedance values 90
6.4.2. Some increase of both phase angle and total impedance values 91
6.4.3. Final drop of both phase angle and total impedance values 91
6.4.4. The EIS and the Visual Inspection Results 92

CHAPTER 7. CONCLUSION 93
7.1. Effects of Geometry on Coating performance 93
7.2. Effects of Contamination on Coating performance 93
7.3. Effects of Rust Cleaning Approach on Coating performance 93
7.4. Effects of Adhesion on Coating performance 94
7.5. Early Coating Evaluation with EIS 94

REFERENCES 95

APPENDIX 98
Pull-Off Test Rig Drawings 98

LIST OF FIGURES

Figure 1: Voltage excitation and current response in EIS (Gamry, 2015) 12
Figure 2: Magnitude and phase angle representation in Bode plot (left) and Nyquist plot representation (right) (David Loveday, Peterson and Rodgers, 2004) 13
Figure 3: Reference new (RN) sample prior to coating application 19
Figure 4: Sample with salt contamination and no rust-cleaning attempt (SN) prior to coating application 19
Figure 5: Sample with no salt contamination and no rust-cleaning attempt (NN) prior coating application 20
Figure 6: Sample with no salt contamination and chemical (rust converter) surface preparation (NC1) prior coating application.....21
Figure 7: Sample with no salt contamination and mechanical surface preparation (NM) prior to coating application.....21
Figure 8: Sample with no salt contamination and both mechanical and chemical (rust converter) surface preparation (NB1) prior to coating application 22
Figure 9: Sample with salt contamination and chemical (rust converter) surface preparation (SC1) prior to coating application 22
Figure 10: Sample with salt contamination and mechanical surface preparation (SM) prior to coating application.....23
Figure 11: Sample with salt contamination and both mechanical and chemical (rust converter) surface preparation (SB1) prior to coating application 24
Figure 12: Samples with salt contamination and both mechanical and chemical (rust remover) surface preparation (SB2) prior to coating application.....24
Figure 13: Exposure time intervals showing the times of inspection.....27
Figure 14: Graphical representation of transition time to corrosion 28
Figure 15: Setup of the pull-off test being performed on a sample 30
Figure 16: New samples on panel racks inside the corrosion chamber 32
Figure 17: PTC1 cell on a large sample 34
Figure 18: Variation in performance of SN samples at 34 hours of exposure (from the left SN-06, SN-12 and SN-14).....36
Figure 19: Variation in performance of SM samples at 68 hours of exposure (from the left SM-06, SM-09 and SM-12).....37
Figure 20: Variation in performance of NN samples at 136 hours of exposure (from the left NN-05, NN-09 and NN-10) 37
Figure 21: Variation in performance of NM samples at 136 hours of exposure (from the left NM-05, NM-09 and NM-11) 37
Figure 22: Variation in performance of SB2 samples at 136 hours of exposure (from the left SB2-05, SB2-06 and SB2-09).....38
Figure 23: Variation in performance of SC1 samples at 264 hours of exposure (from the left SC1-01, SC1-02, SC1-03 and SC1-04) 38
Figure 24: Variation in performance of SB1 samples at 264 hours of exposure (from the left SB1-01, SB1-02, SB1-03 and SB1-04).....39
Figure 25: Variation in performance of NB1 samples at 710 hours of exposure (from the left NB1-01, NB1-02, NB1-03 and NB1-04) 39
Figure 26: Variation in performance of NC1 samples at 710 hours of exposure (from the left NC1-01, NC1-02, NC1-03 and NC1-04) 40

Figure 27: Variation in performance of RN samples at 710 hours of exposure (from the left RN-01, RN-02, RN-03 and RN-04).....40
Figure 28: Reference new samples (RN), a small sample on the top left corner of the larger one at exposure periods of 21 days (left) and 30 days (right). 42
Figure 29: Samples with no salt contamination and chemical (rust converter) surface preparation (NC1), a small sample on the top left corner of the larger one at exposure periods of 21 days (left) and 30 days (right). 43
Figure 30: Samples with no salt contamination and both mechanical (wire brushing) and chemical (rust converter) surface preparations (NB1), a small sample on the top left corner of the larger one at exposure periods of 21 days (left) and 30 days (right). 44
Figure 31: Samples with salt contamination but with both mechanical (wire brushing) and chemical (rust converter) surface preparation (SB1), a small sample on the top left corner of the larger one at exposure periods of 14 days (left) and 21 days (right). 45
Figure 32: Samples with salt contamination but with chemical (rust converter) surface preparation (SC1), a small sample on the top left corner of the larger one at exposure periods of 14 days (left) and 21 days (right).....46
Figure 33: Samples with salt contamination but with both mechanical (wire brushing) and chemical (rust remover) surface preparation (SB2), a small sample on the top left corner of the larger one at exposure periods of 14 days (left) and 21 days (right). 47
Figure 34: Samples with no salt contamination and with mechanical surface preparation (NM), a small sample on the top left corner of the larger one at exposure periods of 14 days (left) and 21 days (right).....48
Figure 35: Samples with no salt contamination but no surface preparation (NN), a small sample on the top left corner of the larger one at exposure periods of 8 days (left) and 14 days (right).....49
Figure 36: Samples with salt contamination but with mechanical surface preparation (SM), a small sample on the top left corner of a larger one at exposure periods of 2 days (left) and 8 days (right). 50
Figure 37: Samples with salt contamination and no surface preparation (SN), a small sample on the top left corner of a larger one at exposure periods of 2 days (left) and 8 days (right). 51
Figure 38: A reference new sample (RN) at 506 and 710 hours of exposure (from left to right).....52
Figure 39: An NC1 sample at 506 and 710 hours of exposure (from left to right) 53
Figure 40: An NB1 sample at 341, 506 and 710 hours of exposure (from left to right).....53
Figure 41: An SB1 sample at 189, 341 and 710 hours of exposure (from left to right).....54
Figure 42: An SC1 sample at 189, 341 and 506 hours of exposure (from left to right).....54
Figure 43: Failure of an SB2 sample at 68 (left) and 136 (right) hours of CCT1 exposure.....55
Figure 44: Failure of a NM sample at 68 (left) and 136 (right) hours of CCT1 exposure.....55

Figure 45: Failure of an NN sample at 68 (left) and 136 (right) hours of CCT1 exposure....55
Figure 46: Failure of an SM sample at 34 (left), 68 (middle) and 136 (right) hours of CCT1 exposure....56
Figure 47: Failure of an SN sample at 17, 34 and 68 hours of CCT1 exposure (from left to right).....56
Figure 48: Transition time to corrosion for the different pre-treatment....61
Figure 49: Dry film thickness (DFT) of visually inspected samples, in decreasing order of coating performance....63
Figure 50: Dry film thickness (DFT) of two sets of NC1 samples....64
Figure 51: Performance of NC1 (top) and NC1* (bottom) samples at one month of exposure, with thick (68.3μm) and thin (54.7μm) dry film thicknesses respectively.....64
Figure 52: Dry film thickness of EIS tested samples, in decreasing order of coating performance....65
Figure 53: Dry film thickness of pull-off tested samples, in order of decreasing coating performance....66
Figure 54: Dry film thickness of pull-off tested samples, in decreasing order of pull strength....66
Figure 55: Change in salt contamination level with decreasing coating performance....68
Figure 56: Schematic of adhesive failure in two interfaces....69
Figure 57: All RN samples test sites showed adhesive failure as the main mode of failure, each row is a sample, and the dollies are on the left of the corresponding test sites.....69
Figure 58: Schematic of cohesive failure in the pre-treatment.....71
Figure 59: All NC1 samples test sites showed cohesive failure in the converted corrosion product underneath the coating, each row is a sample, and the dollies are on the left of the corresponding test sites.....71
Figure 60: All NB1 samples test sites showed cohesive failure in the converted corrosion product underneath the coating, each row is a sample, and the dollies are on the left of the corresponding test sites.....72
Figure 61: All SB1 samples test sites showed cohesive failure in the converted corrosion product underneath the coating, each row is a sample, and the dollies are on the left of the corresponding test sites.....72
Figure 62: All SC1 samples test sites showed cohesive failure in the converted corrosion product underneath the coating, each row is a sample, and the dollies are on the left of the corresponding test sites.....73
Figure 63: All NN samples test sites showed cohesive failure in the corrosion product underneath the coating, each row is a sample, and the dollies are on the left of the corresponding test sites.....73
Figure 64: All SN samples test sites showed cohesive failure in the corrosion product underneath the coating, each row is a sample, and the dollies are on the left of the corresponding test sites.....74
Figure 65: Schematic of cohesive failure in the pre-treatment with some rust/coating adhesive failure.....74
Figure 66: All SB2 samples test sites showing a mixture of both cohesive and adhesive failures, each row is a sample, and the dollies are at the left of the corresponding test sites.....75

Figure 67: All NM samples test sites showing a mixture of both cohesive and adhesive failures, each row is a sample, and the dollies are at the left of the corresponding test sites. 75
Figure 68: All SM samples test sites showing a mixture of both cohesive and adhesive failures, each row is a sample, and the dollies are at the left of the corresponding test sites. 76
Figure 69: Pull-off strength of samples arranged in decreasing coating performance 79
Figure 70: Phase angle at high frequency (10kHz) with surface condition arranged in decreasing coating performance 81
Figure 71: Change of phase angle at high frequency (10kHz) with time of exposure 82
Figure 72: Total impedance at low frequency (1 Hz) with surface condition arranged in decreasing coating performance 84
Figure 73: Change of total impedance at low frequency (1 Hz) with time of exposure 85
Figure 74: Cross section of a coated sample showing how the paint can be thinner on the edges (top right corner) 86
Figure 75: Base Holder drawing 98
Figure 76: Base drawing 99
Figure 77: Actuator drawing 99
Figure 78: Detaching Unit drawing 100
Figure 79: Dolly drawing 101
Figure 80: Pull-Off Tester assembly drawing 102
Figure 81: Pull-Off Tester exploded view 102

LIST OF TABLES

Table 1: Coating failures and probable causes..... 7
Table 2: Combination of contamination control and rust removal approaches for the surface conditions.....18
Table 3: Transition time to corrosion and the parameters used for the calculations.....60
Table 4: Average dry film thickness and respective standard deviation (SD) for each pre-treatment studied.....62
Table 5: Measured conductivity prior to coating application and equivalent NaCl content.....67
Table 6: Table of adhesion failures layers and percentages.....70
Table 7: Cohesive and adhesive failures layers and percentages for the samples with mixed failure mode.....76
Table 8: Table of measured pull strengths to failure with respective averages and standard deviations for each sample condition.....78
Table 9: The phase angle at 10 kHz for each surface condition studied at various exposure periods.....80
Table 10: The Total impedance at 1 Hz for each condition studied at various exposure periods.....83

LIST OF SYMBOLS, CODES AND ACRONYMS

Samples Labelling Codes

In each labelling code, the first letter represents the contamination remaining and the second letter the rust removal method used on the sample plates, where: N=none, S=salt, M=mechanical, C1=chemical rust converter, B1=both M and C1, B2=both M and rust remover.

NB1 – Samples without salt contamination, and both mechanical (wire-brushing) and chemical (rust converter) surface preparation.

NC1 – Samples without salt contamination, and chemical (rust converter) surface preparation.

NM – Samples without salt contamination, and mechanical (wire-brushing) surface preparation.

NN – Samples without salt contamination, and no surface preparation attempt.

SB1 – Samples with salt contamination, and both mechanical and chemical (rust converter) surface preparation.

SB2 – Samples with salt contamination, and both mechanical and chemical (rust remover) surface preparation.

SC1 – Samples with salt contamination, and chemical (rust converter) surface preparation.

SM – Samples with salt contamination, and mechanical (wire-brushing) surface preparation.

SN – Samples with salt contamination, and no surface preparation attempt.

RN – Reference new sample. Brand new sample coated after degreasing.

Acronyms

AC – Alternate Current

ASTM – formerly American Society for Testing and Materials

CCT – Cyclic Corrosion Testing

CME – Centre for Materials Engineering

DC – Direct Current

DFT – Dry Film Thickness

EEC – Equivalent Electrical Circuit

EIS – Electrochemical Impedance Spectroscopy

IMO – International Maritime Organization

ISO – International Organization for Standardization

OCP – Open Circuit Potential

PSPC – Performance Standard for Protective Coating

PTC – Paint Test Cell

SAE – Society of Automotive Engineers

SCE – Standard Calomel Electrode

SD – Standard Deviation

UV – Ultraviolet

Symbols

$U_{(t)}$ – Voltage as a function of time

$I_{(t)}$ – Current as a function of time

U_m – Magnitude of amplitude of perturbation

I_m – Magnitude of amplitude of response

φ – Phase angle

$(\varphi_u - \varphi_i)$ – Phase shift

j – Unit imaginary number

ω – Frequency in rpm

f – Frequency in Hz

$Z_{(j\omega)}$ – Electrochemical impedance

T_g – Glass transition temperature

t - time

CHAPTER 1. INTRODUCTION

1.1. Context of Research

Carbon steel equipment is routinely protected against atmospheric corrosion using organic coating systems, which require maintenance at some point in their lifetime. Despite the high cost involved with maintenance coating, it appears to be inferior in performance when compared to the original coating. While the lifespan of organic coatings in tropical offshore environments can range from five to fifteen years, empirical evidence suggests that repair coatings can last from less than a year (poorly reapplied repair coatings) to just over four years (well reapplied coatings). To date, the gap in performance between original coatings and rehabilitated coatings points to the difficulty in achieving effective surface preparation offshore, which includes limitations of abrasive blast cleaning, temperature, relative humidity and salt contamination on offshore structures.

The coating systems applied to a metal substrate consist of surface pre-treatment, a primer coating, and one or more topcoats, but may also consist of just a single layer coat after surface preparation. The surface pre-treatment is usually done to ensure good adhesion between the substrate and the primer; the requirements of a good primer include good adhesion to the substrate, preventing corrosion on the substrate and providing good paint adhesion; the topcoat needs to have good adhesion properties and high resistance to external factors.

The aging of the organic coatings and subsequent loss of protective ability is probably the biggest concern on their use in an offshore tropical marine environment. Routine maintenance is the solution to this issue, which includes total coating repair and spot repair maintenance. However, the desired results may not be achieved when the repair coating is done on site. Besides relative humidity and salt contamination in the offshore environments, surface preparation has a major effect on the performance of coating repair systems. Abrasive blast cleaning has proven to be one of the best surface preparations available, however its onsite application hindered as the spent abrasive blast grit has to be recovered, which is a difficult goal to achieve. This is one of the reasons why repair coating can be more expensive than the original coating, because the cost of safely containing and disposing of spent blasting media can more than

double or treble the cost of a paint job (ASM International, 1987). Thus, exploring other surface pre-treatment approaches, both mechanical and chemical, is of great importance to the offshore industry.

Unlike the abrasive blasting approach, which can bring the substrate close to its as-new condition, most mechanical preparation methods as well as chemical preparation can only reduce the amount of corrosion product on the substrate prior to repair coating. However, some degree of weathering can help improve paint adhesion, due to other factors affecting adhesion properties such as surface profile and surface chemistry, though this improved adhesion would decrease should the weathering be excessive (Cabanelas, et al., 2007). This opens the possibility of achieving improved repair coating adhesion and subsequently improved coating performance by using surface pre-treatments, which are as simple as wire-brushing or rust remover products of relatively low efficiency.

1.2. Scope and Limitations of Research

Although there is a wide range of possible metal substrate pre-treatments available, this research only covers wire brushing as the mechanical rust cleaning approach, while commercial rust converter and rust remover were chosen as the chemical approach. Likewise, only salt contamination from the seawater exposure and carbon steel corrosion product were considered as the two types of contaminants on surfaces that would have to be addressed by pre-treatment before coating. Furthermore, a wet/dry cyclic corrosion test was chosen as the accelerated exposure test, with the result that the effects of UV radiation on the coating were not studied. In addition, only carbon steel was chosen for coating in this investigation. Finally, during coating maintenance the surface preparation as well as the recoating had to deal with the residue of original damaged/weathered coating on the substrate. Nevertheless, in this investigation the samples were treated as if the coating had completely corroded away and only corrosion product needed to be cleaned from the substrate, overlooking the possible chemical influence of the previous coating on the surface.

Carbon steel was the chosen material for the simple fact that organic coatings are often the choice for corrosion protection of carbon steel offshore equipment. Since the aim is onsite application, use of simple pre-treatment methods avoids creating a false sense of perfection that could be difficult to reproduce on the field, hence the choice of wire-brushing as the mechanical approach, rust converter and rust remover products as the chemical approach. Wet/dry cyclic corrosion tests are known to be quite aggressive and produce results quicker, which is of interest here to best mimic

the corrosive tropical marine environment offshore and due to the time constrain on the investigation.

1.3. Aim of Research

Despite the efforts of coating manufacturers to address the coating maintenance issues mentioned above by developing surface tolerant coating systems, the need for further research still exists to fully understand the factors that affect coating performance, as well as develop effective and efficient surface preparation techniques to work in tandem with these high-performance coating systems.

The parameters affecting coating performance are related to the coating and the substrate, which for the coating includes its dielectric properties, water and oxygen uptake, ion penetration, pigments and inhibitors, ability to resist ageing, environmental exposure and mechanically weakened spots and pinholes. For the substrate, coating performance is affected by surface characteristics, surface chemistry, surface pre-treatment, and electrochemical corrosion reactions at the metal-coating interface. This research focuses on deepening the understanding of the effects of the conditions to which a substrate is exposed prior to surface preparation and the rust treatment prior to repair coating, on the performance of an applied organic coating.

While the impact of surface salt contamination and rust removal/conversion activity directly affects the substrate, this investigation reveals to what extent they affect the organic coating by evaluating and comparing the performance of the coating for different surface preparations. Both the contaminants, i.e. salt and corrosion product as well as the rust treatment, i.e. wire-brushing, rust conversion and rust removal were applied alone or in combination to determine the most effective and efficient surface preparation technique prior to coating.

Since this study aimed to address issues in a tropical marine environment, it has been carried out under corrosive conditions using a specialized chamber with cycling of salt fog from natural seawater, humidity variation and temperature variation so as to mimic a marine environment and while accelerating the test for rapid results production. The use of carbon steel samples represents one of the most widely used offshore materials, whose corrosion protection is done with organic coating. Finally, with a view to further accelerate the testing protocol, electrochemical impedance spectroscopy (EIS) was explored for early evaluation of organic coating performance under the studied conditions.

CHAPTER 2. LITERATURE REVIEW: CORROSION AND ORGANIC COATINGS

2.1. Corrosion

Corrosion is the destructive attack of a metal by an electrochemical process through the operation of coupled half-cell reactions with its environment (Callister, 2003; Revie and Uhlig, 2008; McCafferty, 2010). Although corrosion may be assisted by physical causes such as the ones leading to stress crack corrosion and the effects of tribological wear on corrosion, the physical degradation processes alone are not called corrosion, but referred to with their appropriate names such as wear, erosion, galling, among others. Corrosion is an electrochemical process.

2.2. Organic Coatings

Organic coatings are barrier coatings with complex ingredients often of resins, pigments, additives and are used primarily for corrosion protection of steels. However, they often offer chemical and electrical resistance in addition to corrosion protection. Organic coatings have wide usage in daily life to protect metals from corroding and applications include automobiles, trucks, trains, planes, pipelines, bridges, ships, storage tanks and pressure vessels.

A protective coating system can be comprised of one or more protective layers, with the typical system containing primer, intermediate coat and topcoat. However, the layer largely responsible for corrosion protection is the primer (Rammelt and Reinhard, 1992). Nonetheless, the use of liquid coatings is only recommended on metals with corrosion rates lower than 1.3 mm/year and sites without threat of catastrophic failure (ASM International, 1987). Surface preparation of the metal substrate and the application of the coating under the correct condition prevent early coating deterioration and corrosion underneath the coating.

2.3. Corrosion under Organic Coating

An organic coating or paint film offers corrosion protection to metal substrates in two ways; by acting as a physical barrier between the metal substrate and the corrosive environment, and by working as a reservoir of corrosion inhibitors (González, Fox and Souto, 2004; McCafferty, 2009).

The barrier provided by organic coating is not perfect. Thus, water, oxygen and ions, such as the chloride ion, can penetrate the coating, resulting in corrosion underneath the organic coating at the coating/metal interface (McCafferty, 2009).

Although an organic coating can also fail by non-electrochemical means such as mechanical abrasion or impact, cracking or crazing due to mechanical deformation and oxidation by ultraviolet (UV) radiation (McCafferty, 2009), the electrochemical processes that occur in the narrow region beneath the organic coating, leading to corrosion and de-adhesion, can have a deleterious impact on the performance of an organic coating.

2.4. Adhesion of Organic Coatings

The adhesion properties of an organic coating are related to its anti-corrosion capability. Corrosion underneath an organic coating is often accompanied by loss of adhesion. Furthermore a lack of good adhesion between the organic coating and the metal substrate leads to localized pockets of electrolyte which promote corrosion (McCafferty, 2009).

Adhesion phenomena are not limited to coatings. They are relevant to many technological and scientific areas. Besides coatings, paints and varnishes, adhesion applications include adhesive joints, multi-layered sandwiches, polymer blends, filled polymers and composite materials. Various theories have been formulated for the mechanisms of adhesion, namely (Mittal and Pizzi, 1999):

- Mechanical Interlocking,
- Electronic Theory, also known as electrical double layer, electrostatic, or plate capacitor theory,
- Theory of Weak Boundary Layers – Concept of Interphase,
- Adsorption or Thermodynamic Theory, also referred to as wettability or acid-base theory,
- Diffusion Theory and
- Chemical Bonding Theory.

For organic coating applications, metal/polymer adhesion is of interest and the fundamental theories governing it are (McCafferty, 2009):

1) The Adsorption Theory: Here, the adsorption forces between the two entities being joined defines the adhesive bond.

2) The Chemical Reaction Theory: Here, the adhesion is due to a chemical reaction between the polymer and the metal.

3) The Mechanical Interlocking Theory: Here, the bond is formed through mechanical interlocking or keying of the polymer into cavities and pores on the surface of the metal.

4) The Electrostatic Theory: Here, the adhesive bond relies on the existence of an electrostatic charge between the two adhering surfaces.

To improve organic coating performance, the parameters affecting adhesion between an organic coating and a metal substrate must be understood. Hence, researchers have been working on identifying the causes of poor adhesion.

Cabanelas et al. (2007) showed in their studies that a galvanized steel surface offers better paint adhesion after a certain degree of weathering (long-term atmospheric exposure) than a smooth surface, although this good adhesion would decrease should the weathering become excessive. Collazo et al. (2003) shared this view when studying the performance of different paints on galvanized steel surfaces. However, coating adhesion on galvanized steel substrates is dependent not only on the degree of weathering (defined by mechanical keying) since other factors such as surface contamination as well as the surface chemistry of the galvanized layer resulting from fabrication and service also affect the adhesion properties of the coating. In a review on developments of surface treatment technologies for hot-dip galvanized steel relevant to adhesion of organic coatings, Maeda (1996) referred to the above factors as they affect adhesion, and apparently they are closely related to the chemical reactivity of galvanized steel surfaces.

These conclusions from Maeda's review cannot be directly applied to the present research since the samples used in this project are not galvanized steel but bare carbon steel, which offers a different surface chemistry to a coating. However, the impact of the weathering degree is expected to play a role in this project since the likely adhesion mechanism will be the mechanical interlocking theory where surface roughness predominates over the chemical reactivity.

2.5. Coating Failures and Defects

There is a number of factors that lead to coating failure and defects, and the coating can fail differently depending on these factors. Table 1 below summarises the types of coating failures and defects of interest in the current work and their respective probable causes (Fitzsimons and Parry, 2016).

Table 1: Coating failures and probable causes

Failure	Description	Probable causes
 **Alligatoring (Crocodiling)**	"Very large (macro) crazing/cracking that resembles the skin of an alligator or crocodile. Cracks may penetrate through to the undercoat or down to the substrate. "	"Internal stresses in the coating where the surface shrinks faster than the body of the paint film. Excessive film thickness and limited paint flexibility. Application of a hard topcoat over a more flexible softer undercoat. Application of topcoat before the undercoat has dried."
 **Blistering**	"Dome-shaped projections or blisters in the dry paint film through local loss of adhesion and lifting of the film from the underlying surface. Blisters may contain liquid, vapor, gas, or crystals."	"Many mechanisms can be involved, including osmotic gradients associated with soluble salts, soluble pigments, corrosion products, retained solvents, and solvents from cargoes. Non-osmotic blistering is associated with cathodic disbonding, thermal gradients related to cold-wall effects, and compressive stress."
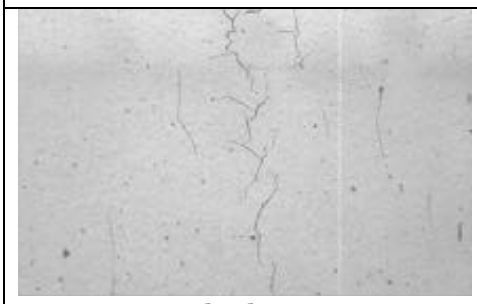 **Checking**	"Fine cracks that do not penetrate the topcoat of a paint system. Some checking can be so minute that it is impossible to see without magnification."	"Typically, a formulation and/or a specification problem. As with cracking, stresses are developed that cause the surface of the paint film to become brittle and crack. Limited paint flexibility."
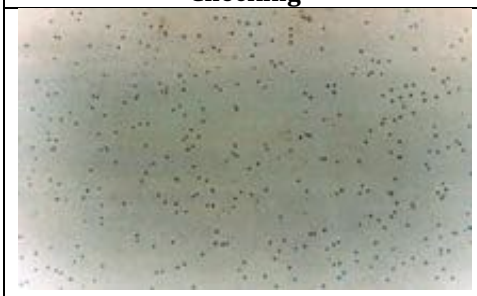 **Cissing**	"Surface breaks in a wet paint film, where the paint has receded to expose the underlying substrate. The paint is unable to wet–out the substrate. Can be very large."	"Surface contamination by either moisture or foreign matter such as oil, grease, or silicone. Also known to happen when incorrect solvent blends have been used."

Failure	Description	Probable causes
 **Cracking**	"The splitting of a dry paint film through at least one coat to form visible cracks, which may penetrate down to the substrate. Cracking comes in several forms, from minute cracking to severe cracking."	"Cracking is generally a stress-related failure and can be attributed to surface movement, aging, absorption and desorption of moisture, and general lack of flexibility of the coating. The thicker the paint film, the greater the possibility it will crack."
 **Crazing**	"Similar to checking but the cracks are generally wider and penetrate deeper into the film."	"Application temperature too low, incompatibility with previous coating, aging, or high film thickness."
 **Rust Rashing**	"Fine spots of rust that appear on a paint film, often a thin primer coat. The initial spots rapidly spread over the surface, resulting in a film of rust through which the individual spots are difficult to discern. Also from holidays."	"Low film thickness, often in combination with a high surface profile."
 **Rust Spotting**	"Individual spots of rust that appear on a paint film and frequently start as localized spotting but rapidly increase in density."	"Low film thickness (more likely creating rust rashing), voids and holidays (more likely creating rust rashing), but also defects in the steel, such as laminations and inclusions. Too high a surface profile may cause penetration of peaks through a paint film and cause rust spotting. May also occur from metallic contamination of a coated surface by grinding dust and so on."

Failure	Description	Probable causes
 **Rust Staining**	"A light staining on the surface of the paint caused by the precipitation of ferrous oxide from adjacent exposed steel."	"Water runoff from a rusty surface above a soundly coated surface. Rust staining occurs when the rust is wetted-out and contaminated water runs over and discolors other items or locations. Usually more of an eyesore than a defect. The coating itself may not be defective, only stained."
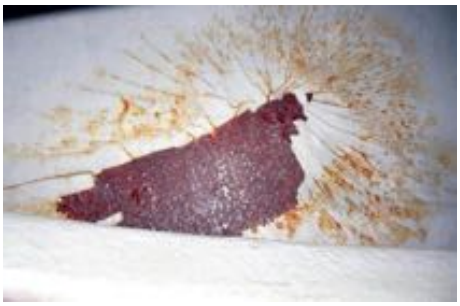 **Stress Cracking**	"Paint coatings with visible cracks, which may penetrate down to the substrate."	"Stress cracking can be attributed to surface movement, aging, absorption and desorption of moisture, thermal cycling, and general lack of flexibility of the coating. The thicker the paint film, the greater the possibility that cracking may occur. Often occurs around welds and changes in section."
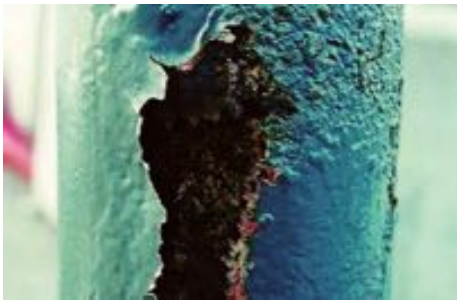 **Undercutting**	"Visual corrosion beneath a paint film, often called creep. Corrosion travels beneath the paint film and lifts the paint from the substrate. Severe cases can show as blistering, flaking, cracks, and exposed rust."	"Application of paint to corroded substrate. Rust creep from areas of mechanical damage and missing primer coat. Can be found in areas of poor design or access, where inadequate preparation and coating thickness was applied. Could also be due to lack of maintenance."

The contents on this table are direct quotes from *Coating Failure and Defects – A Comprehensive Field Guide*, by Corrosionpedia.com in partnership with Fitz's Atlas 2 and ASM Handbook Volume 5B.

CHAPTER 3. LITERATURE REVIEW: CORROSION TESTS FOR ORGANIC COATINGS

There is a wide range of test methods available to investigate the physical and chemical behaviour of organic coatings and these include both electrochemical methods and accelerated exposure tests.

The accelerated tests are useful for time constrained test works since they are relatively quick procedures of making data available for analysis. A brief description of the tests to be used in this research project are given below.

3.1. Accelerated Exposure Test

Accelerated exposure testing is useful for testing the performance of an organic coating since a coated substrate may take many years under normal exposure before corrosion breakthrough occurs. However, if a decision is made to employ an accelerated exposure test then a well-designed test protocol must be in place. This protocol needs to create a stress environment that will lead the system under test to fail with the same mechanism observed in the field, and must then provide a means to measure how and when the test caused the system to fail (Bierwagen *et al.*, 2003).

3.1.1. Effect of Temperature on Coating Deterioration

Temperature is a common parameter employed to accelerate organic coating degradation. Recall that, with time, both electrolyte and oxygen find their way through the organic coating into the substrate and promote corrosion. The rate of diffusion of electrolyte, the transport of oxygen through the coating as well as molecular mobility increase with temperature, thus degrading the barrier property of the coating and increasing the rate of corrosion (Bierwagen *et al.*, 2003; Loveday, Peterson and Rodgers, 2005). There is a limit to how far temperature can be increased to accelerate coating deterioration without altering the failure mechanism. Temperatures above the glass transition temperature (T_g) of an organic coating significantly decrease its barrier and electrical resistance properties rendering the accelerated test unreliable (Bierwagen *et al.*, 2003). Therefore, other ways to accelerate the corrosion process such as fog of variable humidity and salt content, thermal cycling and wet-dry cycling are often used.

3.1.2. Continuous and Cycling Protocols in Accelerated tests

The ASTM B117 salt fog test is widely used as an accelerated exposure test in place of immersion testing, which is time consuming. However, this stress environment does not adequately mimic any actual environment and in some cases, the temperature may exceed the T_g of the organic coating under study, which can lead to a change in the failure mechanism. Furthermore Bierwagen et al. (2003) described this test protocol as very weak and almost unusable because, after the exposure, the panels are only qualitatively examined. Atmospheric environments often display varying humidity, salt fog, temperatures, UV exposure from the sun and in some cases, chemical pollution. Thus, the use of cyclic protocols brings the test conditions close to those experienced under actual field exposure.

Cyclic protocols for accelerated exposure tests not only provide a more realistic failure mechanism but also give quicker results than a similar environment with continuous exposure and no variation. For instance Skerry, Alavi and Lindgren (1988) compared the corrosion products obtained from different accelerated test protocols and found the corrosion product of 48 hours of wet/dry cycling similar to that derived from four weeks of outdoor exposure. Nevertheless, the site of the outdoor test may affect the corrosion produced compared to that created by a specific test protocol e.g. a specific wet/dry protocol may create corrosion product that resembles that created by a tropical marine environment. An important aspect of these tests is that they provide no information on the degradation mechanism of the protective coating, but only a qualitative estimation of the protective properties (Rammelt and Reinhard, 1992). Hence, the advantage of using electrochemical methods such as electrochemical impedance spectroscopy to rapidly evaluate coating deterioration.

3.2. Electrochemical Impedance Spectroscopy (EIS)

Electrochemical Impedance Spectroscopy (EIS) is an experimental electrochemical measurement technique that has gained widespread application in the study of organic coating performance.

3.2.1. Basics of EIS Technique

In EIS, a continuous perturbation, i.e. a small amplitude AC signal, is applied to a steady state system and the relaxation of the electrochemical system to a new steady state, i.e. the system response, is subsequently studied. The system response of interest for EIS is that from the application of a sinusoidal

signal (Lasia, 1999). Figure 1 below shows a voltage excitation and the corresponding current response of the system in EIS.

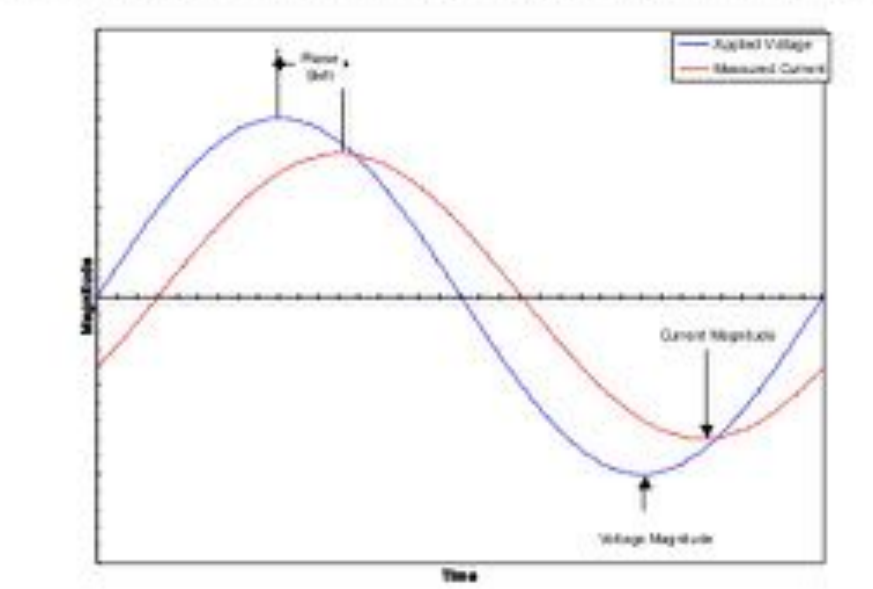

Figure 1: Voltage excitation and current response in EIS (Gamry, 2015)

As seen on Figure 1 above, a small sinusoidal voltage will result in a sinusoidal current response, and can be represented by the expressions below.

$$U_{(t)} = U_m \sin(\omega t + \varphi_u)$$

$$I_{(t)} = I_m \sin(\omega t + \varphi_i)$$

where:

$U_{(t)}$ – voltage as a function of time

$I_{(t)}$ – Current as a function of time

U_m – magnitude of amplitude of perturbation

I_m – magnitude of amplitude of response

$(\varphi_u - \varphi_i)$ – phase shift

Using Laplace transformation, the equations above can be simplified from functions of time into functions of frequency (s). Substituting s by $j\omega$ with $j=\sqrt{-1}$ (unit imaginary number) and $\omega=2\pi f$ (frequency), the ratio of the new functions of voltage and current defines the frequency-dependent electrochemical impedance $Z_{(j\omega)}$ (Rammelt and Reinhard, 1992; Lasia, 1999).

3.2.2. Impedance Data Representation

There are various ways to plot the impedance data. The most used are the Nyquist plot, where it is measured at different frequencies and plotted in a complex plane, and the Bode plot that presents the logarithm of the modulus of the impedance and the phase angle as a function of the logarithm of the frequency (Figure 2).

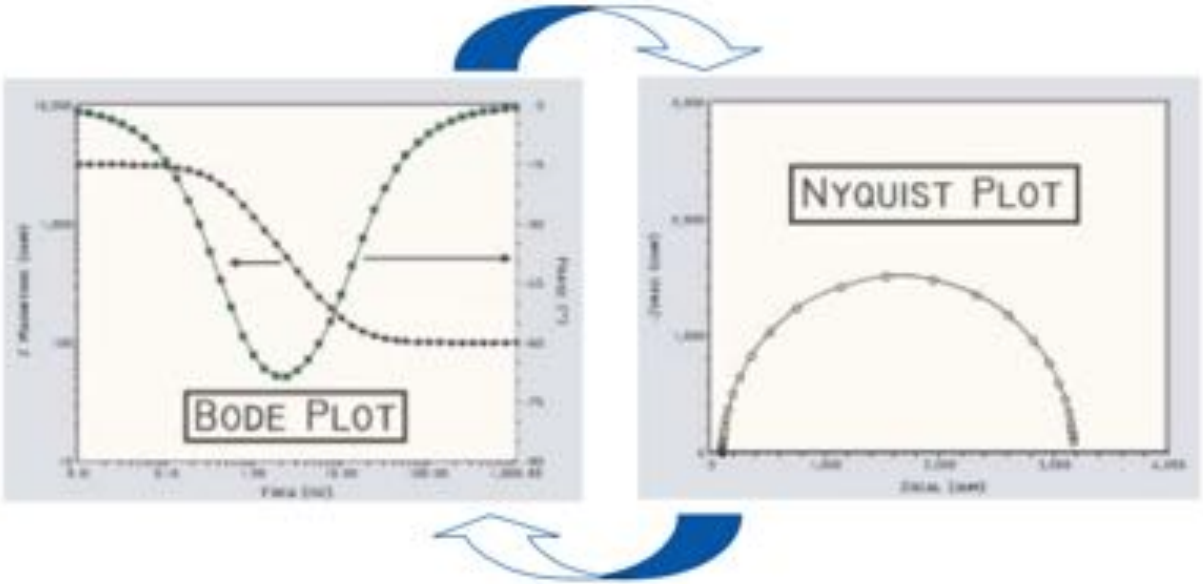

Figure 2: Magnitude and phase angle representation in Bode plot (left) and Nyquist plot representation (right) (David Loveday, Peterson and Rodgers, 2004)

To determine the coating properties and degradation mechanism, the impedance data is usually analysed through a wide range of frequencies. It is convenient to use an equivalent electrical circuit, which converts the main processes into circuit elements (capacitances, resistances, inductances and distributed circuit elements) to depict the metal/coating system, since the EIS primarily characterizes a system in terms of its electrical properties (Rammelt and Reinhard, 1992). However, various analysis methods to evaluate organic coatings from their EIS data have emerged over the years, and they usually do not include all the parameters available from the EIS measurement.

3.2.3. EIS Data Analysis

There is a wide range of methods used for the analysis of the collected data. The choice of analysis is highly influenced by the system under study and the aim of the investigation. For the study of organic coatings and their corrosion protective properties, the following methods are often used among others: 1) equivalent electrical circuit, 2) phase angle at high and medium as well as low frequencies, 3) total impedance at low frequency, 4) minimum of phase angle and its frequency, 5)

frequency breakpoint, 6) frequency at maximum phase angle, 7) open circuit potential analysis, 8) electrical and electrochemical resistances and 9) areas under Bode plots.

Equivalent electrical circuit (EEC) is the most common method of EIS data analysis for organic coating evaluation, providing measurements of coating resistance, coating capacitance, double layer capacitance and charge transfer resistance. However, only a detailed computer assisted analysis of the impedance data can provide more information on the possible degradation and corrosion mechanisms, and evaluation of the system parameters (Rammelt and Reinhard, 1992). By making use of an analogy of the organic coating system to an electrical circuit, an equivalent theoretical circuit is chosen that fits the experimental plot and its parameters are calculated. Despite past arguments questioning the reliability of the correlation between the circuit elements and the system parameters, as more than one circuit may be fit to a set of data points, EEC is widely accepted so that its use extends to validation of some of the more recent analysis methods.

3.2.4. Phase Angle at High Frequency

Previous studies of phase angle at high frequency show that these result agrees very closely with the parameters extracted from EIS models such as coating resistance and coating capacitance (Mahdavian and Attar, 2006). Furthermore, phase angle response can be used to evaluate organic coating performance regardless of the frequency range. However, the response may be faster or slower depending on whether it is measured in the high, medium or low frequency ranges. Zou et al. (2008) argue that phase angle at low frequency range best represents the performance of the coating at the early stages of exposure but that phase angle at high frequency gives a better representation when the coating has been exposed for longer. Finally, the middle range frequency (10 Hz) best reflects the variation of the coating resistance and the resistance at both early and late stages of exposure.

Coating thickness can affect the response of phase angle. Despite the identical response at low frequencies of a sample with a varying thickness profile compared to a sample with uniform thickness, there is a considerable difference in their responses at high frequencies (Touzain, 2010). Unlike the thickness, the sample size does not affect the phase angle plot, regardless of the frequency applied (Touzain, 2010).

3.2.5. Stages of Organic Coating Performance and Corresponding Phase Angle Responses at High Frequency

During the deterioration of organic coatings and subsequent corrosion progression, the following phase angle response can be observed at different stages of exposure:

- *At the early stage, the phase angle value is closest to 90˚ since the coating system shows a more capacitive response*: newly applied coating (near perfect) has very large coating resistance (due to its insulating nature) and capacitance, leading to current flowing through the capacitor.
- *During the intermediate progression of the exposure, the phase angle value gradually decreases (away from 90˚ and towards 0˚). This is due to the system showing a mixed resistive-capacitive response*: with exposure, the coating gradually becomes permeable decreasing the coating resistance and increasing its capacitance (as the dielectric of water can be about 80 times higher than the coating's), promoting the splitting of current through both the resistor and the capacitor.
- *In the late stages of exposure, the phase angle value quickly drops (towards 0˚) since the coating system shows a more resistive response*: upon saturation of the coating with electrolyte, the capacitance stabilizes while the resistance may continue to drop, hence the current flows primarily through the resistor.

Some variations may occur in the middle stages of the above process, such as increases in the phase angle values explained by corrosion products blocking the pores and effects of inhibitor formulated with the coating. The above phase angle responses are corroborated by many researchers (Merten *et al.*, no date; D Loveday, Peterson and Rodgers, 2004; González, Fox and Souto, 2004; Mahdavian and Attar, 2006; Zuo *et al.*, 2008; Akbarinezhad, Ebrahimi and Faridi, 2009).

3.2.6. Total Impedance at Low Frequency

Impedance at low frequencies is quite popular for evaluation of organic coating performance. The analysis is usually based on the correlation between the barrier property of the coating and its insulating property. In short, the higher the total impedance of the coating remains for long period of exposure, the higher the coating performance.

Both charge transfer resistance and coating resistance are almost the only constituents of total impedance at low frequency since it is a near DC response of the system (Mahdavian and Attar, 2006).

3.2.7. Advantages of Phase Angle at High Frequency and Total Impedance at Low Frequency over other Analysis Methods

Phase angle at high frequency and total impedance at low frequency are very fast EIS methods to evaluate organic coating systems, which makes them ideal for experiments

involving a large number of samples. Their applicability to coating degradation studies are presented in the work of Mahdavian and Attar (2006) for phase angle at high frequency, and van Westing et al. (1993) for total impedance at low frequency. Since they are the methods of choice in this research, it is worthy pointing out the advantages they hold over other methods.

- No need for selection of an equivalent circuit: the system to be studied can be so complex that selecting an adequate equivalent electrical circuit may become problematic.
- No signal drift or data scatter at low frequencies (only for phase angle): the lower the frequency the longer the plot time, which causes signal drift and data scatter due to the changes the system undergoes with time. This is avoided using phase angle at high frequency since the plotting at higher frequencies is much quicker.
- No time-consuming task of extracting the parameter from the model: even upon selection of an adequate equivalent electrical circuit, extracting the values of the circuit elements corresponding to system parameters is still a lengthy procedure.
- No error in calculation: the values of both phase angle and total impedance are used as measured without any further calculation thus avoiding possible calculation errors.

CHAPTER 4. EXPERIMENTAL PROCEDURES AND MATERIALS

4.1. Materials

4.1.1. Metal Substrate

The metallic substrates used were Type QD panels, manufactured by Q-Lab. They have a smooth and bright finish, with the materials information as provided by the manufacturer given below:

- SAE Material Designation: 1008/1010
- ASTM Material Specifications: A1008
- ISO Material Specifications: 3574 Type CR1
- ASTM Panel Specifications: D609 -Type 3
- ISO Panel Specifications: 1514-Type 3
- Roughness Ra (micro-inches): <20
- Surface Finish: Smooth
- Temper: 1/4 hard
- Hardness (Rockwell): B50-B65
- Tensile Strength (kpsi): 45-65
- Tensile Strength (MPa): 310-448
- Q-Shaped Hole: Yes

The chemical composition of SAE 1008/1010 steel panels is:

0.60% max Manganese
0.15% max Carbon
0.030% max Phosphorus
0.035% max Sulfur.

The dimensions of the samples were 152mm x 305 mm x 0,51 mm (Q-LAB type QD-612) and 76mm x 152 mm x 0,51 mm (Q-LAB type QD-36). The majority of the tests used the QD-612 panel, while the QD-36 was only used for pull-off testing and to investigate the effect of sample size.

4.1.2. Organic Coating

Jotamastic Smart Pack, a two-pack solvent free chemically resistant coating, was used for this research work. This coating comprises two components, known as the base and curing agent, which are mixed immediately before application so that a chemical reaction occurs and the polymerization reaction continues after application to produce a densely cross-linked film with good solvent and chemical resistance.

The coating was applied with airless spray equipment to a dry film thickness (DFT) of 60 – 80 µm, measured with an Elcometer coating thickness gauge that works with electromagnetic induction principle, which is within the manufacturer's recommended DFT of 50 – 120 µm. After surface preparation to the desired surface condition, the coating was applied and allowed to cure for 10 days before testing commenced.

4.1.3. Rust Converter

The rust converter used was navy steel, a water borne, eco-friendly product that acted both as stabilizer of adherent rust and as primer of rusted steel.

4.1.4. Rust Remover

The rust remover used was SurTec® 414 neutral activator of neutral pH-value, which can remove rust and oxide films.

4.2. Surface Conditions Studied

The samples were prepared to different surface conditions before applying the Jotamastic coating. The surface conditions ranged from clean new samples free of contamination to corroded samples with contamination. Table 2 below shows the different surface conditions the samples were subjected to.

Table 2: Combination of contamination control and rust removal approaches for the surface conditions

Samples	**New**		**Weathered**							
Surface Conditions	RN	SN	SC1	SM	SB1	SB2	NN	NC1	NM	NB1
Exposure to salt-fog (natural seawater)		X	X	X	X	X	X	X	X	X
Contamination Remaining on the Surface										
*None	X						X	X	X	X
*Salt (from seawater)		X	X	X	X	X				
Rust Removal Approach										
*None	X	X					X			
*Chemical 1 (rust converter)			X					X		
*Mechanical (wire brushing)				X					X	
* Both Mechanical & Chemical 1					X					X
* Both Mechanical & Chemical 2 (rust remover)						X				

As seen on Table 2 above, with the exception of reference new samples (RN), every surface condition involved pre-corroding the samples before any preparation. In each labelling code, the first letter represents the contamination remaining and the second letter the rust removal method used on the sample plates.

The use of the word “None” for contamination, signifies that an effort was made to remove contamination from the specific pre-corroded plate (see Section 5.5, page 67).

4.2.1. Reference New Samples (RN)

A set of brand new samples was used as reference. Figure 3 below shows the appearance of the surface of the RN samples prior to testing.

Figure 3: Reference new (RN) sample prior to coating application

4.2.2. Samples with Salt Contamination and no Rust-Cleaning Attempt (SN)

All other surface condition involved exposing the samples so as to corrode and contaminate the plates, so that the additional preparation methods could be carried out. Figure 4 below shows the appearance of the samples after exposure.

Figure 4: Sample with salt contamination and no rust-cleaning attempt (SN) prior to coating application

A set of these samples was coated without any attempt to improve surface condition so that they could be used as the reference fully corroded substrate (SN). The remaining samples were divided into two batches; one set was cleaned to remove salt contamination (see 4.2.3 – 4.2.6) while the other set was left with salt contamination.

4.2.3. Samples with no Salt Contamination and no Rust-Cleaning Attempt (NN)

Half of the remaining samples from the SN samples were cleaned with deionized water to remove soluble salts. The resulting surface condition was salt cleaned and fully corroded. The appearance of NN samples is shown in Figure 5

Figure 5: Sample with no salt contamination and no rust-cleaning attempt (NN) prior coating application

Some of the NN samples were coated to provide another condition to test. Chemical rust treatment approach was used on a third of the remaining NN samples and one third were mechanically treated.

4.2.4. Samples with no Salt Contamination and Chemical (Rust Converter) Surface Preparation (NC1)

This surface condition was obtained by applying rust converter to NN samples. The appearance of the samples after rust converter application and ready to be coated can be seen on Figure 6 below.

Figure 6: Sample with no salt contamination and chemical (rust converter) surface preparation (NC1) prior coating application

Figure 6 above shows a salt-cleaned sample that was then chemically treated with rust converter (NC1). Rust converter was only applied to some of the NN samples, the rest were kept for further treatment.

4.2.5. Samples with no Salt Contamination and Mechanical Surface Preparation (NM)

The remaining NN samples were wire brushed to achieve the pre-treatment grade of St 2-C, which conforms to ISO 8501-1 producing the surface shown in Figure 7 below.

Figure 7: Sample with no salt contamination and mechanical surface preparation (NM) prior to coating application

The sample on Figure 7 above was salt-cleaned then wire brushed to produce condition NM. One half of these samples was further pre-treated to produce another surface condition namely NB1 in Section 4.2.6 below.

4.2.6. Samples with no Salt Contamination and both Mechanical and Chemical (Rust Converter) Surface Preparation (NB1)

Application of rust converter onto the remaining NM samples resulted in the surface condition NB1, whose appearance is shown in Figure 8 below.

Figure 8: Sample with no salt contamination and both mechanical and chemical (rust converter) surface preparation (NB1) prior to coating application

The surface condition in Figure 8 was achieved through salt removal, followed by mechanical wire brushing and then rust converter application to give condition NB1. The following surface conditions were achieved without cleaning soluble salts from the sample plates.

4.2.7. Samples with Salt Contamination and Chemical (Rust Converter) Surface Preparation (SC1)

This surface condition was obtained by applying rust converter on SN samples. After rust converter application, these samples, Figure 9 below, are ready to be coated.

Figure 9: Sample with salt contamination and chemical (rust converter) surface preparation (SC1) prior to coating application

Figure 9 above displays a sample treated with rust converter right after exposure when still containing salt contamination (SC1). Rust converter was only applied to some of the remaining SN samples, the rest were kept for further treatment.

4.2.8. Samples with Salt Contamination and Mechanical Surface Preparation (SM)

Mechanical wire brushing was performed on a set of SN samples to achieve St 2-C pre-treatment grade, as per ISO 8501-1, producing the surface shown on Figure 10 below.

Figure 10: Sample with salt contamination and mechanical surface preparation (SM) prior to coating application

The sample on Figure 10 above contains salt contamination and was wire brushed to St 2 grade. While one set of these SM samples were ready to be coated, the remaining SM plates were further pre-treated to produce two other surface conditions.

4.2.9. Samples with Salt Contamination and both Mechanical and Chemical (Rust Converter) Surface Preparation (SB1)

Application of rust converter onto half of the remaining SM samples resulted in another surface condition (SB1), with appearance shown on Figure 11 below.

Figure 11: Sample with salt contamination and both mechanical and chemical (rust converter) surface preparation (SB1) prior to coating application

This surface condition (SB1), shown on Figure 11 above, was accomplished by wire brushing salt contaminated samples followed by application of chemical rust converter.

4.2.10. Samples with Salt Contamination and both Mechanical and Chemical (Rust Remover) Surface Preparation (SB2)

Application of rust remover onto the remaining SM samples resulted on one last surface condition (SB2), whose appearance is shown on Figure 12 below.

Figure 12: Samples with salt contamination and both mechanical and chemical (rust remover) surface preparation (SB2) prior to coating application

The surface condition shown on Figure 12 above (SB2) was achieved through wire brushing of the salt contaminated sample followed by treatment with a rust remover product.

4.3. Sample Preparation

The sample plates were prepared as described under Section 4.2 above. However, protocols had to be followed to achieve uniform surface condition across all samples. These procedures are described below.

4.3.1. Pre-Corrosion Procedure

Since this study is directed to maintenance coating, it was necessary that the samples be pre-corroded and pre-treated to a certain degree to try to mimic the somewhat poor surface treatment that is sometimes achieved in the field.

The metal plates were exposed for a fixed time in a salt fog chamber so as to pre-corrode them. For uniformity, all the plate samples were exposed to the pre-programmed CCT1 cycle in a Q-Fog chamber for 17 hours, with exposure always starting from the beginning of the fog step of the cycle (details of CCT1 on Section 4.6.2, page 32). This exposure was meant to achieve Rust Grade C (International Organization for Standardization, 2011). Natural seawater was used to produce the salt fog inside the corrosion chamber so as to remain as true to the offshore environment as possible.

The following parameters were used on the corrosion chamber for the pre-corrosion process: two CCT-1 cycles (17 hours), air pressure of 15 psi and pump speed 90 rpm; resulting in a fog deposition rate of 1.5 ml/hr per 80 cm^2, averaged over two collection locations in the chamber. Note that for the fog deposition rate the total time for all steps in the cycle were considered, not only the time of the fog step alone.

Pre-corrosion of the sample plates to the desired rust grade was followed by various cleaning and surface preparation procedures prior to coating application.

4.3.2. Salt Cleaning Procedure

The soluble salts from the pre-exposure were washed away with distilled water. This was done in batches containing 14 large and 5 small plates, using 4.5 litres of distilled water, and washed by hand (wearing latex gloves) for five minutes whilst immersed in the water. The process was repeated with a second bath of clean water, reversing the order of removing the plates from the water.

4.3.3. Mechanical Preparation Procedure (Wire Brushing)

The mechanical rust removal method used in this work was hand tool cleaning as it is meant to undress the unfeasibility of deploying the best available surface preparation equipment to the offshore rigs. The samples were wire brushed from Rust Grade C to achieve the pre-treatment grade of St 2-C, which conforms to ISO 8501-1(International Organization for Standardization, 2011).

Two carbon steel wire brushes were used, one brush for each degree of salt contamination. The brushing procedure consisted of 10 brushing cycles per pass, with two longitudinal passes and five transverse passes required to cover the width and the length of the small plates whilst five longitudinal and 10 transverse passes, were necessary for the larger plates.

4.3.4. Chemical Surface Preparation

The chemical surface preparation made use of commercially available products. As the study aims to address maintenance coating issues, rust converters appeared to be best suited to maintenance because the converted rust product would hopefully act as a protective primer ready to be coated. The purpose is to determine the relative merits of removing rust to rust conversion prior to coating application. However, the situation is further complicated by the fact that salt contamination can influence rust conversion and hence the comparison of removing rust and rust conversion will also be affected by the amount of rust and degree of salt contamination in the rusted surface.

The application of the rust converter and the rust remover was carried out as recommended by the manufacturers except that in this study most of the samples were pre-weathered and pre-treated before application of the chemicals.

4.3.4 (a) Rust Converter Application

A foam brush was used to apply the rust converter product onto the surface of the samples. The application involved dipping and reapplying the converter product immediately after the first pass. An average temperature of 18˚C was recorded on the days of rust converter application.

4.3.4 (b) Rust Remover Approach

The samples were immersed into the prepared rust remover product for 30 minutes, and then removed and rinsed with distilled water; the samples were coated after drying. The preparation of rust remover product consisted of diluting 100ml of SurTec 414 with deionized water to approximately 1 litre, and then neutralizing with 0.1 N

sodium hydroxide solution. The amount of 0.1 N sodium hydroxide solution required for neutralization was determined by titration, using phenolphthalein (0.1 % in ethanol) as an indicator.

4.4. Visual Inspection Criteria

4.4.1. Transition Time to Corrosion Based on Visual Inspection

Following exposure in the chamber, after visual inspection, the condition of the coated plates was photographically recorded at various fixed time intervals, e.g. 8 hours, 17 hours, one day and so on. However, the degradation observed on any two consecutive photographs varied substantially depending on the surface pre-treatment applied. This suggests that coating breakthrough occurred at different times prior to the next observation in any consecutive set. Hence, a need arose to establish criteria to estimate the transition time to corrosion, i.e. from little observed corrosion to extensive corrosion.

The transition time to corrosion is defined here as the time elapsed to 25% of the coating presenting any kind of failure. Which is visually rated as follows: any value <12.5% is recorded as 0% and any value ≥12.5% is recorded as 25%. The edges were not considered for determining the percentage failure.

4.4.2. Criteria for Determining Transition Time to Corrosion from Visual Inspection

The coating condition was photographically recorded at times $t_0 = 0$ (prior to exposure) up to t_n = 710 hours (30 days of exposure) for the studied surface preparation conditions. A generalized timeline of exposure is shown on Figure 13 below.

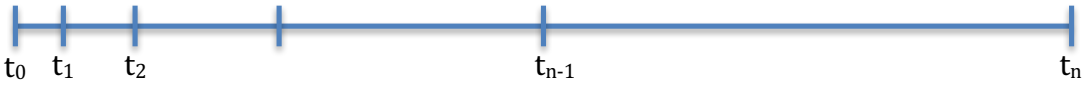

Figure 13: Exposure time intervals showing the times of inspection.

As represented in Figure 13 above, the intervals at earlier stages of exposure are shorter than those on the later stages, so as to accommodate the rapid change in plate condition at the beginning of any test exposure period as well as the rapid corrosion that occurred on certain surface preparation conditioned test plates.

4.4.2 (a) Procedure

1. The percentage coating damaged was estimated at the time of inspection. The percentage damage was rated as: 0%, 25%, 50%, 75% or 100% failure of the coating area on the plates. To simplify observation the following rules were used

   I. Record 0% when inspection estimate <12.5%
   II. Record 25% when inspection estimate between 12.5% and 37.5%
   III. Record 50% when inspection estimate between 37.5% and 62.5%
   IV. Record 75% when inspection estimate between 62.5% and 87.5%
   V. Record 100% when inspection estimate >87.5%

2. Based on recorded percentage failure, a rule to assign the start of corrosion in the period between the inspection of a plate and its next inspection was set up, and the rule is as follows: the time elapsed since corrosion started corresponds to a percentage of the time interval between the current inspection and the previous one, where this percentage is the recorded percentage failure. Note that, uniform corrosion rate was assumed from the time corrosion starts to the time of observation.

   Example: For 75% failure recorded at total exposure of t_n = 24h, with previous inspection done in the last 8 hours (at t_{n-1}=16h), corrosion occurred during the last 75% of 8 hours i.e. it has been corroding for the last 6 hours (8x0.75=6).

3. Knowing the total exposure period and the time elapsed since corrosion started, the transition time to corrosion (time to corrosion initiation, t_{corr}), from first exposure to the start of corrosion, can easily be calculated by subtracting these two. For the above example, this would be t_{corr} = 24 – 6 = 18 hours. See the diagram below for clarity.

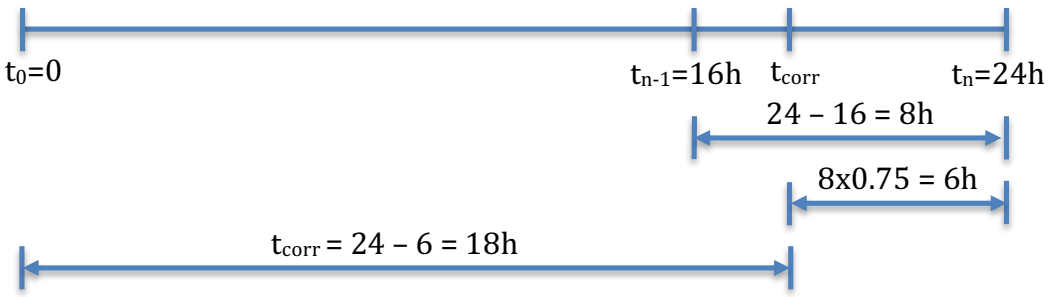

Figure 14: Graphical representation of transition time to corrosion

Alternatively, use the expression bellow:

$$t_{corr} = t_n - (t_n - t_{n-1})\frac{f_p}{100}$$ Equation 1

where:

t_{corr} - transition time to corrosion

t_n - time of inspection (exposure time at highlighted pictures under Section 5.3.1, page 52)

t_{n-1} - time of previous inspection (time at the picture on the left of highlighted pictures under Section 5.3.1, page 52)

f_p - recorded percentage failure at t_n.

4.5. Pull-Off Adhesion Testing

The adhesion of the coating to the substrate was evaluated by pull-off testing. A test rig was designed to use with a tensile tester in CME (Centre for Materials Engineering) laboratory, UCT.

4.5.1. Apparatus

4.5.1 (a) ***Tensile Tester:*** the tensile machine on Figure 15 (Instron Universal Testing System) provides a co-axial pull force between the grip (detaching unit) and the base, and measures the pull strength.

4.5.1 (b) ***Pull-off Test Rig:*** provides a torsion free and self-aligning mounting for the samples in the tensile machine (drawings of the rig in APPENDIX).

4.5.1 (b) (i) Base Holder: attaches the base of the rig to the base of the tensile machine.

4.5.1 (b) (ii) Base: holds the actuator and provides the self-aligning capability through a self-aligning spherical roller bearing.

4.5.1 (b) (iii) Actuator: has an annular flat surface to press uniformly against the surface of the coating and around the detaching unit.

4.5.1 (b) (iv) Detaching Unit: has a T-groove to engage the head of the dolly and a means to be attached to the load cell of the tensile machine.

4.5.1 (b) (v) Dolly/Loading Fixture: to be adhered to the coating on its flat end and attached to the detaching unit on the other end (head).

4.5.1 (c) ***Solvent***: ethanol to clean contaminants such as fingerprints, moisture and oxides from the surface of the dolly.

4.5.1 (d) ***Fine Sandpaper:*** a very fine grade (400 grit) to avoid introducing flaws or leaving residue while cleaning the coating.

4.5.1 (e) ***Adhesive:*** Spabond 340LV to glue the dolly to the coating without affecting the coating properties.

4.5.1 (f) ***Cotton Swabs:*** to remove excess adhesive and defining the adhered area.

The setup of the pull-off test can be seen in Figure 15 below

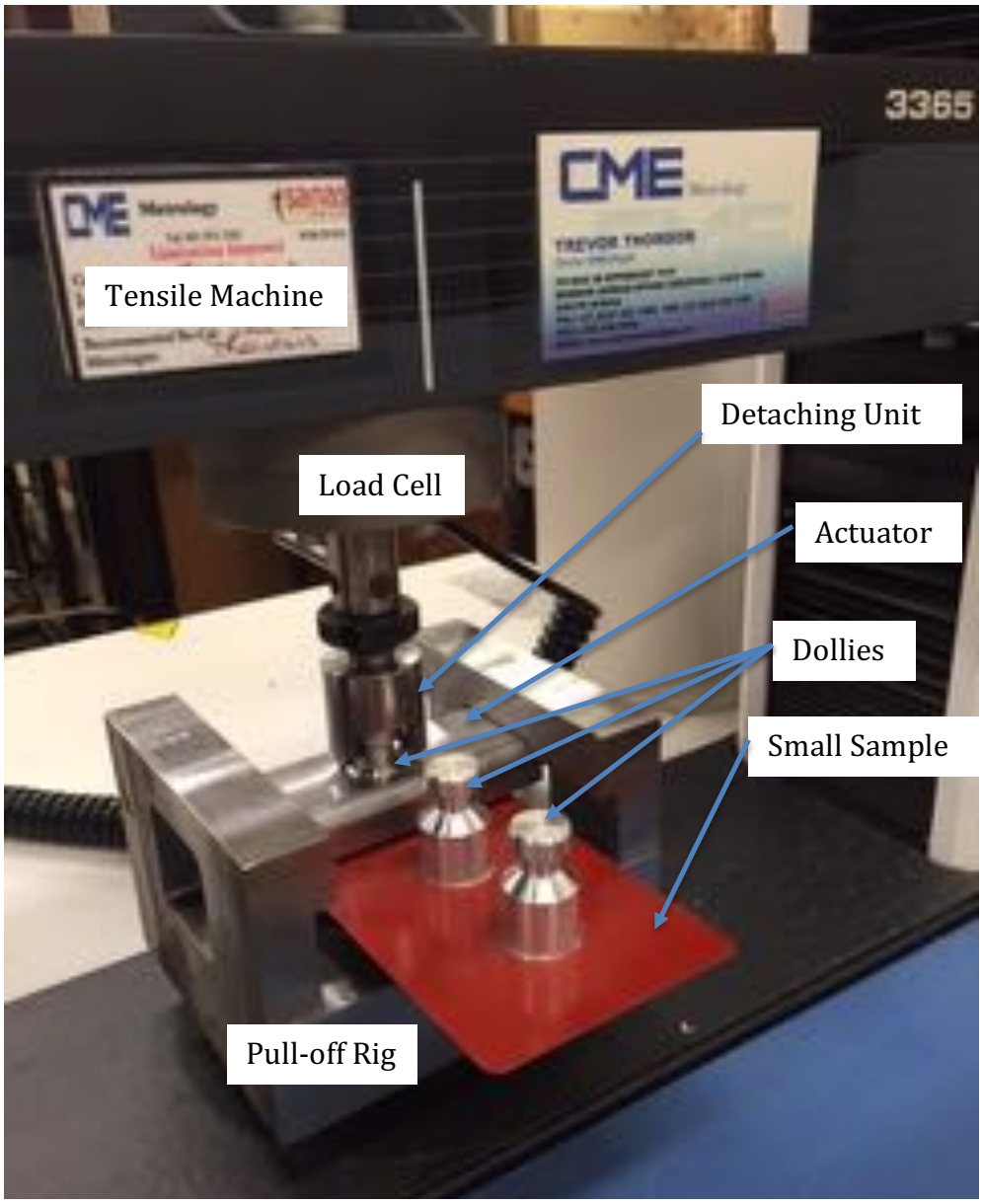

Figure 15: Setup of the pull-off test being performed on a sample

4.5.2. Specimen Preparation for Pull-Off

Specimen preparation for pull-off testing consists mainly of gluing the dolly to the substrate. To ensure adhesion of the adhesive to the coating surface, the coating was only lightly abraded with 400 grit sandpaper to avoid reducing coating thickness and damaging the coating. The particles from abrasion were removed by solvent cleaning. The dolly was cleaned with sandpaper to remove the aluminium oxide film built on the metal surface. Some adhesive was used on the sandpaper at the end to prevent new oxide film formation and avoid premature failure in the oxide layer.

The adhesive was prepared as recommended by the manufacturer and applied on both the coating and the dolly to ensure good wetting of the surfaces. Although another brand of adhesive, a two-part epoxy adhesive (pratley steel quickset), was tested, it was found to be unsatisfactory for the test work.

4.5.3. Pull-Off Test Procedure

The pull-off test was performed at a pull rate of 0.10 mm/sec, which was set on the machine Bluehill software along with other required specifications such as test area geometry (circular) and dimension (diameter = 20mm). These parameters allow for the automatic calculation of the pull strength by the Bluehill software.

With the pull-off rig mounted on the tensile machine, the detaching unit is brought down with the loading cell to a height inside the base that the head of a dolly can be slid into the T-groove of the detaching unit. This is done once the actuator is placed around a dolly attached to a sample, then the sample is lifted to as close as possible to the actuator to reduce testing time. Care must be taken to avoid bumping with the dolly and pre-stress the coating. Finally, the run button is hit on the Bluehill software, and the test is run to failure then the stop button is pressed. The results obtained can be found under results (Section 5.6.4, page 78). Note that the samples for pull-off testing were not exposed after coating application.

4.6. Accelerated Exposure Testing

After coating application, samples were exposed to accelerated test conditions to evaluate the degradation rate of the coating and subsequent corrosive attack. The evaluation was performed by visual inspection and EIS measurement.

4.6.1. Apparatus

4.6.1 (a) ***Cabinet (Q-FOG Chamber):*** this is the corrosion chamber used for the accelerated exposure.

4.6.1 (a) (i) Test Panel Racks: used to hold the samples inside the chamber at an inclination of 15˚ from the vertical. ASTM B117 Standard recommends inclinations from 15˚ to 30˚ from the vertical, since it also recommends that salt solution from one specimen shall not drip on any other specimen, racks with 15˚ inclination is preferred to accommodate more specimens at once. Figure 16 below shows the panel racks with new samples inside the corrosion chamber.

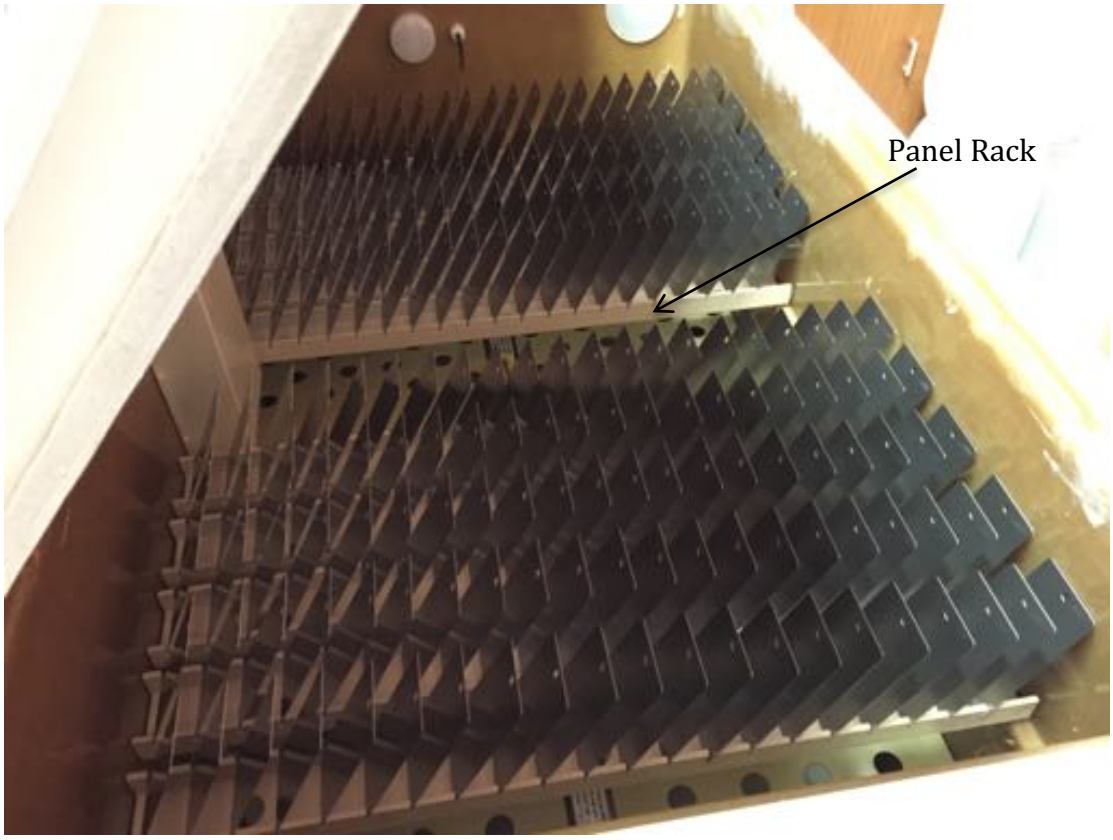

Figure 16: New samples on panel racks inside the corrosion chamber

4.6.2. Exposure Test Procedure

The procedure used for accelerated exposure is CCT-1, also known as CCT-A. Some Japanese automotive manufacturers specified this test (Q-LAB, 2011). Conveniently, it is pre-programmed on the corrosion chamber used (Q-FOG CCT model).

4.6.2 (a) Test Cycle Steps of CCT-1

Step 1	Fog at 35˚C for 4 hours
Step 2	Dry at 60˚C for 2 hours
Step 3	Dry at 40˚C for 30 minutes
Step 4	Humid (up to 100%) at 50˚C for 2 hours
Step 5	Final step – go to step 1

Note that Step 3 is only added to improve transition.

4.6.2 (b) Salt Solution

Natural seawater, collected from lagoon beach in Cape Town (South Africa), was used as the exposure solution and replaced every week so as to remain fresh.

The quantity and uniformity of the salt fog was verified before starting the test. The fog deposition rate was 1.8 mL/h per 80 cm^2 (collected for 17 hours of continuous fog), which is within the recommended range of 1.0 to 2.0 mL/h (Q-LAB, 2011). The samples were moved around inside the chamber to promote uniform exposure during the test. Furthermore, all samples were exposed to equivalent exposure periods by ensuring that the steps involved on a given exposure period were the same for all samples. Samples were periodically removed from the chamber for visual evaluation and EIS testing.

4.7. Salt contamination test

The salt contamination on the surface of the samples was measured using the Bresle test method. A defined volume of pure water is brought in contact with the surface then the conductivity of the water is measured; the result gives the equivalent amount of salt on the surface.

4.7.1. Apparatus

4.7.1 (a) ***Conductivity Meter and Sensor:*** Elcometer 138 was used to measure the conductivity of the water after exposure to the surface.

4.7.1 (b) ***Bresle Patches:*** Elcometer 135 was used to contain the pure water against the surface.

4.7.1 (c) ***Syringe and Needles:*** to insert and remove the water into and from the patches.

4.7.2. Salt Measurement Procedure

The test procedure used is US NAVY PPI 63101-000 (Elcometer, no date). This procedure requires only 10 to 15 seconds of contact between the surface and the water, which makes it favourable for surface conditions containing corrosion products as they tend to absorb water. The measured conductivity values (in µS/cm) multiplied by a factor of 1.1 gave the IMO PSPC equivalent NaCl in mg/m^2 (International Maritime Organization – Performance Standard for Protective Coating).

4.8. Electrochemical Impedance Spectroscopy (EIS) Testing

One of the biggest advantages of EIS testing is the ability to provide results long before any visual sign can be identified. This project compared visual assessment of coated steel plates against EIS evaluation of the coated plates.

4.8.1. Apparatus

4.8.1 (a) ***Potentiostat:*** VersaSTAT 3 was the potentiostat/galvanostat used to carry out the AC impedance tests.

4.8.1 (b) ***Faraday Cage:*** to lessen the current and voltage noises picked up by the working and reference electrodes (D Loveday, Peterson and Rodgers, 2004).

4.8.1 (c) ***Computer:*** to aid data collection.

4.8.1 (d) ***Electrochemical Cell:*** the cell used is a PTC1, see Figure 17 below, with a graphite rod as counter electrode and a saturated calomel electrode (SCE) as reference electrode.

Faraday
Cage

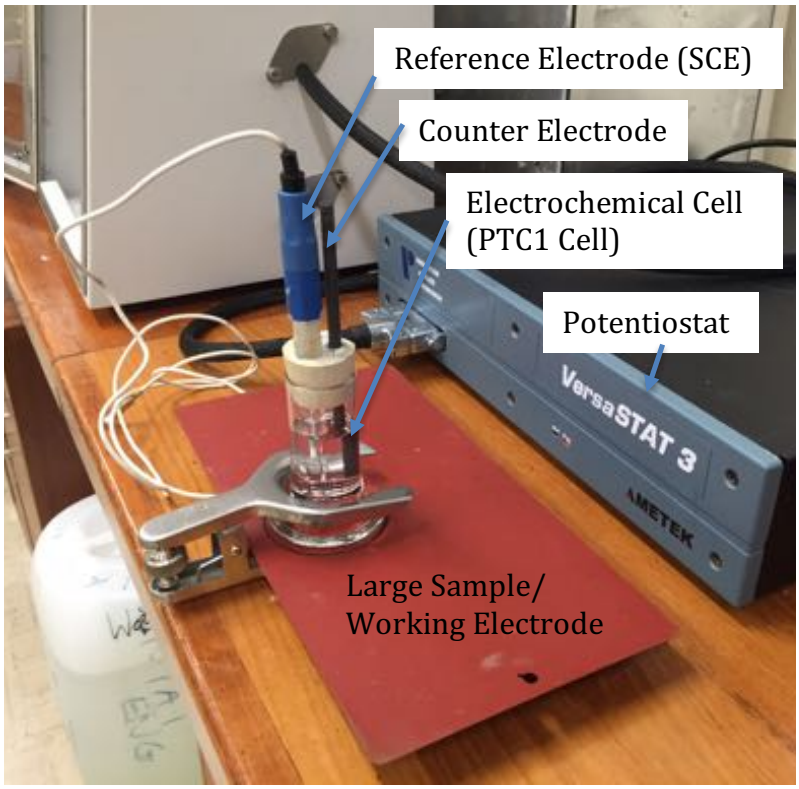

Figure 17: PTC1 cell on a large sample

4.8.2. Specimen Preparation for EIS measurement

To ensure the EIS testing is always performed on the same area of the samples every time they were taken from the corrosion chamber, the test area on the plates was permanently outlined using a marker pen using the cell body as template. This prevents changes in coating thickness within samples as well as other coating properties being interpreted as the result of coating deterioration. Furthermore, the samples were conditioned (immersed in the test solution) for 20 minutes before running the impedance test.

4.8.3. Electrolyte used

The electrolyte used in the EIS testing experiment was synthetic seawater as prepared in accordance with ASTM D1141 standard (2013).

4.8.4. EIS measurement Procedure

The EIS test was performed using a three-electrode (working, reference and counter electrodes) electrochemical cell. The coated sample was the working electrode, which required removing a small portion of the coating outside the test area to allow connection of the lead of the potentiostat. The perturbation amplitude was 10 mV and

the scan frequency range studied was 10 kHz to 1 Hz. The measurements were done at the open circuit potential (OCP), and the test was set to plot the average of five readings per plot.

The analysis of the data points obtained was done using phase angle at high frequency (10 kHz) and total impedance at low frequency (1 Hz) methods. The results obtained can be found on Section 5.7 (page 79).

CHAPTER 5. RESULTS

5.1. Consistency in the Visual Inspection Results

Before comparing how the coating performs from one surface condition to another, it is important to look at the result for consistency, i.e. for coating performance among replicates. By recording the variations within replicates, it is possible to decide on the acceptability of the results.

The semi-quantitative approach in 4.4.2 (page 27) was used to determine the time for coating deterioration to start, i.e. the transition time to corrosion, as a measure of coating performance.

Figures 18 to 22 below present three situations of samples SN, SM, NN, NM and SB2, and Figures 23 to 27 present four situations of samples SC1, SB1, NB1, NC1 and RN at the transition time to corrosion. The samples below are presented in increasing order of thickness from the images on the left to the image on the right. The surface conditions are presented in chronological order of transition time to corrosion, i.e. from the condition with the smallest transition time to corrosion (SN) to the condition with the largest time to corrosion (RN).

Figure 18: Variation in performance of SN samples at 34 hours of exposure (from the left SN-06, SN-12 and SN-14)

Figure 19: Variation in performance of SM samples at 68 hours of exposure (from the left SM-06, SM-09 and SM-12)

Figure 20: Variation in performance of NN samples at 136 hours of exposure (from the left NN-05, NN-09 and NN-10)

Figure 21: Variation in performance of NM samples at 136 hours of exposure (from the left NM-05, NM-09 and NM-11)

Figure 22: Variation in performance of SB2 samples at 136 hours of exposure (from the left SB2-05, SB2-06 and SB2-09)

The plates shown in Figures 18 to 22 were used for EIS testing, so the focus is on the testing areas within the marked circle. The difference in performance across the samples with identical pre-treatment is minimal and shows good consistency across the plates i.e. similar appearance in terms of type and degree of failure.

While Figures 18 to 22 show the zone on the test plates that was tested by EIS, Figures 23 to 27 show the entire test plate. Here the visually assessed test plates are presented as opposed to the EIS tested plates, since by the time they showed visual signs of coating deterioration, EIS measurement was no longer being performed.

Figure 23: Variation in performance of SC1 samples at 264 hours of exposure (from the left SC1-01, SC1-02, SC1-03 and SC1-04)

Figure 24: Variation in performance of SB1 samples at 264 hours of exposure (from the left SB1-01, SB1-02, SB1-03 and SB1-04)

Figure 25: Variation in performance of NB1 samples at 710 hours of exposure (from the left NB1-01, NB1-02, NB1-03 and NB1-04)

Figure 26: Variation in performance of NC1 samples at 710 hours of exposure (from the left NC1-01, NC1-02, NC1-03 and NC1-04)

Figure 27: Variation in performance of RN samples at 710 hours of exposure (from the left RN-01, RN-02, RN-03 and RN-04)

Figures 23 to 27 show that although coating degradation can vary across a single plate, the outcome from one plate to another within each pre-treatment type is very similar, thus showing a consistency in the test results.

The edge of the test plates is a critical region where corrosion initiates and corrosion initiation is a catalyst for complete failure. Figures 18 to 27 illustrate that coating deterioration could consist of different types of failure, occur at different locations on

any one test plate and also be influenced by the specific pre-treatment applied to the plate prior to coating. Other factors affecting coating deterioration, such as sample size, can also be explored.

5.2. Effect of Sample Size on Coating Performance

Corrosion of steel in seawater occurs with the seawater as the electrolyte and the metal surface as the electrodes. Both anodic and cathodic regions are present on the same surface due to inhomogeneity in the material and the difference in oxygen concentration at different sites of the surface of the metal.

An organic coating is applied to the steel substrate to prevent corrosion. By isolating the electrodes (metal) from the electrolyte (seawater), organic coatings protect metals from corroding. However, the isolation of the steel surface provided by an organic coating is not perfect and electrolyte reaches the metal through pores in the coating and this permeation usually depends on time of exposure of the coating to the liquid.

As electrolyte reaches the metal substrate, anodic and cathodic sites are formed under the organic coating leading to corrosion initiation. The size of the samples influences the number of cathodic and anodic sites formed since there is always some inhomogeneity in the metal. Likewise, the availability of critical corrosion initiation sites such as the plate edge is plate size dependent. Therefore, samples dimensions may affect the corrosion rate of the coated metal substrate and subsequent coating deterioration.

Figures 26 to 37 below show a comparison between plates of different sizes with dimensions 76 mm x 152 mm and 152mm x 305 mm. In addition, each of the studied conditions is presented at two distinct periods of exposure. The smaller samples are on the top-left corner of the larger ones.

Figure 28 below shows two RN samples of different sizes at 21 and 30 days of exposure. The dry film thickness of the coating is 60 µm for both plates.

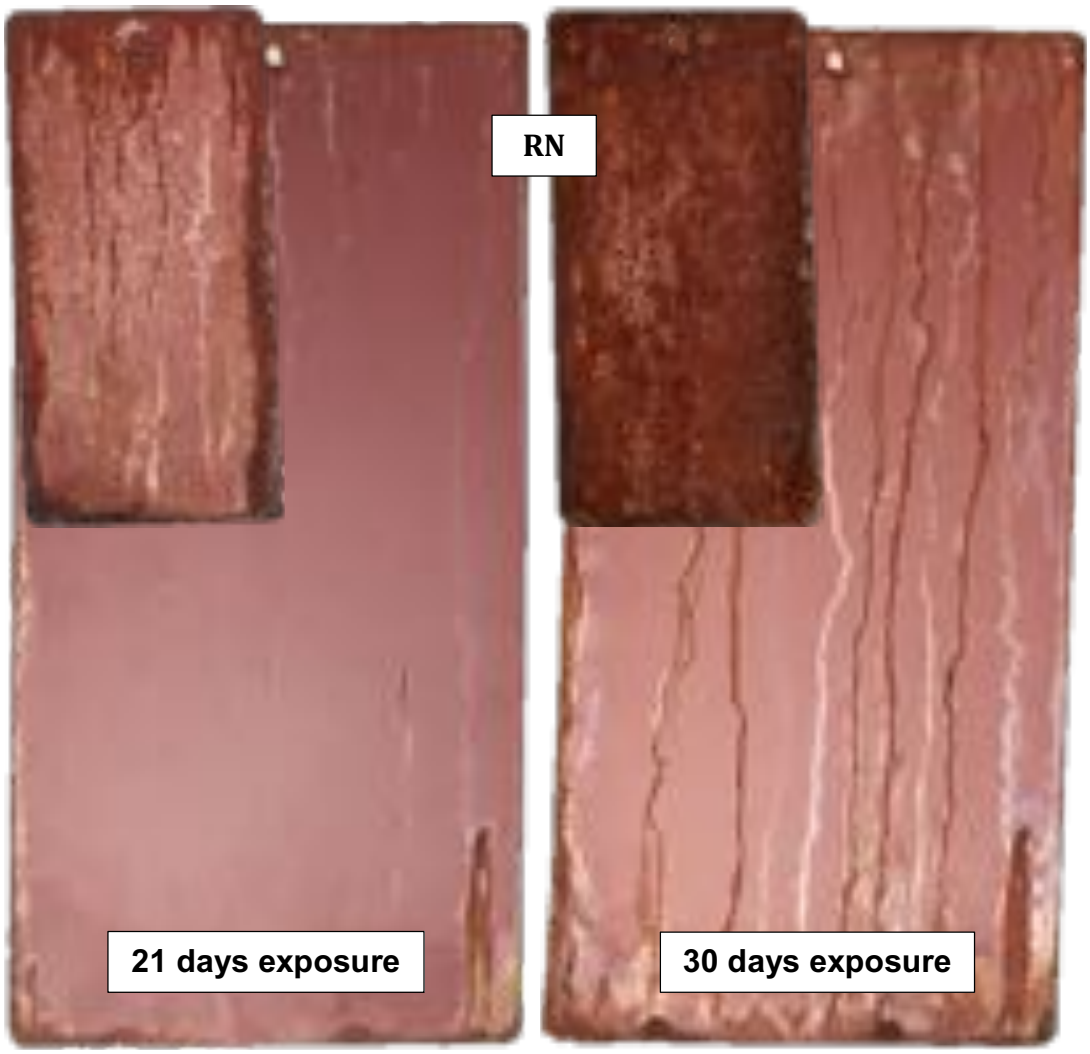

Figure 28: Reference new samples (RN), a small sample on the top left corner of the larger one at exposure periods of 21 days (left) and 30 days (right).

The edge of a sample is a critical feature as it is where corrosion is most likely to start. This is seen at 21 days of exposure on the left image of Figure 28, most clearly on the smaller sample. From the images for both 21 and 30 days of exposure, the smaller sample shows a higher corrosion rate.

Figure 29 below shows the NC1 plates at 21 and 30 days of exposure. The dry film thicknesses of the coating are 69 µm and 68 µm for the large and small samples respectively.

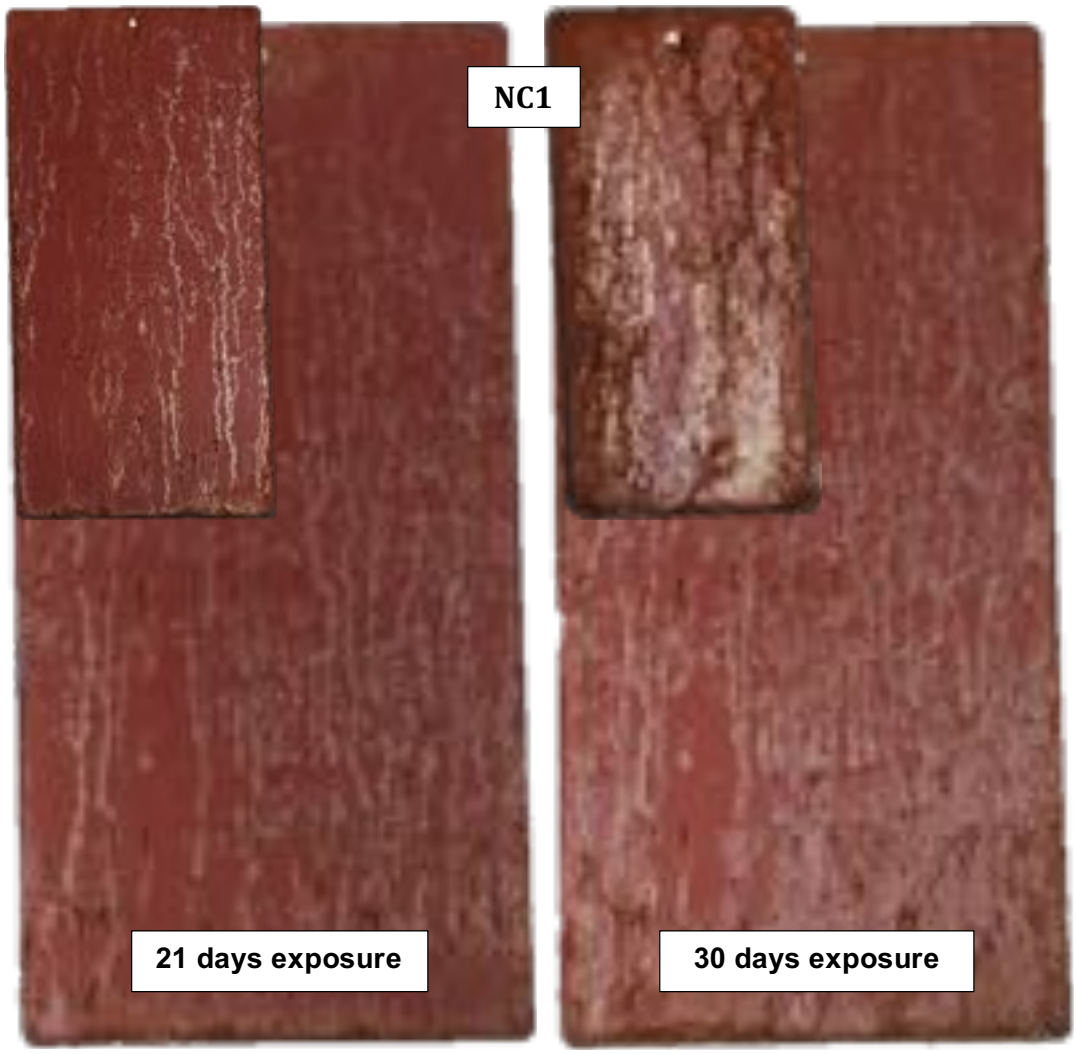

Figure 29: Samples with no salt contamination and chemical (rust converter) surface preparation (NC1), a small sample on the top left corner of the larger one at exposure periods of 21 days (left) and 30 days (right).

At this stage, the failure observed is mostly *checking*. There is also some corrosion attack on the edge of the plates but without clear distinction between the two plates. In contrast, the image for 30 days exposure shows significant corrosion on the smaller sample, mainly starting from the edge. Nevertheless, the larger sample has not undergone significant changes from 21 to 30 days of exposure.

Figure 30 below shows the NB1 plates at 21 and 30 days of exposure. The dry film thicknesses of the coating are 67 µm and 68 µm for the large and small samples respectively.

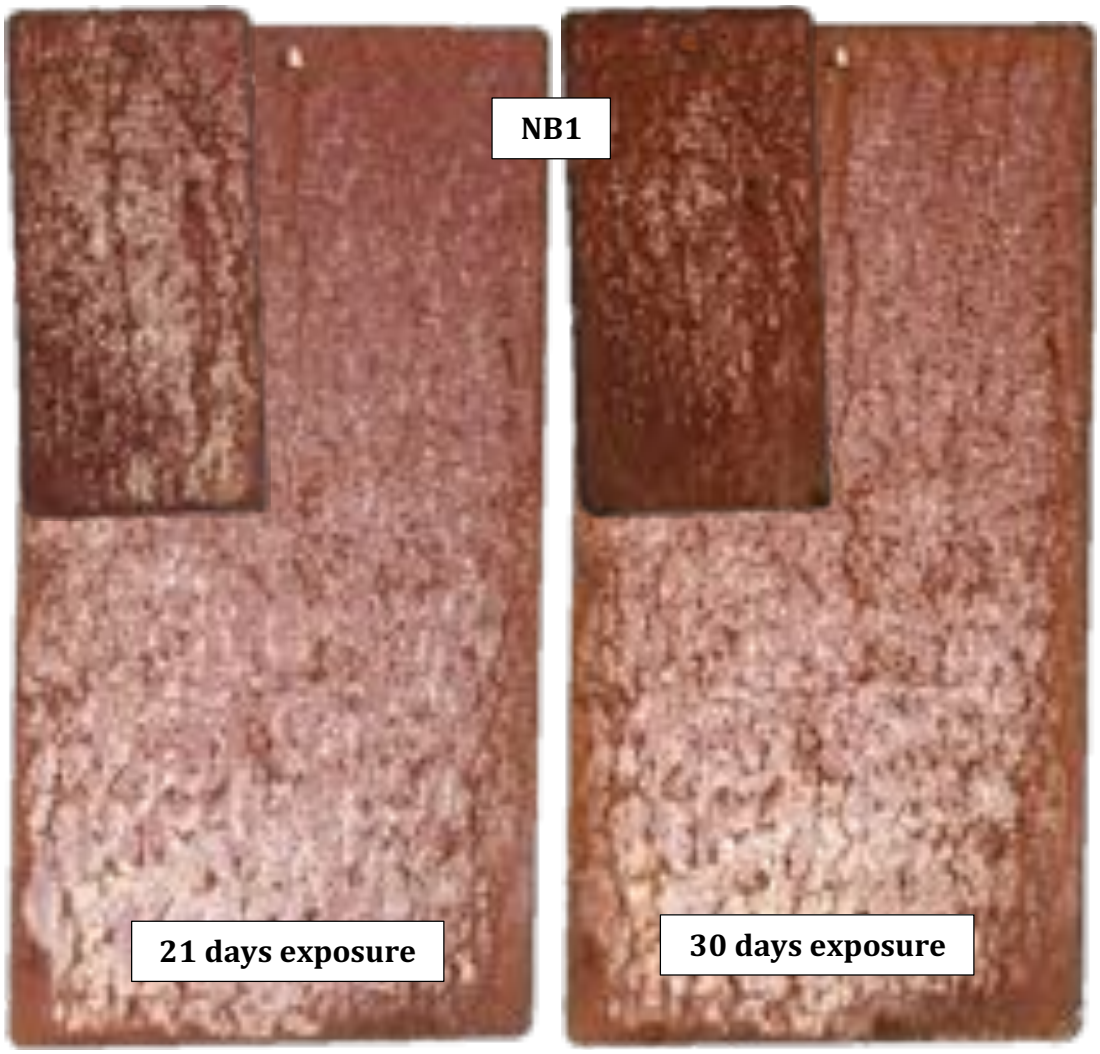

Figure 30: Samples with no salt contamination and both mechanical (wire brushing) and chemical (rust converter) surface preparations (NB1), a small sample on the top left corner of the larger one at exposure periods of 21 days (left) and 30 days (right).

Figure 30 above shows that the coating degradation on NB1 samples is widely spread on the surface of the samples except at the edge. The small plates show more degradation than the large plates. Furthermore, the increase in corrosion from 21 to 30 days exposure for the small plate is greater than the increase in corrosion on the larger plate.

Figure 31 below shows two SB1 samples of different sizes at 14 and 21 days exposure. The dry film thicknesses of the coating are 69 µm and 68 µm for the large and small samples respectively.

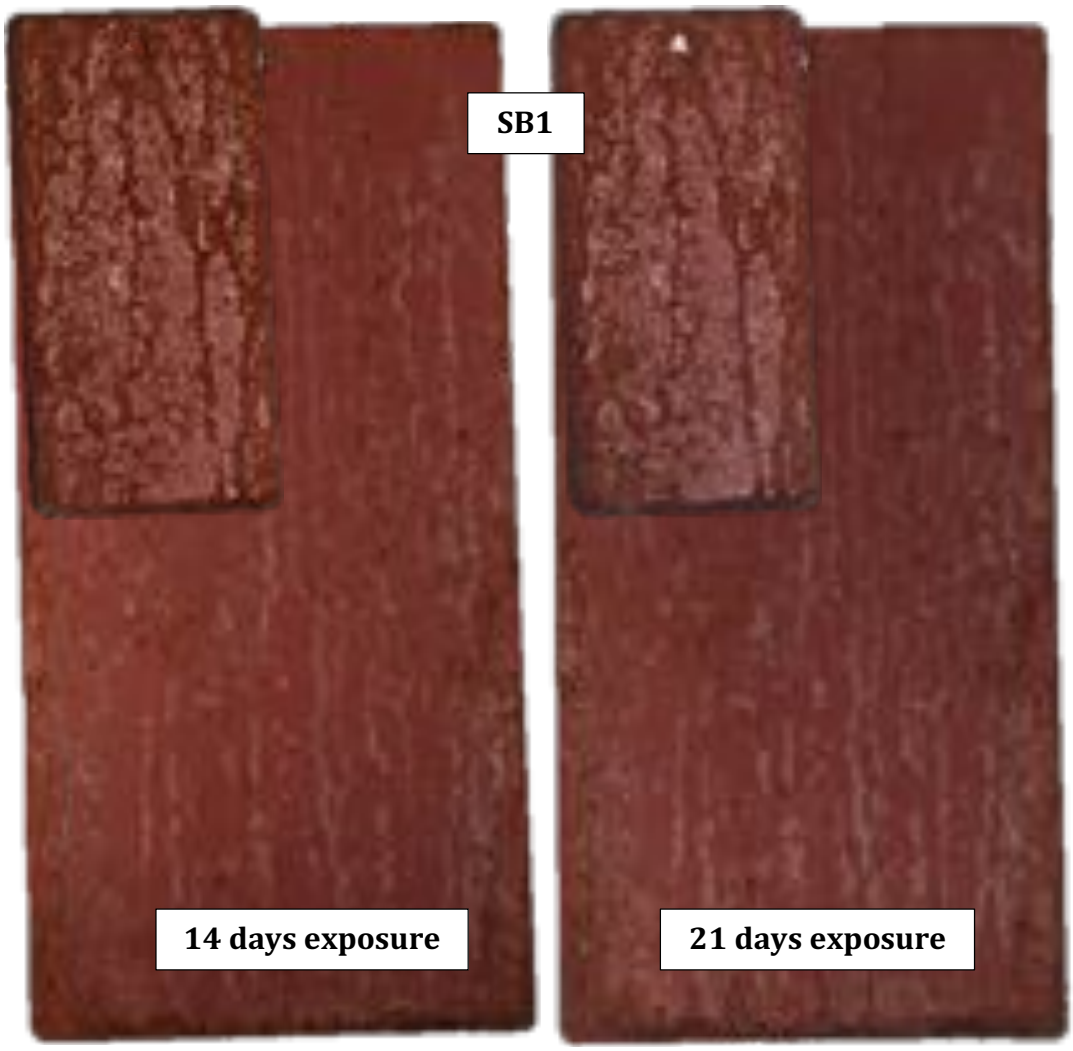

Figure 31: Samples with salt contamination but with both mechanical (wire brushing) and chemical (rust converter) surface preparation (SB1), a small sample on the top left corner of the larger one at exposure periods of 14 days (left) and 21 days (right).

Figure 31 above shows that the coating degradation on SB1 samples is widely spread on the surface of the samples. However, the small plate shows more extensive degradation level than the large plate. There is no clear increase in corrosion from 14 to 21 days exposure on either sample.

Figure 32 below shows two SC1 samples. The dry film thickness of the coating is 71 µm for both large and small samples.

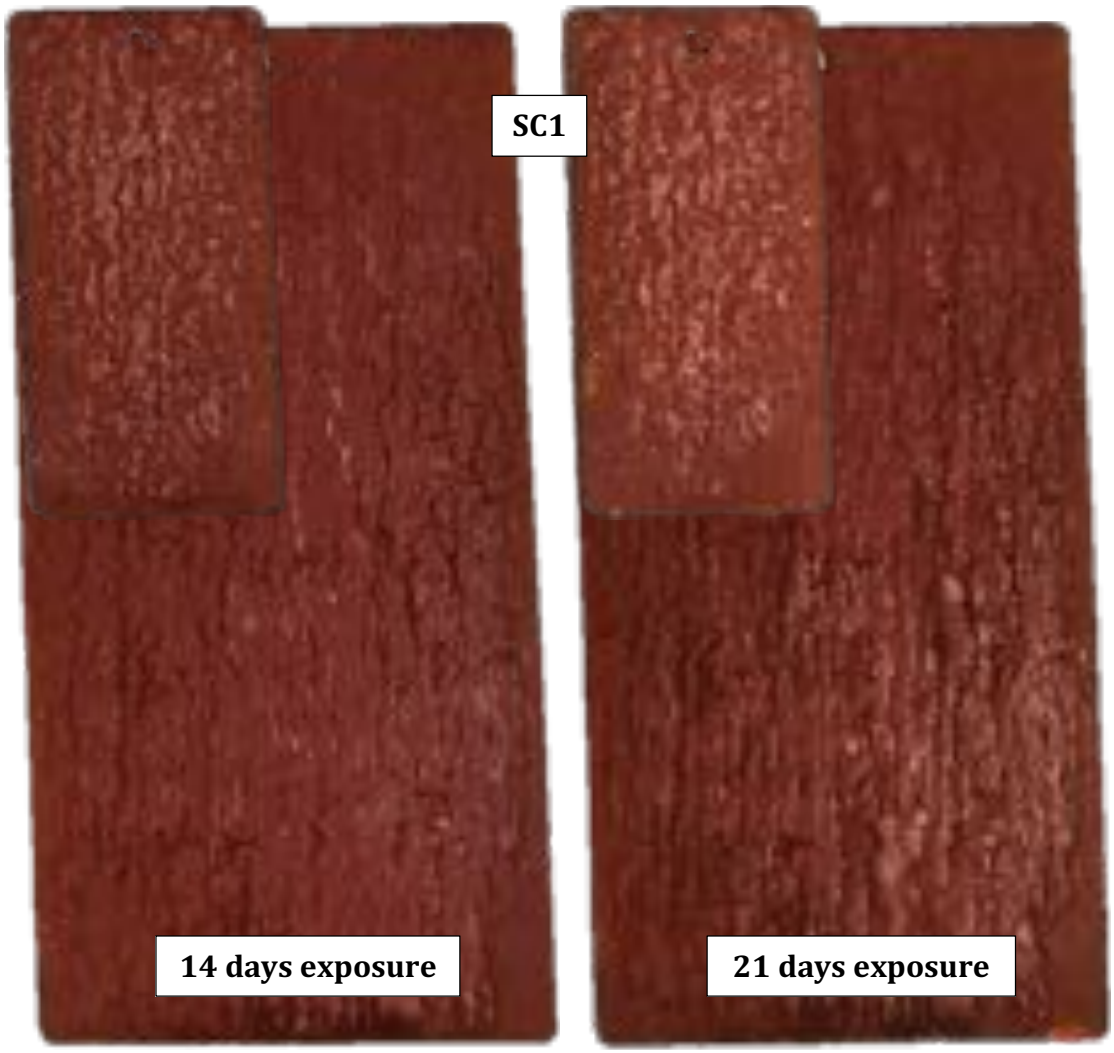

Figure 32: Samples with salt contamination but with chemical (rust converter) surface preparation (SC1), a small sample on the top left corner of the larger one at exposure periods of 14 days (left) and 21 days (right).

Figure 32 above shows that the coating degradation on SC1 samples is widely spread on the surface of the samples. There is a clear increase in coating deterioration on the large plate from 14 to 21 days of exposure. The failure on the large plate at 21 days exposure is mostly *undercutting*.

Figure 33 below shows two SB2 samples of different sizes at 14 and 21 days exposure. The dry film thicknesses of the coating are 74 µm and 62 µm for the large and small samples respectively.

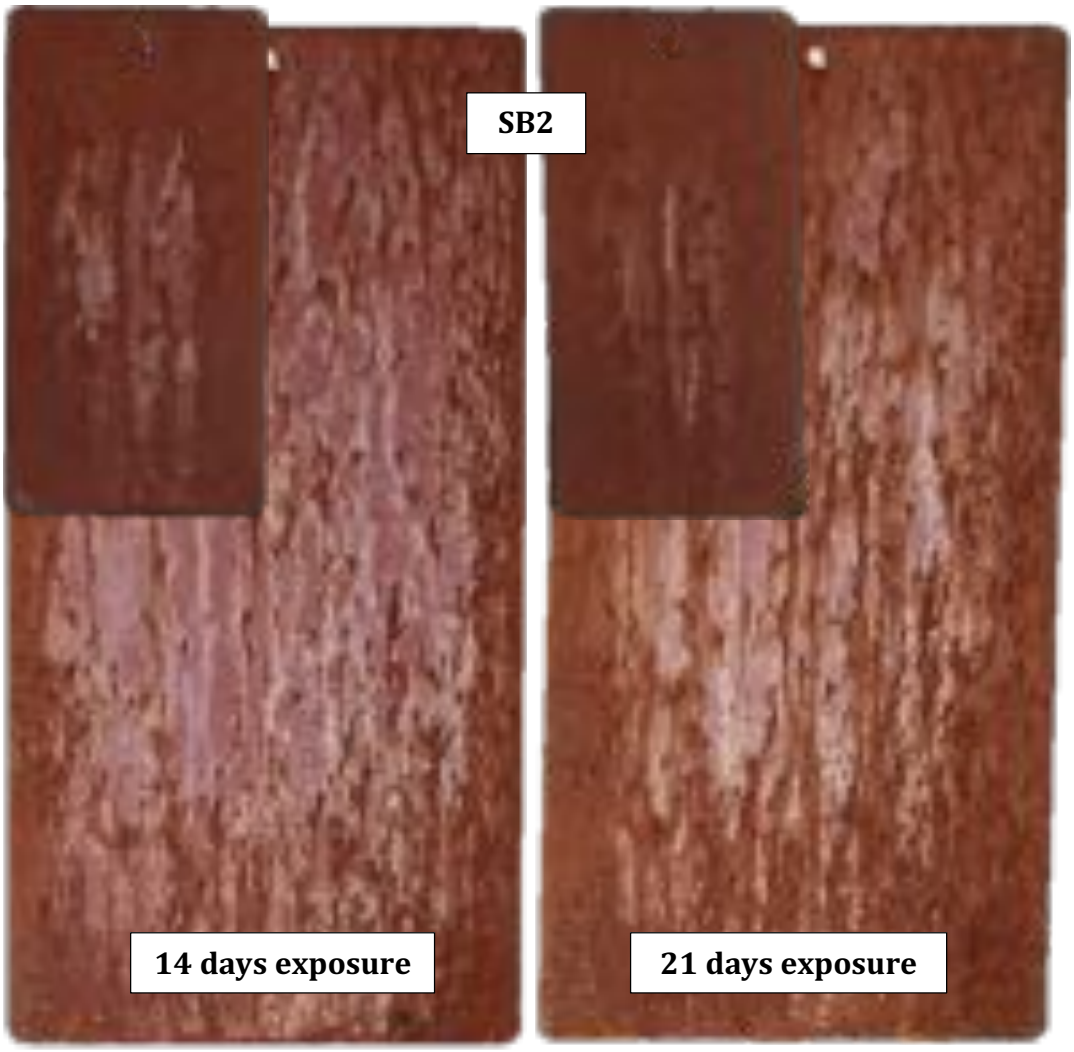

Figure 33: Samples with salt contamination but with both mechanical (wire brushing) and chemical (rust remover) surface preparation (SB2), a small sample on the top left corner of the larger one at exposure periods of 14 days (left) and 21 days (right).

Figure 33 shows that the coating degradation on SB1 samples is widely spread on the surface of the plates. The small plate shows greater degradation than the large one. There is an increase in coating degradation from 14 to 21 days exposure on both samples.

Figure 34 below shows two NM samples of different sizes at 14 and 21 days of exposure. The dry film thicknesses of the coating are 62 µm and 63 µm for the large and small samples respectively.

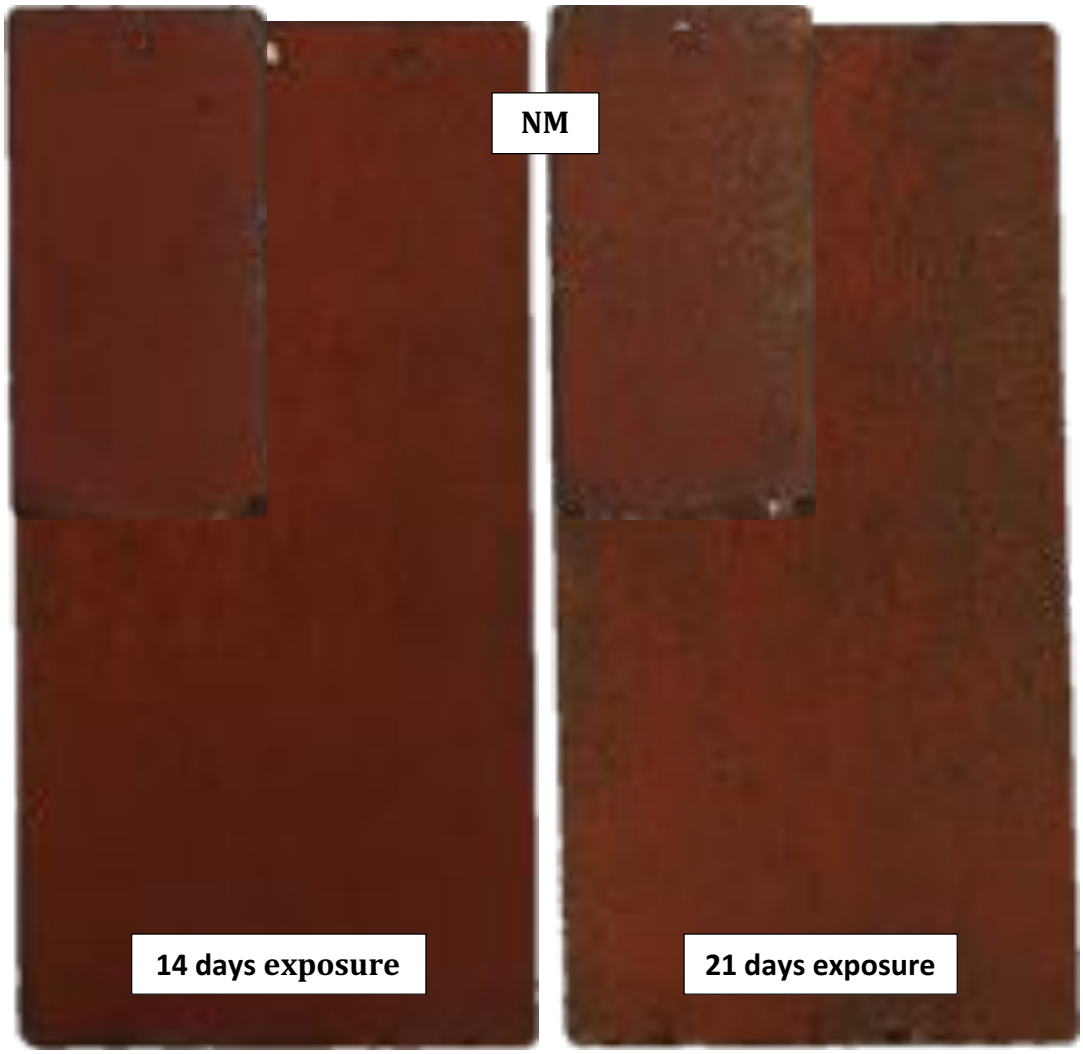

Figure 34: Samples with no salt contamination and with mechanical surface preparation (NM), a small sample on the top left corner of the larger one at exposure periods of 14 days (left) and 21 days (right).

The black spots seen on NM in Figure 34 above, represent *cissing*. Although there is a clear increase in corrosion breakthrough from 14 to 21 days exposure, there is no clear distinction between the small and large samples.

Figure 35 below shows NN samples of different sizes at 8 and 14 days of exposure. The dry film thicknesses of the coating are 74 µm and 72 µm for the large and small samples respectively.

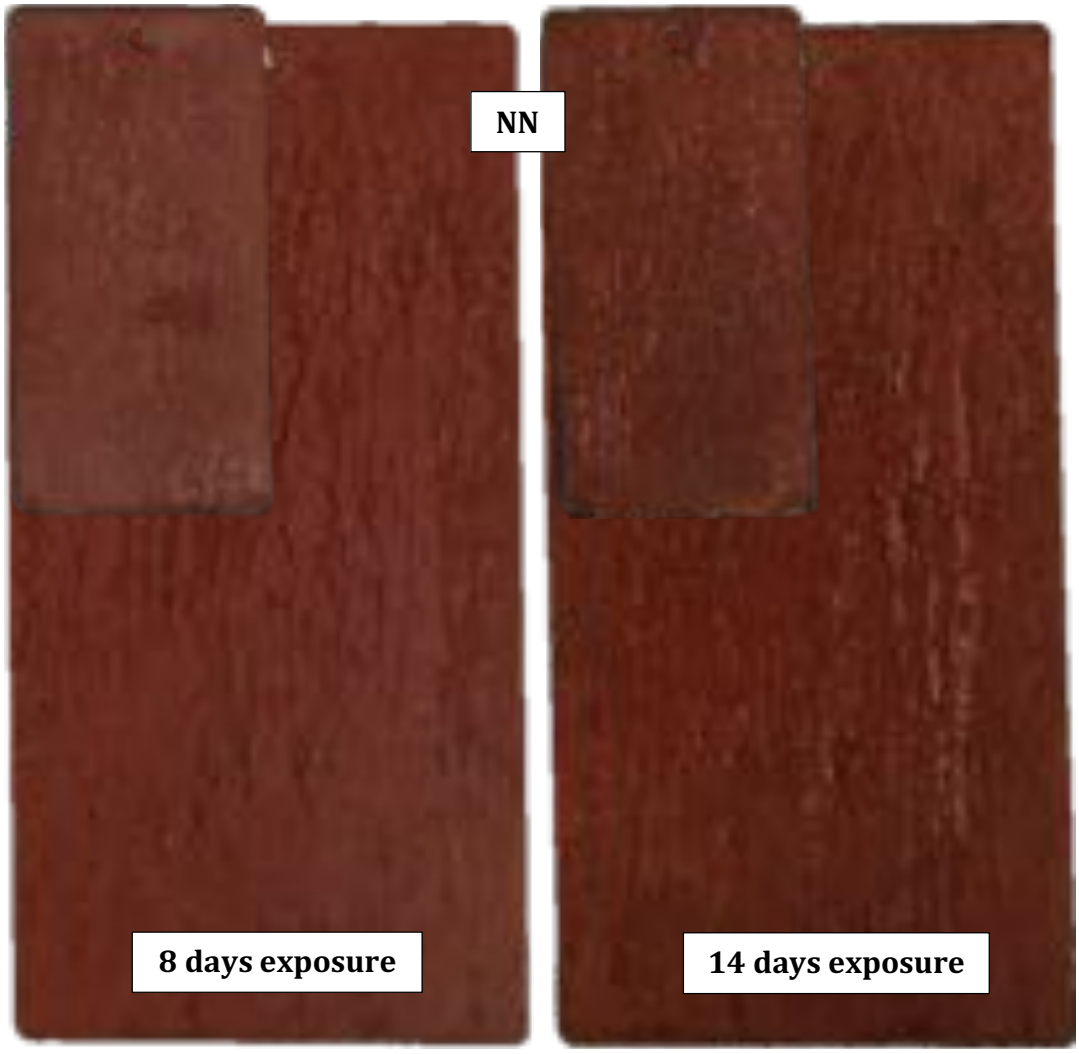

Figure 35: Samples with no salt contamination but no surface preparation (NN), a small sample on the top left corner of the larger one at exposure periods of 8 days (left) and 14 days (right).

Figure 35 shows an increase in deterioration on both samples from eight to 14 days exposure. Despite the whitish colour and possible *rust rashing* on the left image of the smaller sample (8 days exposure), there is more corrosion breakthrough on the larger sample, i.e. more rust formed underneath the coating damaged the coating and is seen on the surface.

Figure 36 below shows two SM samples of different sizes at 8 and 14 days of exposure. The dry film thicknesses of the coating are 62 µm and 64 µm for the large and small samples respectively.

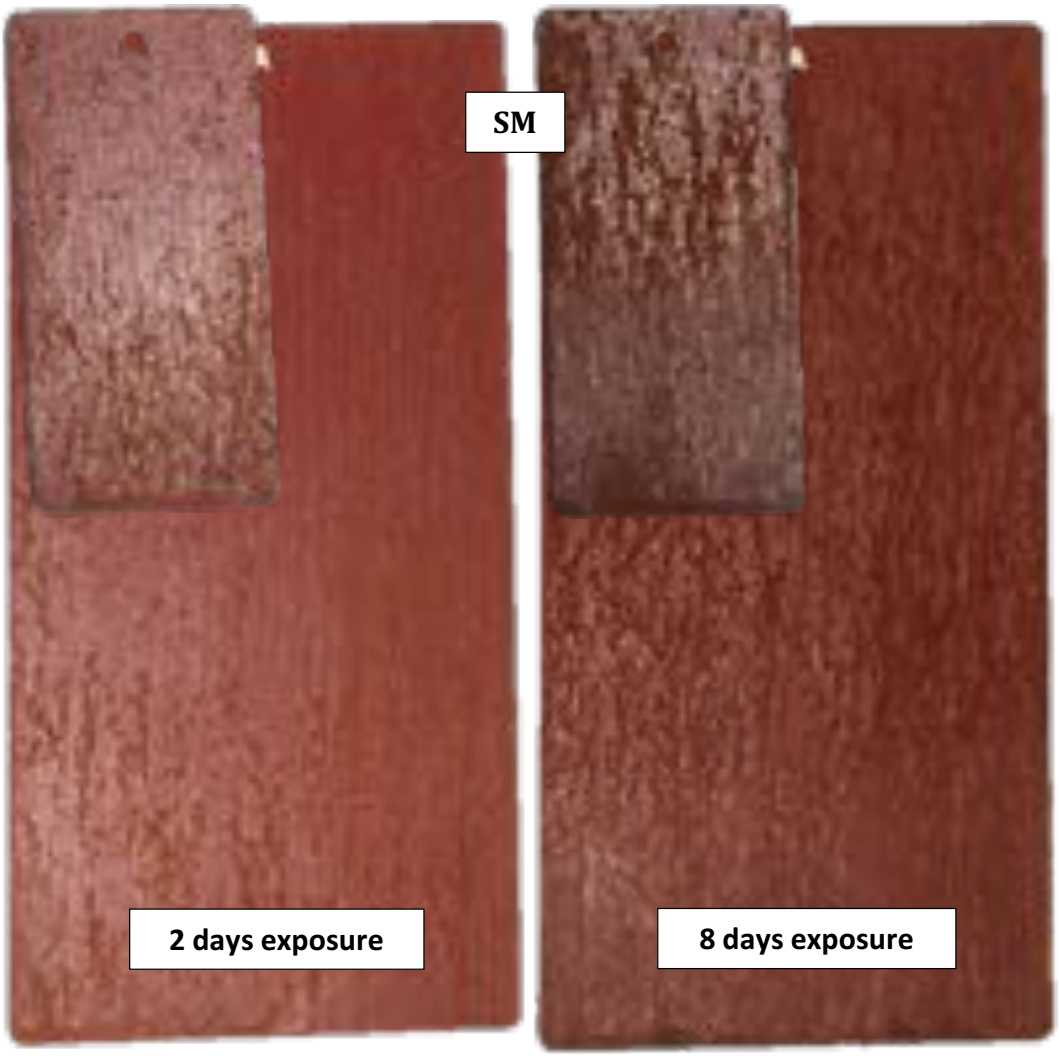

Figure 36: Samples with salt contamination but with mechanical surface preparation (SM), a small sample on the top left corner of a larger one at exposure periods of 2 days (left) and 8 days (right).

Figure 36 shows an increase in coating deterioration on both samples from 2 to 8 days of exposure. The breakthrough is concentrated on the bottom half of the samples as seen on the left image (2 days exposure). However, there is no clear distinction in the level of degradation between the two plate sizes.

Figure 37 below shows two SN samples of different sizes at two and eight days of exposure. The dry film thicknesses of the coating are 69 µm and 67 µm for the large and small samples respectively.

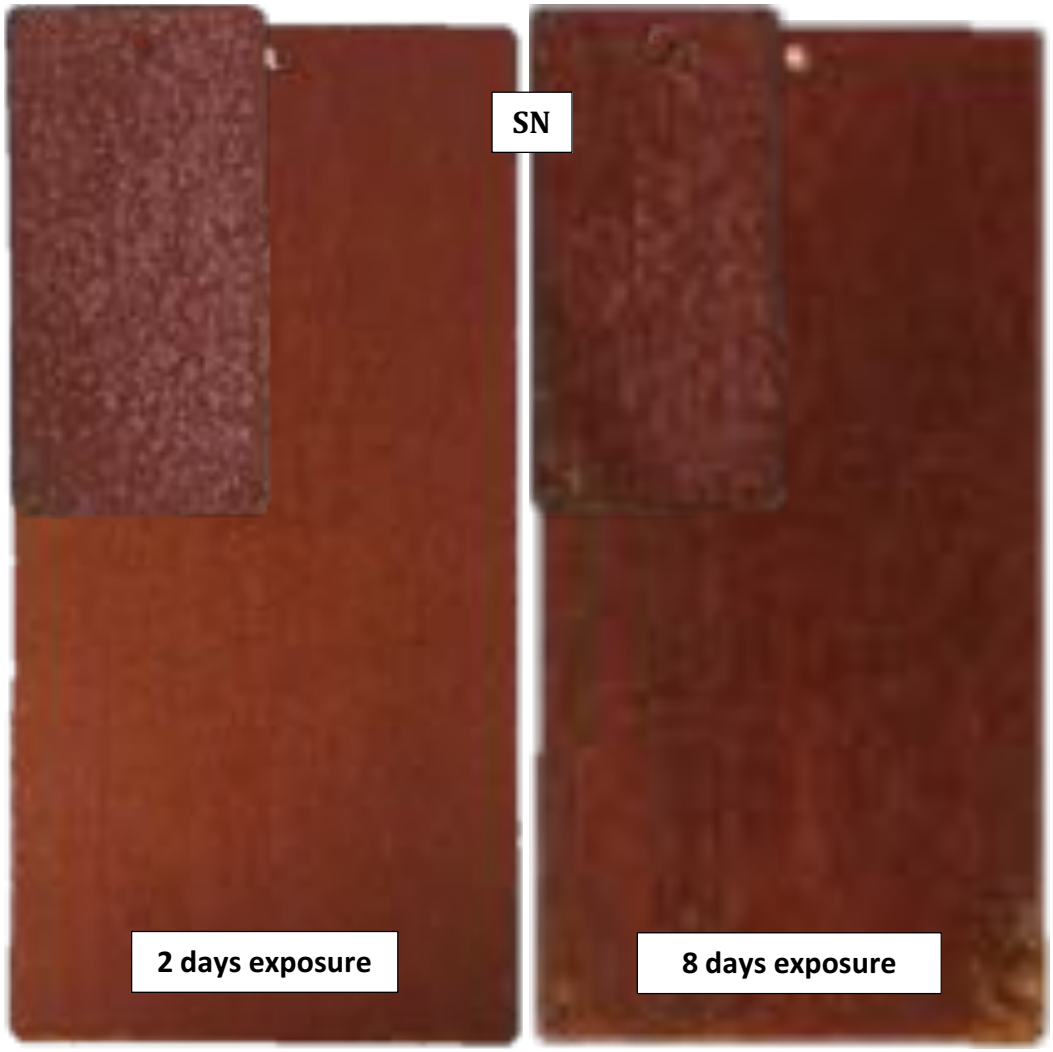

Figure 37: Samples with salt contamination and no surface preparation (SN), a small sample on the top left corner of a larger one at exposure periods of 2 days (left) and 8 days (right).

Figure 37 shows that at 2 days exposure the coating has failed with the entire surface of the larger sample covered in rust rashing. At 8 days exposure, the coating has undergone severe damage. On the other hand, the smaller sample shows only progressive damage (damage got worse with time) of the coating without clear *rust rashing* at either two or eight days exposure.

5.3. Coating Performance Based on Visual Inspection

5.3.1. Visual Condition of the Samples at Transition Time

Figures 38 to 47 below show the samples used for the visual evaluation of the coating performance for all surface conditions tested. Due to the variation in the level of degradation for sample plates within a set that underwent identical pre-treatment, the plates shown are those that are most representative of the degradation visible within that surface condition set. Furthermore, Figures 43 to 47 show the samples used for EIS measurement that reached the transition to corrosion during the EIS measurement. In addition, the photographs for analysis, regarding the type and percentage failure (see Sections 5.3.2 and 5.3.3), are highlighted with blue borderline and one or two adjacent pictures are shown for clarity.

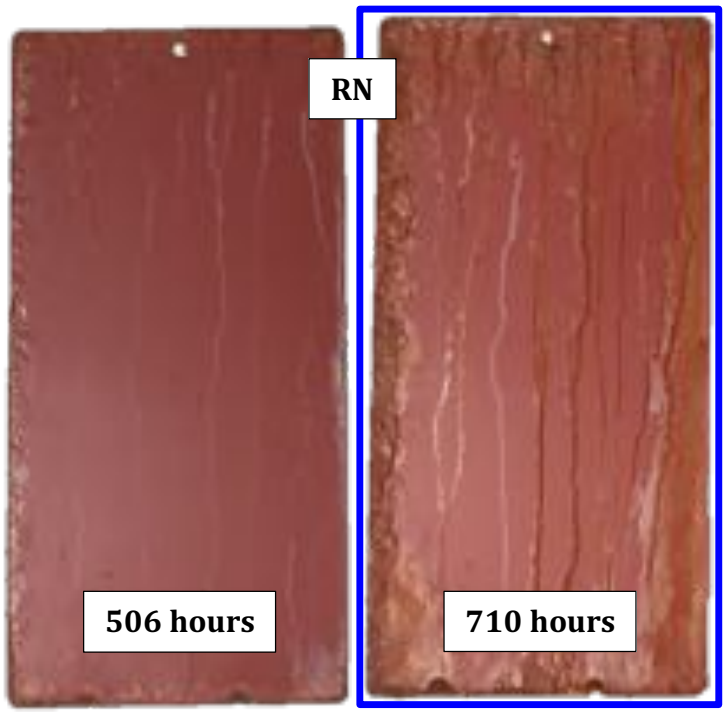

Figure 38: A reference new sample (RN) at 506 and 710 hours of exposure (from left to right)

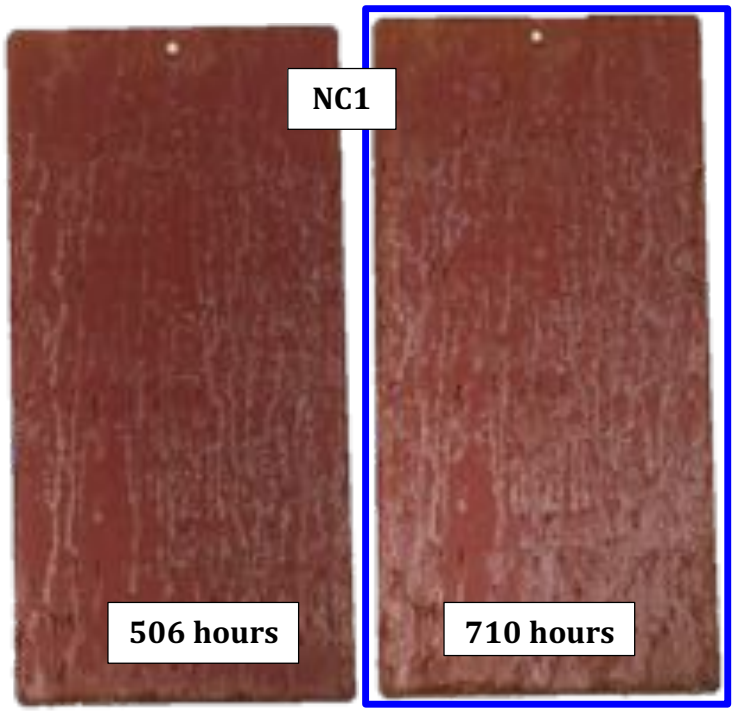

Figure 39: An NC1 sample at 506 and 710 hours of exposure (from left to right)

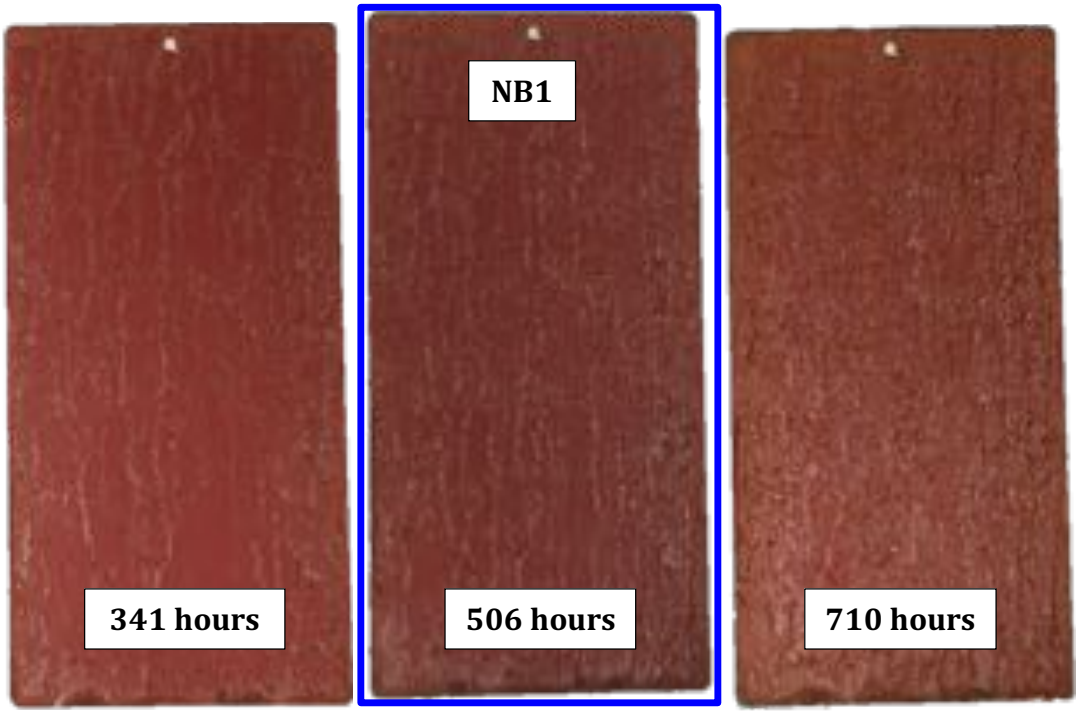

Figure 40: An NB1 sample at 341, 506 and 710 hours of exposure (from left to right)

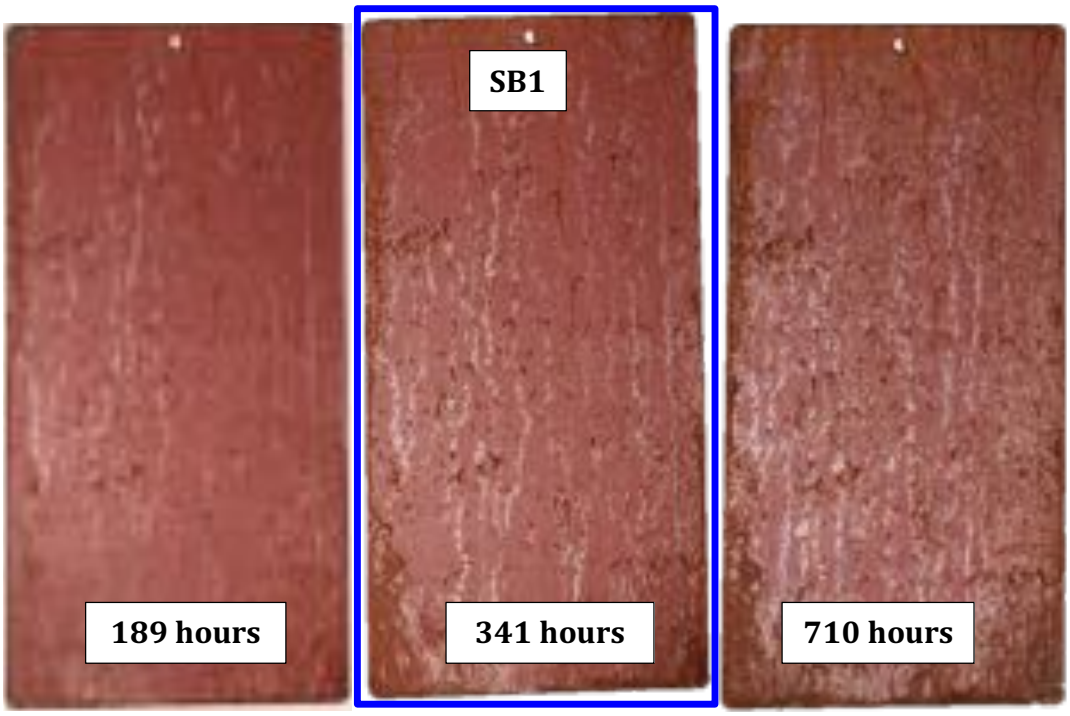

Figure 41: An SB1 sample at 189, 341 and 710 hours of exposure (from left to right)

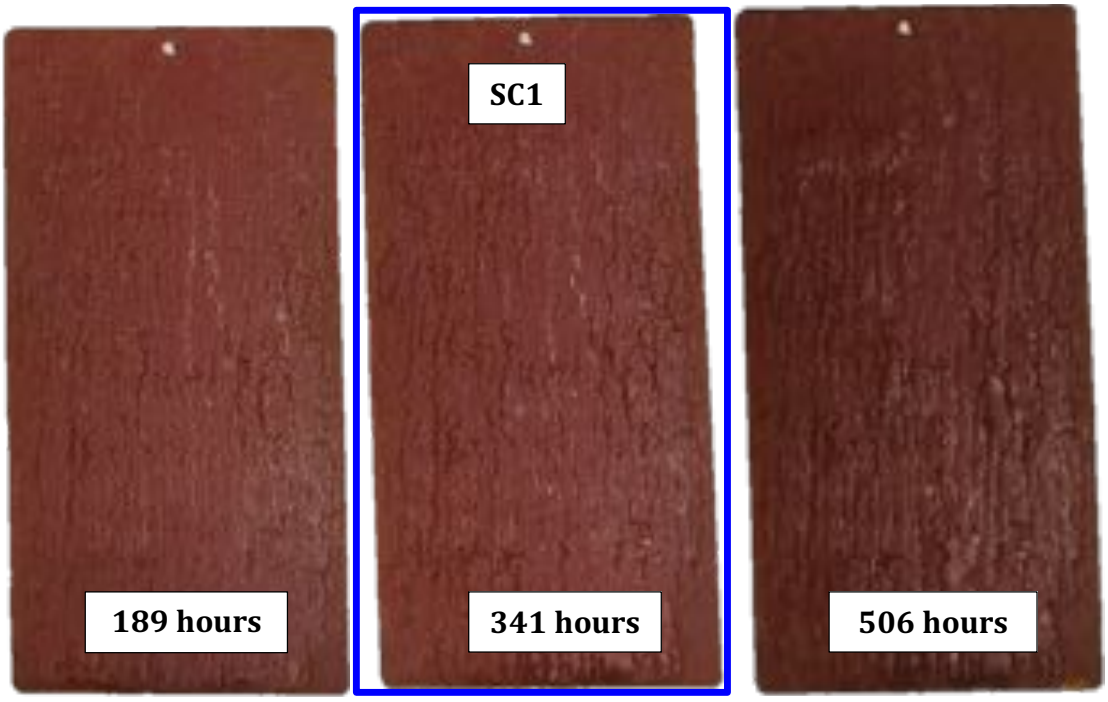

Figure 42: An SC1 sample at 189, 341 and 506 hours of exposure (from left to right)

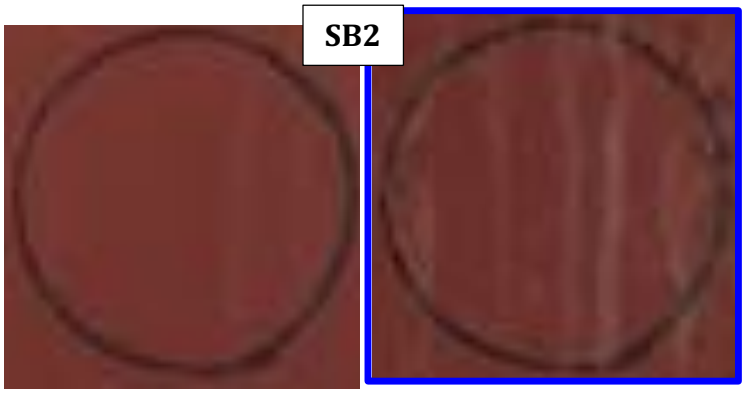

Figure 43: Failure of an SB2 sample at 68 (left) and 136 (right) hours of CCT1 exposure

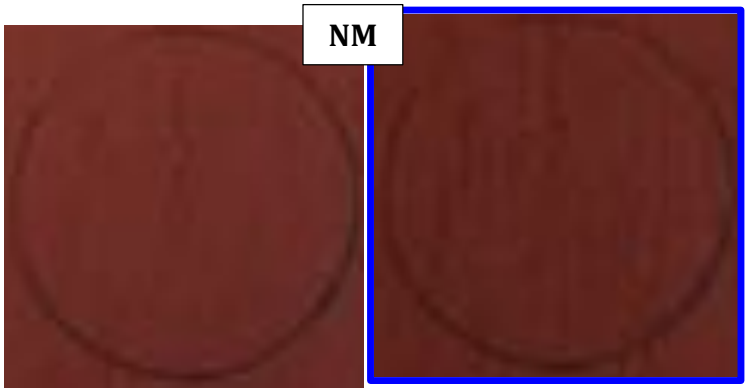

Figure 44: Failure of a NM sample at 68 (left) and 136 (right) hours of CCT1 exposure

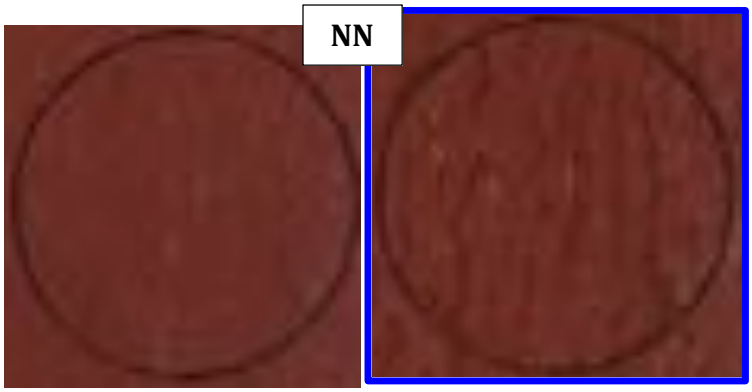

Figure 45: Failure of an NN sample at 68 (left) and 136 (right) hours of CCT1 exposure

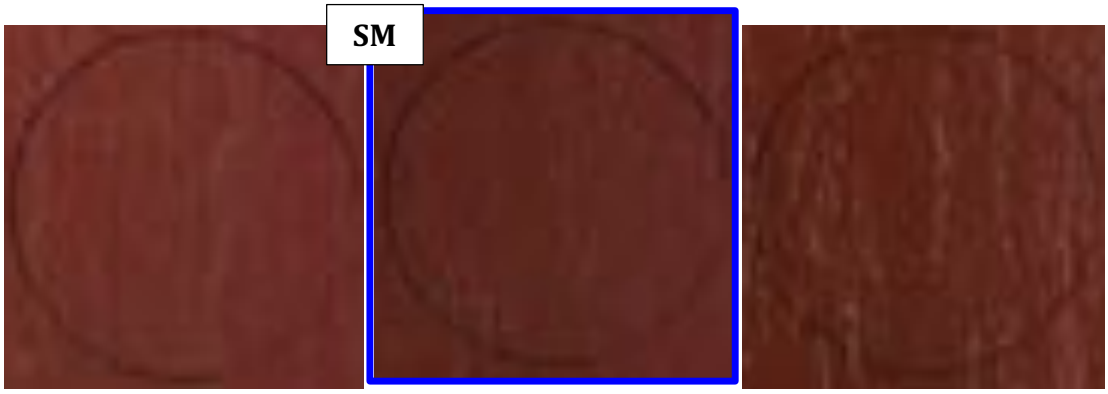

Figure 46: Failure of an SM sample at 34 (left), 68 (middle) and 136 (right) hours of CCT1 exposure

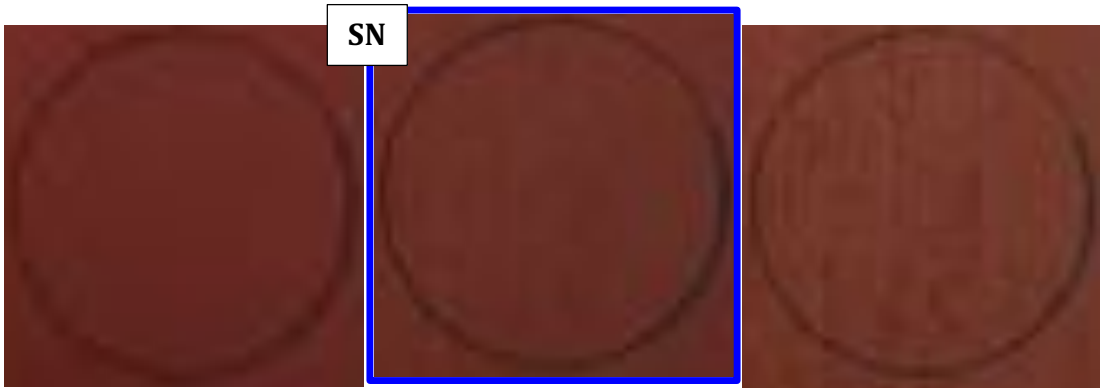

Figure 47: Failure of an SN sample at 17, 34 and 68 hours of CCT1 exposure (from left to right).

5.3.2. Types of Failure Observed on the Samples

5.3.2 (a) Failures on RN Samples

The corrosion attack on the reference new samples was mainly on the edges of the plates (Figure 38). Thus, the water runoff from the damaged edges stained the sound coating. For that reason, *rust staining* is predominantly observed (right image of Figure 38). The attack on the edges of the sample plates gradually moved inwards as *blistering*.

5.3.2 (b) Failures on NC1 Samples

The individual spots on NC1 plates where corrosion breakthrough occurred were mostly elongated (Figure 39). This may lead to the incorrect assignment of the failure modes involving cracking or crazing such as *checking* or *alligatoring*. However, the actual mode of failure is *rust spotting* with the spot density increasing in the direction of the water runoff.

5.3.2 (c) Failures on NB1 Samples

Figure 40 shows that NB1 samples experienced *rust spotting*. However, the increasing roughness observed on the middle and right-hand images indicates coating disbondment resulting from corrosion under the coating. The NB1 plates developed both *rust spotting* and some *undercutting*.

5.3.2 (d) Failures on SB1 Samples

The corrosion failure of SB1 samples was manifested as *rust spotting* (Figure 41). The development of rust spots on SB1 was over a much shorter exposure period than NC1.

5.3.2 (e) Failures on SC1 Samples

The degree of coating uplift on SC1 samples in the right-hand image of Figure 42 is a clear indication of delamination from *undercutting* failure. It is interesting to note that despite the high degradation level observed, there is negligible amount of corrosion product on the surface of the coating.

5.3.2 (f) Failures on SB2 Samples

The distinct corrosion sites on the surface of SB2 samples (Figure 43) clearly show that the failure on SB2 samples appears as *rust spotting*.

5.3.2 (g) Failures on NM Samples

The type of failure on NM samples (Figure 44) is considered to be *rust rashing* where the corrosion sites are on the pathways of water runoff. The black spot just above the centre of the testing area (right image of Figure 44) could be considered *cissing*, although the spot did not occur while the coating was still completely wet.

5.3.2 (h) Failures on NN Samples

The failure on the NN sample has also occurred on the vertical pathways of the water runoff (Figure 45). This was classified as *rust spotting* because there is actual breakdown of the coating. Some rust rashing was observed during the previous inspection (left image of Figure 45) but in negligible amounts.

5.3.2 (i) Failures on SM Samples

Figure 46 shows three distinct stages on the failure of the SM sample. Firstly, on the left image, *rust staining*, secondly on the middle image, a mixture of *rust rashing* and *rust spotting* and finally, on the right image, further degradation of these failure modes.

5.3.2 (j) Failures on SN Samples

On Figure 47 above for the SN samples, it is clearer on the third image (68h) that *rust rashing* is the type of failure present if compared with the first image (17h), since the colour similarity between the coating and the corrosion product can be misleading.

5.3.3. Estimated Percentage Failure on Transition Period

To determine the coating failure of the samples, some tolerance is required since the degradation happens gradually and on the first signs of deterioration it may not be considered as failed coating depending on the predefined criteria. For that reason, based on the criteria predefined for this work (Section 4.4, page 27), the percentage failure of the different samples is:

- 0% to 25% of blistering from the edges for RN samples at 710 hours of exposure: Since the failure is still very close to the edges and *rust staining* is not included in quantifying coating degradation, the failure percentage is closer to 0% (see Figure 38).
- 0% to 25% of *rust spotting* on NC1 samples at 710 hours of exposure: The quantification included rust spots near the edges because they did not result from damaged edges (see Figure 39). Hence, the percentage failure was estimated to be closer to 25%.
- 25% to 50% of *rust spotting* and *undercutting* on NB1 samples at 506 hours of exposure: Although looking at how much rust has surfaced (through *rust spotting*) the damage may seem minimal; but by taking *undercutting* into account the failure is estimated closer to 50% (see Figure 40).
- 0% to 25% of *rust spotting* on SB1 samples at 341 hours of exposure (see Figure 41): Corroded sites adjacent to the edges were excluded since they may have been influenced by the corrosion of the edges, yet the estimated failure is closer to 25%.
- 50% to 75% of *undercutting* on SC1 samples at 341 hours of exposure (see Figure 42): Due to the failure being underneath the coating arising from *undercutting* and judging by the change in surface roughness it is estimated that the failure is closer to 50%.
- 0% to 25% of *rust spotting* on SB2 samples at 136 hours of exposure (see Figure 43): There is a clear transition here since the photographs go from a

perfect coating (left hand side) to a coating with *rust spotting* (right hand side). However, it is estimated closer to 0%.

- 25% to 50% of *rust rashing* on NM samples at 136 hours of exposure (see Figure 44): based on the number of pathways for water runoff, this failure estimated to be closer to 25%.
- 25% to 50% of *rust spotting* on NN samples at 136 hours of exposure (see Figure 45): Combining the pathways of water runoff observed with the severity of rust, the failure can be estimated closer to 50%.
- 25% to 50% of *rust rashing* and rust spotting on SM samples at 68 hours of exposure (see Figure 46): Judging by how much coating is still undamaged, the failure is estimated closer to 50%.
- 25% to 50% of *rust rashing* on SN samples at 34 hours of exposure: Based on the amount of rust on the top of the coating and the difficulty in distinguishing between *rust stain* and the coating the estimation of damage is difficult (see Figure 47). However, considering how widely spread on the surface it is, the failure is estimated closer to 50%.

5.3.4. Determining Transition Time to Corrosion

The transition time to corrosion can be calculated using the expression on Equation 1 (page 28). Table 3 below shows the calculated transition time to corrosion and the parameters used in these calculations, namely time of inspection (t_n), time of previous inspection (t_{n-1}), duration of last exposure to the fog chamber ($t_n - t_{n-1}$) and recorded percentage failure (f_p).

Table 3: Transition time to corrosion and the parameters used for the calculations

Sample	Exposure Time (hours)			Percentage Failure (%)	Time to Corrosion (h)
Code	t_{n-1}	t_n	$t_n - t_{n-1}$	f_p	t_{corr}
RN	506	710	204	0	710
NC1	506	710	204	25	659
NB1	341	506	165	50	424
SB1	189	341	152	25	303
SC1	189	341	152	50	265
SB2	68	136	68	0	136
NM	68	136	68	25	119
NN	68	136	68	50	102
SM	34	68	34	50	51
SN	17	34	17	50	26

Figure 48 below shows a graphical representation of the transition time to corrosion of the samples with different surface pre-treatments in order of performance.

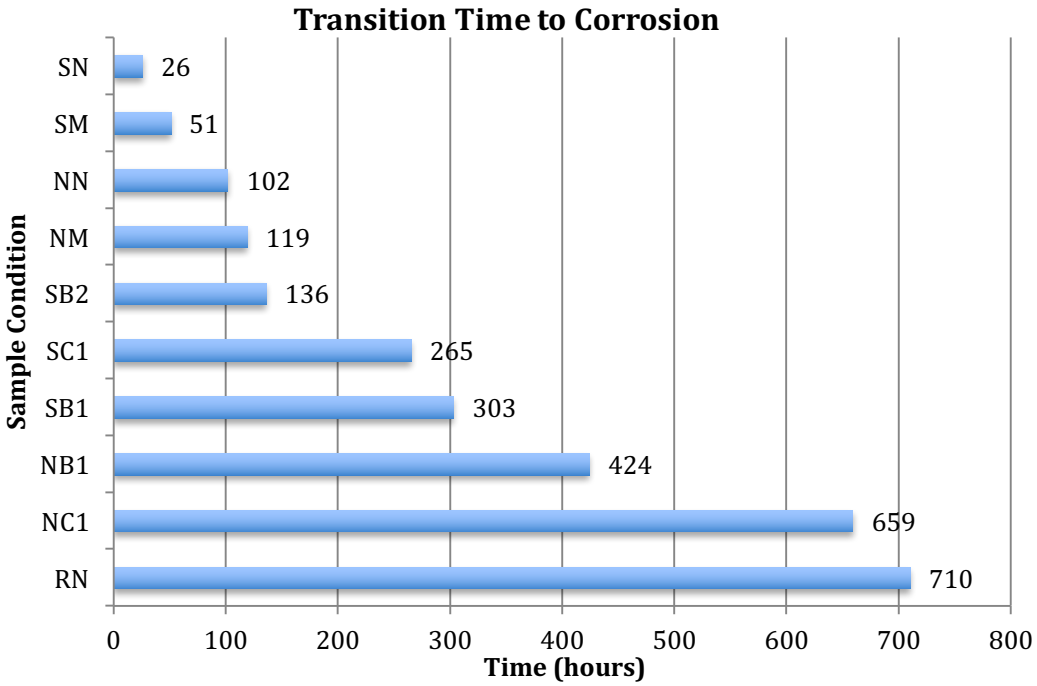

Figure 48: Transition time to corrosion for the different pre-treatment

This order of performance is derived from the test work in this study and is based on actual corrosion recorded on the surface of the coated test plates after various surface preparations and exposure times.

5.4. Dry Film Thickness Results

Numerous factors affect the performance of organic coating on steel substrates, which can offer a number of variables to be considered in the study of coating performance. Thus, an effort was made to keep the coating thicknesses constant in order to study other variables. Nevertheless, due to the application method and the difference in surface roughness among the various surface conditions studied (including salt contamination, corrosion product and converted corrosion product underneath the coatings), there are still some variations in coating thicknesses on each sample plate and from sample to sample within a set. Table 4 shows the average dry film thicknesses per surface condition and the respective standard deviations (SD).

Table 4: Average dry film thickness and respective standard deviation (SD) for each pre-treatment studied

Pre-treatment	Dry Film Thickness (DFT) of Samples (µm)					
	Visually Inspected		EIS Tested		Pull-Off Tested	
Code	Average	SD	Average	SD	Average	SD
RN	66.7	4.93	74.3	15.28	59.9	8.91
NC1	68.3	5.03	70.7	11.06	87.9	2.21
NB1	77.3	3.79	83.3	2.08	50.9	13.01
SB1	69.3	2.52	77.7	18.15	76.5	1.53
SC1	68.0	3.61	71.7	5.69	60.2	1.60
SB2	76.0	1.00	77.0	7.00	59.0	10.16
NM	61.3	1.15	67.7	6.11	46.0	0.35
NN	69.0	5.57	69.7	5.03	47.6	0.58
SM	67.3	5.03	68.0	4.58	60.3	17.64
SN	67.3	5.69	70.0	8.19	114.1	2.62

For better visualization, the values on Table 4 above were represented on charts as seen in the figures below.

5.4.1. Dry Film Thickness of Visually Inspected Samples

Figure 49 below shows the dry film thicknesses of the samples inspected visually. The different conditions are arranged in order of coating performance based on the visual inspection ranking.

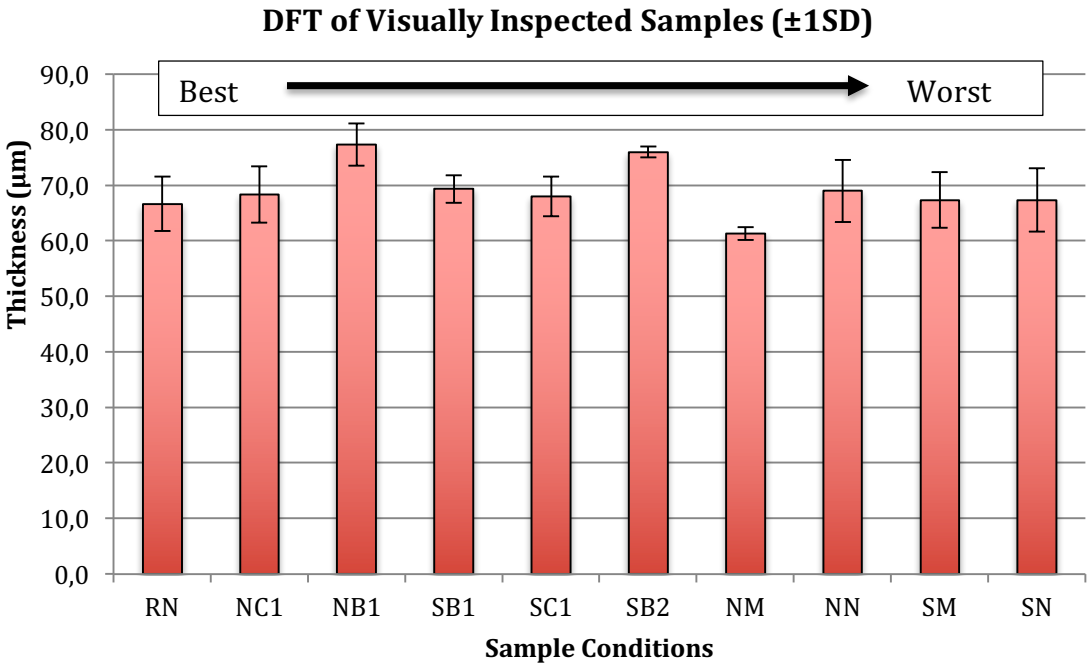

Figure 49: Dry film thickness (DFT) of visually inspected samples, in decreasing order of coating performance

It is seen from Figure 49 that there is some variation from one condition to another as well as from one sample to another within a set. However, there is no direct correlation between coating thickness and coating performance since there is neither decrease nor increase in thickness despite the decrease in performance from left to right.

The results on Figure 49 above address small thickness changes when constant thickness was attempted. However, for the effect of thickness on coating performance, other parameters were kept constant including pre-treatment. Figure 50 below show the thickness of two sets of NC1 samples that were coated to distinct dry film thicknesses.

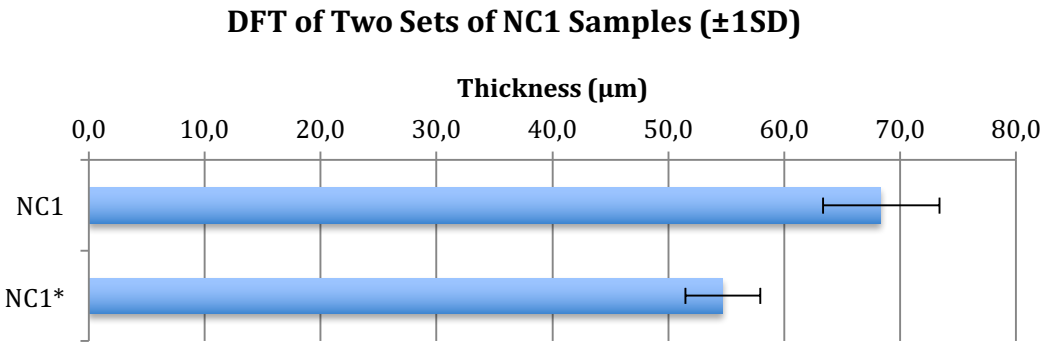

Figure 50: Dry film thickness (DFT) of two sets of NC1 samples

Figure 50 above shows clear distinction in thickness between the two sets of samples (NC1 and NC1*). Their coating performance can be evaluated from Figure 51 below.

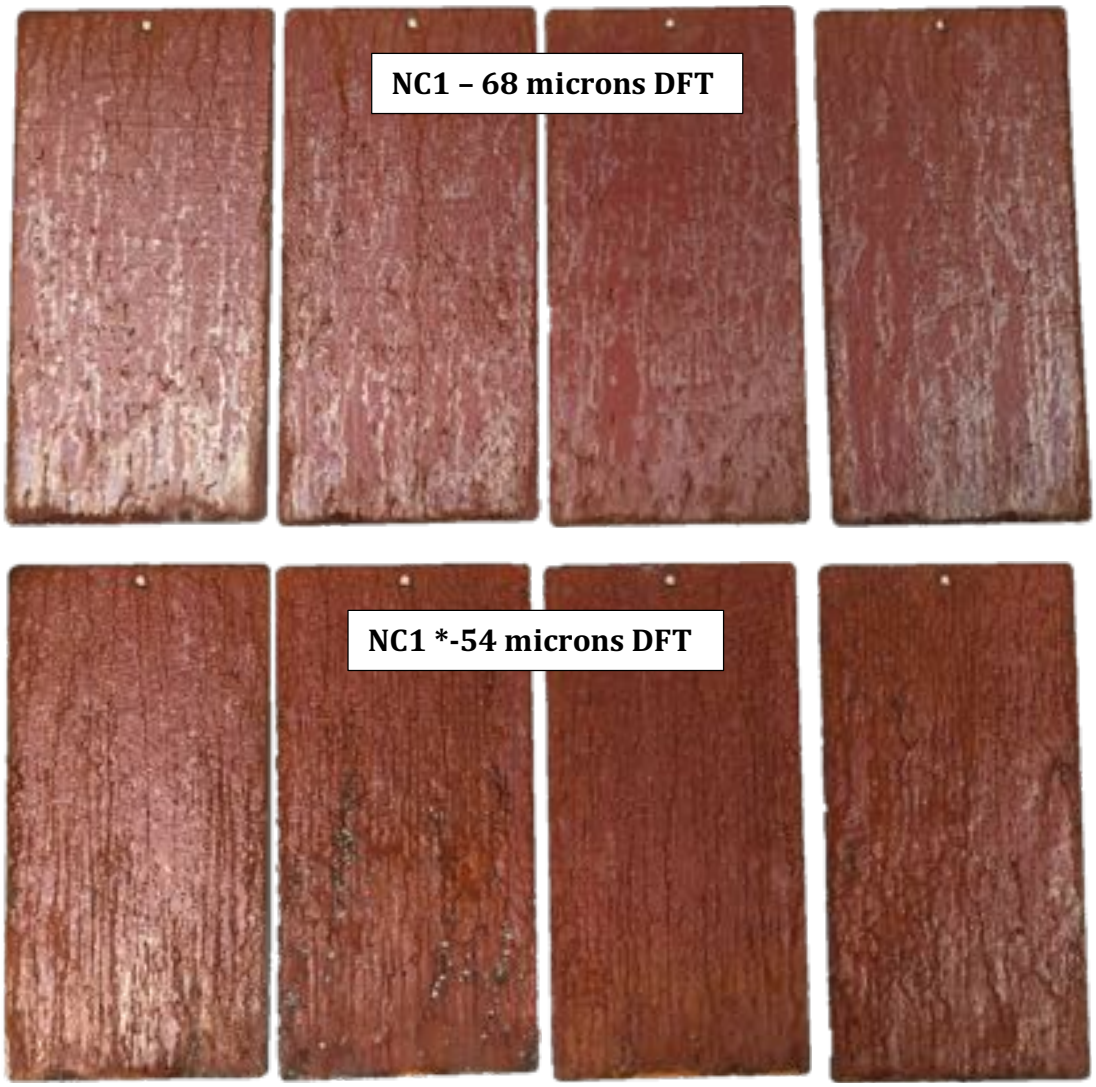

Figure 51: Performance of NC1 (top) and NC1* (bottom) samples at one month of exposure, with thick (68.3µm) and thin (54.7µm) dry film thicknesses respectively.

Figure 51 above shows both sets of NC1 samples. The thicker samples show about 25% coating failure and the thinner samples show highly damaged coatings. Therefore, if all other parameters are equal, coating performance decreases with decreasing dry film thickness.

5.4.2. Dry Film Thickness of EIS Tested samples

Despite being used for EIS testing, these samples are organized in order of decreasing coating performance as evaluated from visual inspection. Figure 52 below shows their dry film thicknesses (DFT).

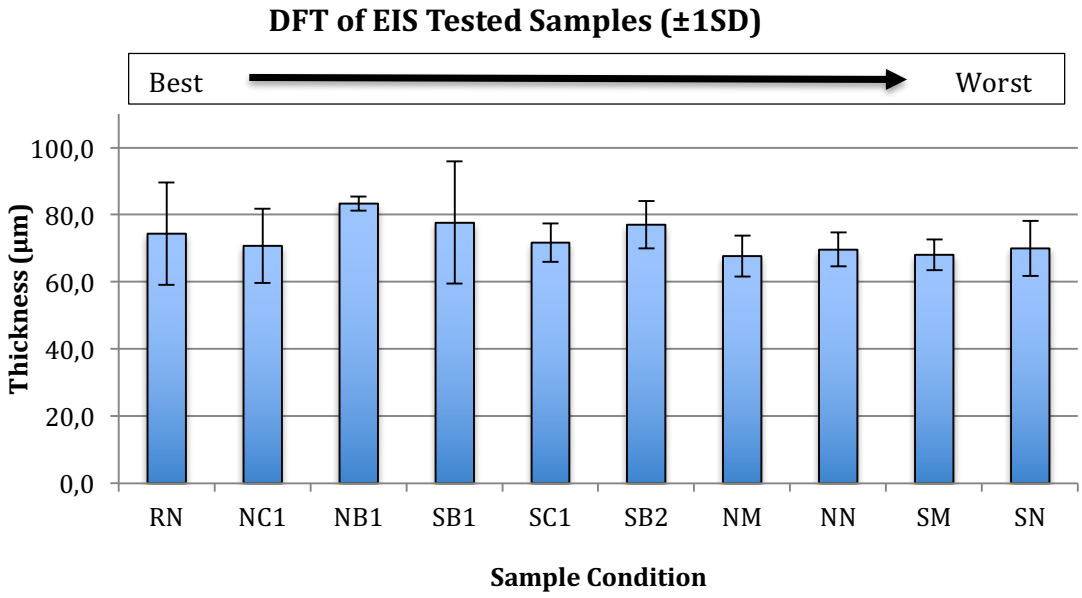

Figure 52: Dry film thickness of EIS tested samples, in decreasing order of coating performance

Figure 52 above shows that although the samples are organized in decreasing coating performance, the dry film thickness is neither in increasing nor decreasing order. Therefore, the variation on dry film thickness is too small to affect the coating performance.

5.4.3. Dry Film Thickness of Adhesion Pull-Off Tested samples

The direct correlation between dry film thickness and pull strength is presented in this section, but first the thickness of pull-off tested samples are presented with relation to the visual inspection performance. The samples used for adhesion pull-off testing in decreasing order of performance are presented on Figure 53 below.

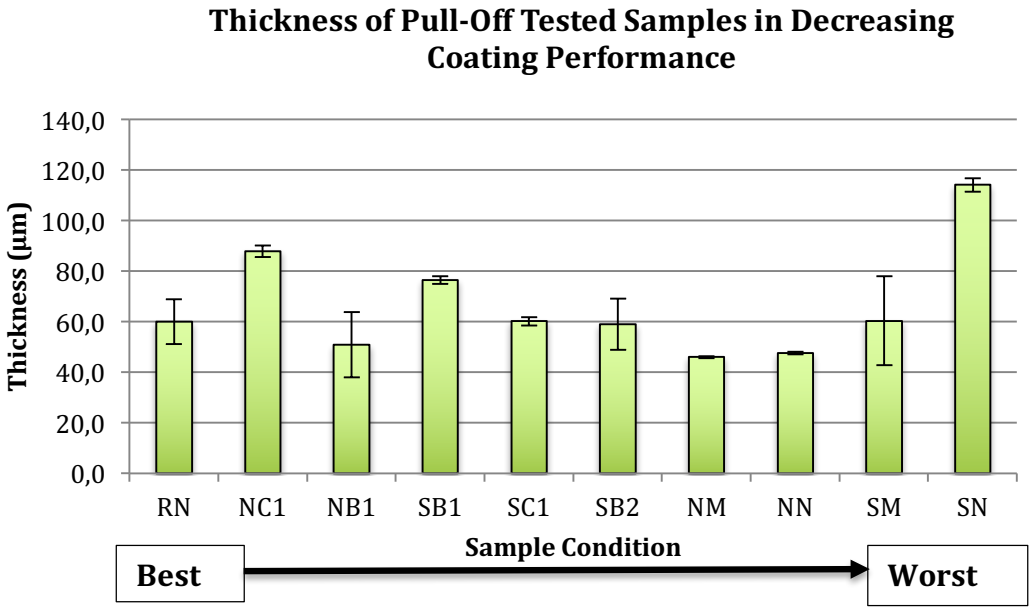

Figure 53: Dry film thickness of pull-off tested samples, in order of decreasing coating performance

Figure 53 above shows that coating performance and dry film thickness are not correlated, when the difference in DFT is the result of the coating application method used. In addition, these samples need to be compared in terms of adhesion performance since it is the property evaluated during pull-off testing. Hence, the same data are represented on Figure 54 below, but in decreasing order of pull strength.

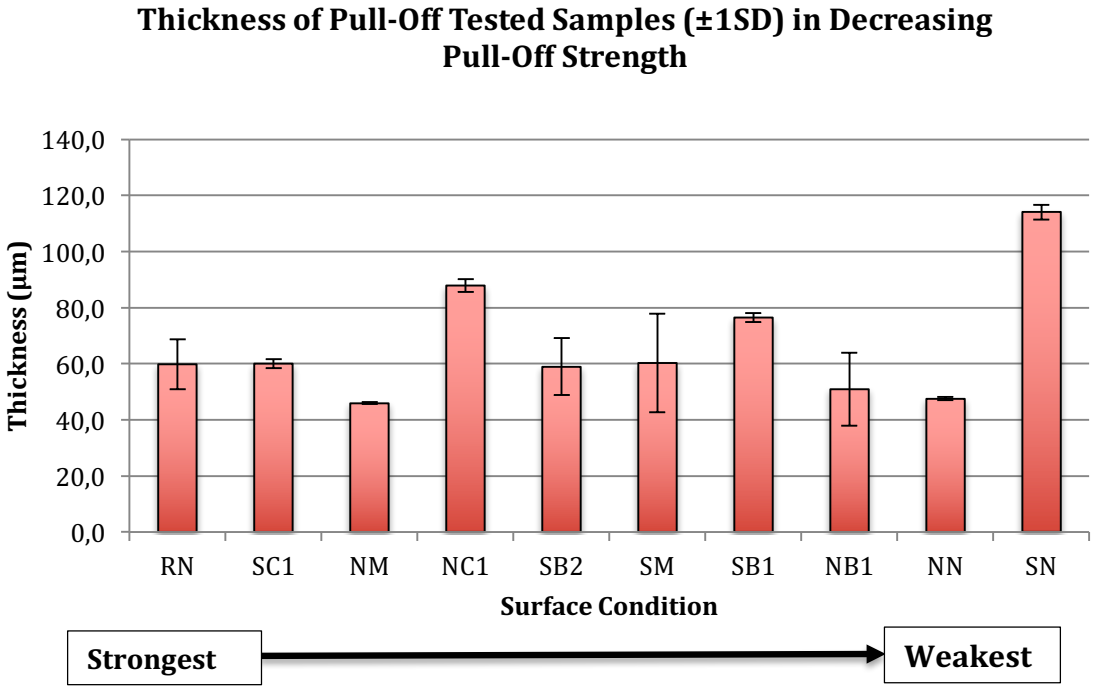

Figure 54: Dry film thickness of pull-off tested samples, in decreasing order of pull strength

From Figure 54 above, there is no clear correlation between dry film thickness and pull-off strength since RN, NC1 and SN as well as SB2 to SB1 show increasing DFT with decreasing pull strength while RN to NM and NB1 to NN show decreasing DFT with decreasing pull strength. The pull-off strength values will be presented later on Section 5.6.4 (page 78).

5.5. Salt Contamination Results

The salt contamination was measured with the Bresle method. The results obtained are presented on Table 5 below.

Table 5: Measured conductivity prior to coating application and equivalent NaCl content

Sample Condition	Conductivity (µS/cm)	NaCl (mg/m^2)	Standard Deviation (mg/m^2)
RN	–	–	–
NC1	130.2	143.2	2.30
NB1	123.6	136.0	27.63
SB1	360.0	396.0	105.22
SC1	538.0	591.8	196.37
SB2	68.2	75.0	12.58
NM	123.6	136.0	27.63
NN	130.2	143.2	2.30
SM	360.0	396.0	105.22
SN	538.0	591.8	196.37

Shown in Table 5 above, the equivalent NaCl content was determined as per IMO PSPC (see Section 4.7.2). Note that the salt measurement was performed before rust converter and rust remover application.

The reference new samples (RN) were not tested for salt contamination since they were not exposed to the fog chamber and degreasing was performed prior to coating application.

The surface conditions were arranged in order of performance and their corresponding salt content was plotted, hence the correlation between salt contamination and performance can easily be seen in Figure 55 below.

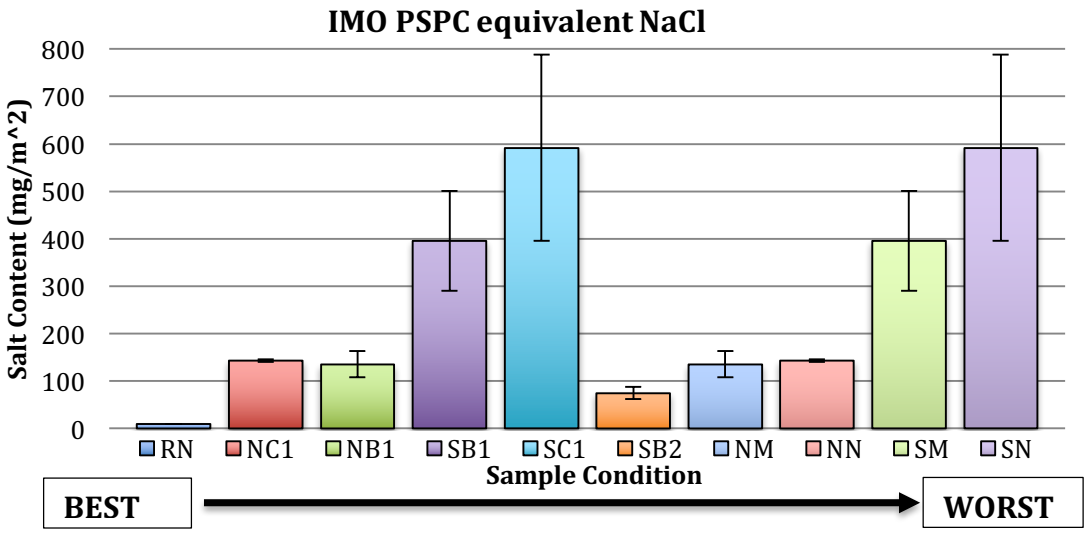

Figure 55: Change in salt contamination level with decreasing coating performance

From Figure 55 above, the best performing condition is the one with the least amount of salt contamination (RN) and the poorest performing one has the highest amount of salt contamination (SN). Despite the clear performance differences between samples treated with and without rust converter, it is safe to say that coating performance decreases with increasing salt contamination.

5.6. Pull-Off Test Results

The pull-off test performed on the coated plates involves applying a pull force perpendicular to the coating surface and measure the force required to detach the coating from the substrate. In the pull-off test to failure, it is important to not only record the force required to detach the coating from the substrate, but also to record the nature of the failure and the extent of the damage to different layers.

Three modes of failure were observed on the tests performed:

i. Adhesive Failure: disbondment at the interface between two layers.
ii. Cohesive Failure: rupture within a layer.
iii. Mixed Mode of Failure: a mixture of both modes of failure in more than one layer and/or interface.

5.6.1. Samples with Adhesive Failure

Figure 56 shows a schematic of adhesive failure between substrate and coating, and between the adhesive and the dolly.

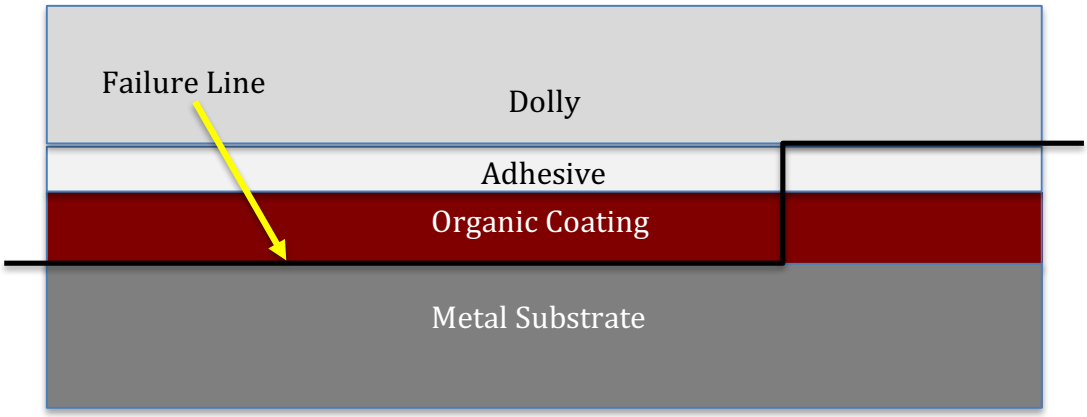

Figure 56: Schematic of adhesive failure in two interfaces.

The schematic on Figure 56 above shows the case where adhesive failure occurs at two different interfaces on a single testing site, which is not always the case, as it will be shown later on.

Adhesive failure is the main mode of failure observed on RN samples, but there is a slight indication of small amount of cohesive failure too, as seen in Figure 57 below.

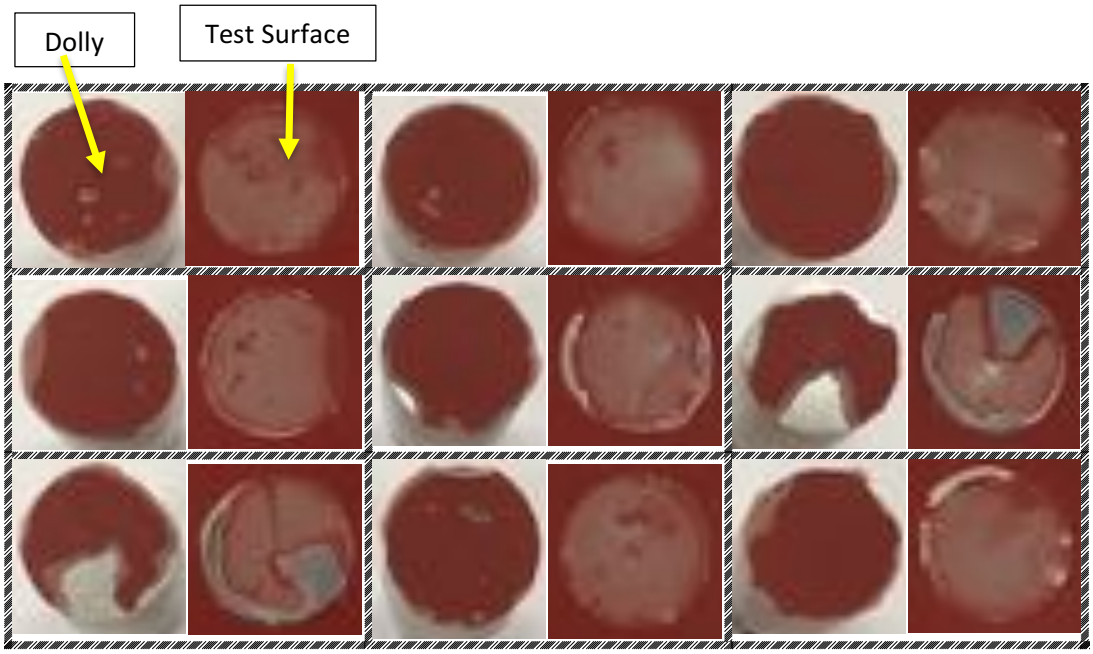

Figure 57: All RN samples test sites showed adhesive failure as the main mode of failure, each row is a sample, and the dollies are on the left of the corresponding test sites.

The test sites in Figure 57 above show the failure modes from the pull-off test to failure of RN samples. The dark red colour on the dolly face and the visible substrate on the sample test site demonstrate substrate/coating adhesive failure, while the grey on the sample test site and the bare metal on the dolly face show failure of the adhesive attaching the dolly to the coating. In addition, on some substrate/coating adhesive failures there are darker red spots on the substrate, which is coating cohesive failure when the corresponding location on the dolly is also red. Finally, the observed failure is adhesive failure on the coating/adhesive interface when the corresponding location on the dolly is grey. The visually estimated adhesive failure percentages are presented on Table 6 below.

Table 6: Table of adhesion failures layers and percentages

Test Site	Layers	%	Layers	%	Other %
RN-7.1	Substrate & Coating	97	Adhesive & Dolly	1	2
RN-7.2	Substrate & Coating	98	Adhesive & Dolly	1	1
RN-7.3	Substrate & Coating	99	Adhesive & Dolly	1	0
RN-10.1	Substrate & Coating	98	Adhesive & Dolly	1	1
RN-10.2	Substrate & Coating	98	Adhesive & Dolly	1	1
RN-10.3	Substrate & Coating	74	Adhesive & Dolly	25	1
RN-15.1	Substrate & Coating	75	Adhesive & Dolly	23	2
RN-15.2	Substrate & Coating	98	Adhesive & Dolly	1	1
RN-15.3	Substrate & Coating	98	Adhesive & Dolly	1	1

The category marked “Other”, on Table 6 , includes glue failure (adhesive failure on the coating-to-adhesive interface) and cohesive failure. Test site coding in Table 6 is as follows: RN-15.2 = Plate Treatment Code letters – Plate number in the set - location number on plate where pull-off test was performed.

5.6.2. Samples with Cohesive Failure

Cohesive failure is represented in the diagram in Figure 58, which shows cohesive failure in the pre-treatment layer (rust or converted rust).

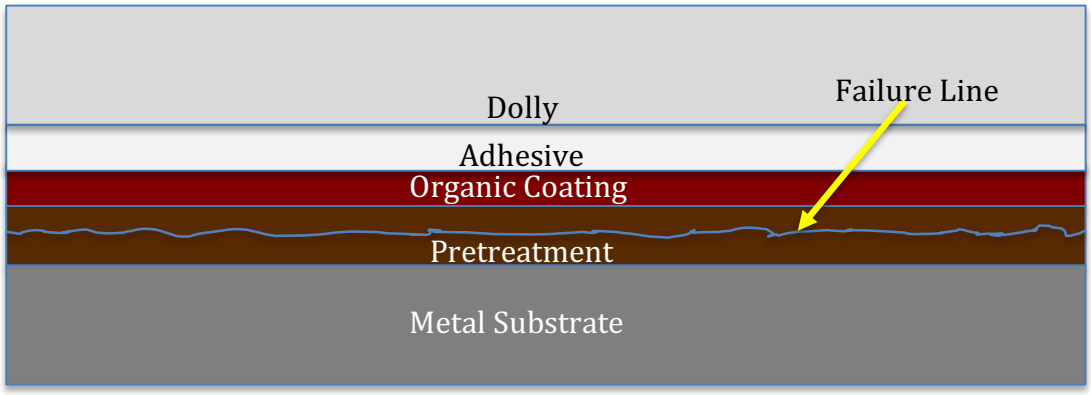

Figure 58: Schematic of cohesive failure in the pre-treatment.

Figure 58 above shows failure entirely on the pre-treatment (rust or converted rust). Most coated test plates in this research underwent this type of failure as seen on the pictures below (Figures 59 to 64).

Figure 59: All NC1 samples test sites showed cohesive failure in the converted corrosion product underneath the coating, each row is a sample, and the dollies are on the left of the corresponding test sites.

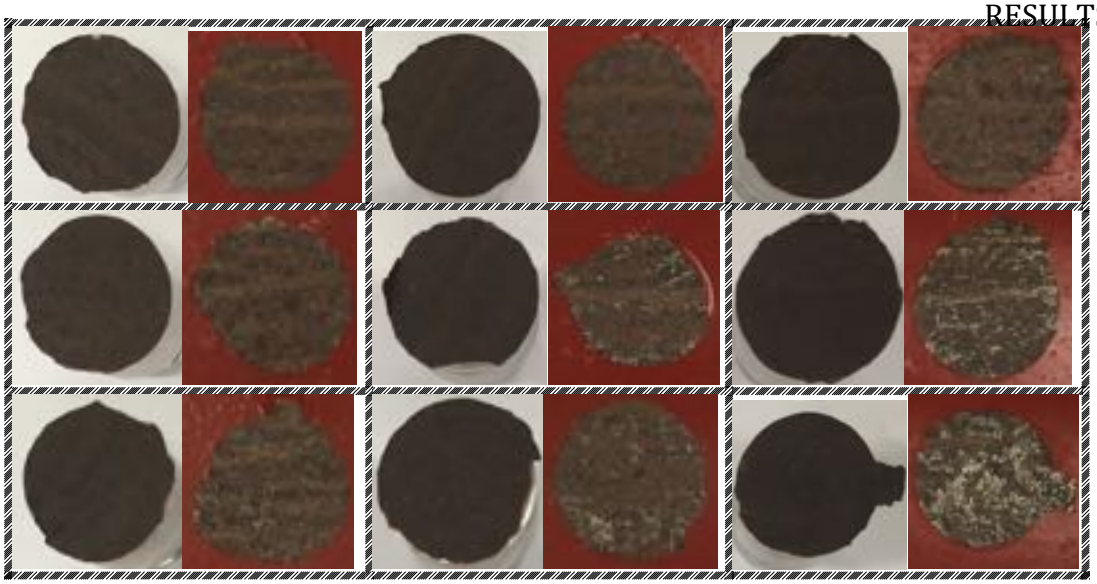

Figure 60: All NB1 samples test sites showed cohesive failure in the converted corrosion product underneath the coating, each row is a sample, and the dollies are on the left of the corresponding test sites.

Figure 61: All SB1 samples test sites showed cohesive failure in the converted corrosion product underneath the coating, each row is a sample, and the dollies are on the left of the corresponding test sites.

Figure 62: All SC1 samples test sites showed cohesive failure in the converted corrosion product underneath the coating, each row is a sample, and the dollies are on the left of the corresponding test sites.

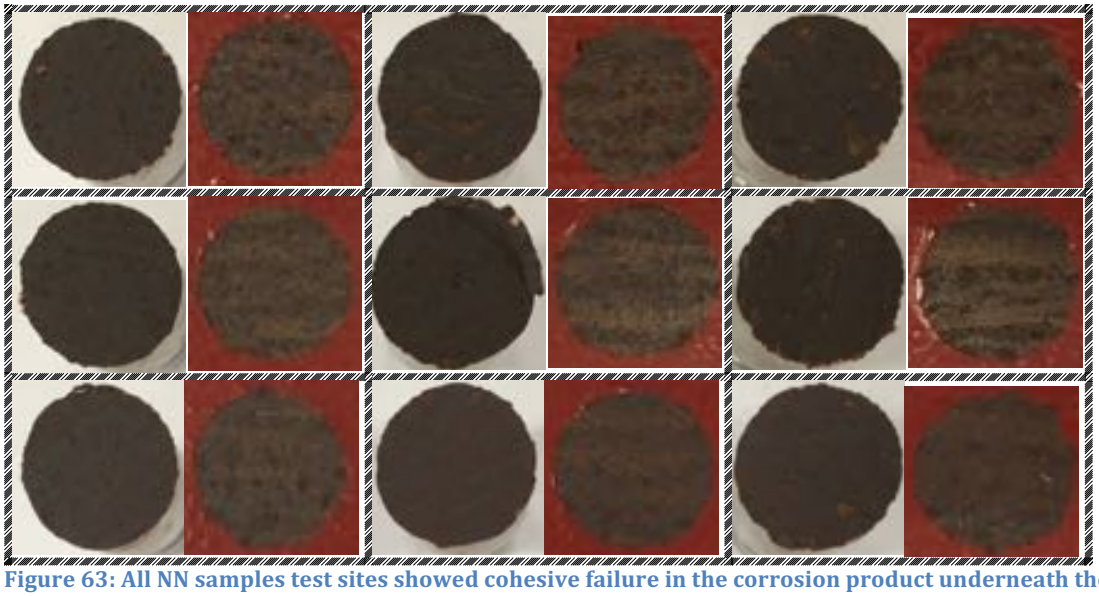

Figure 63: All NN samples test sites showed cohesive failure in the corrosion product underneath the coating, each row is a sample, and the dollies are on the left of the corresponding test sites.

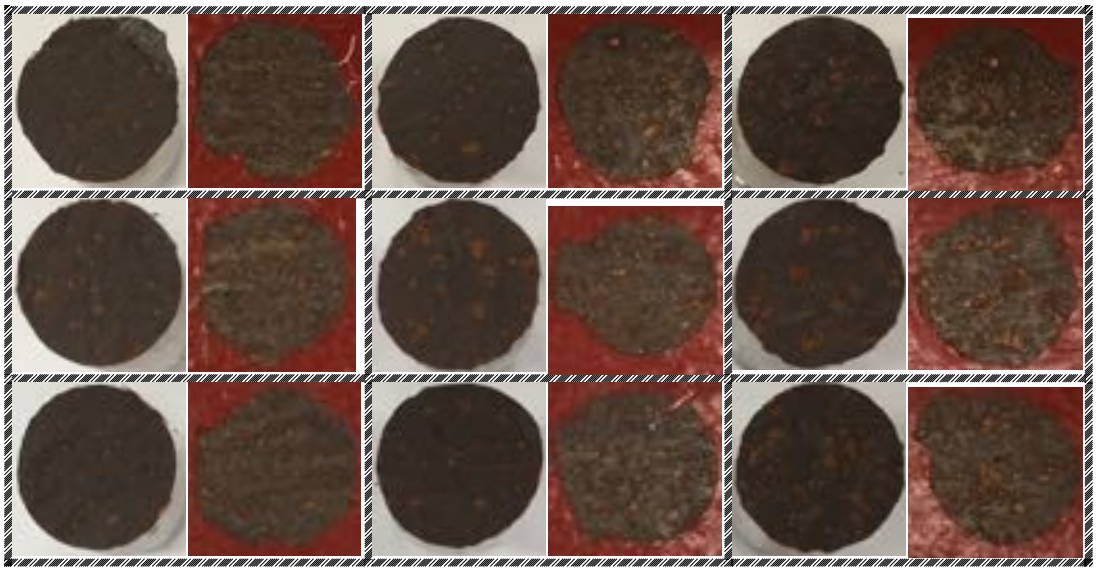

Figure 64: All SN samples test sites showed cohesive failure in the corrosion product underneath the coating, each row is a sample, and the dollies are on the left of the corresponding test sites.

Figures 59 to 62 show samples pre-treated with rust converter (NC1, NB1, SB1 and SC1) and these samples underwent 100% cohesive failure in the converted compound. Figures 63 and 64 show samples on which no rust removal was carried out (NN and SN) and these samples underwent 100% cohesive failure in the rust layer.

5.6.3. Samples with Mixed Failure Modes

Some test samples exhibited both cohesive and adhesive failure. The schematic in Figure 65 illustrates cohesive failure in the corrosion product layer very close to the rust-to-coating interface resulting in quite a few spots of rust-to-coating adhesive failure.

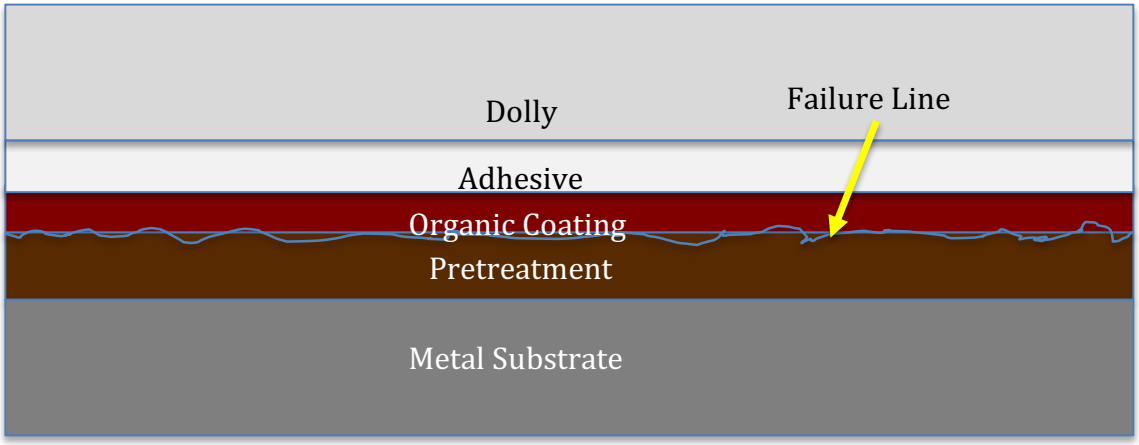

Figure 65: Schematic of cohesive failure in the pre-treatment with some rust/coating adhesive failure.

As seen on Figure 65 above, failure occurs very close to the rust/coating interface with considerable cohesive failure on the rust and some on the coating. These are the predominant failure modes and location, but there are other failure locations on the tested samples as shown on the pictures of Figures 66 to 68 below.

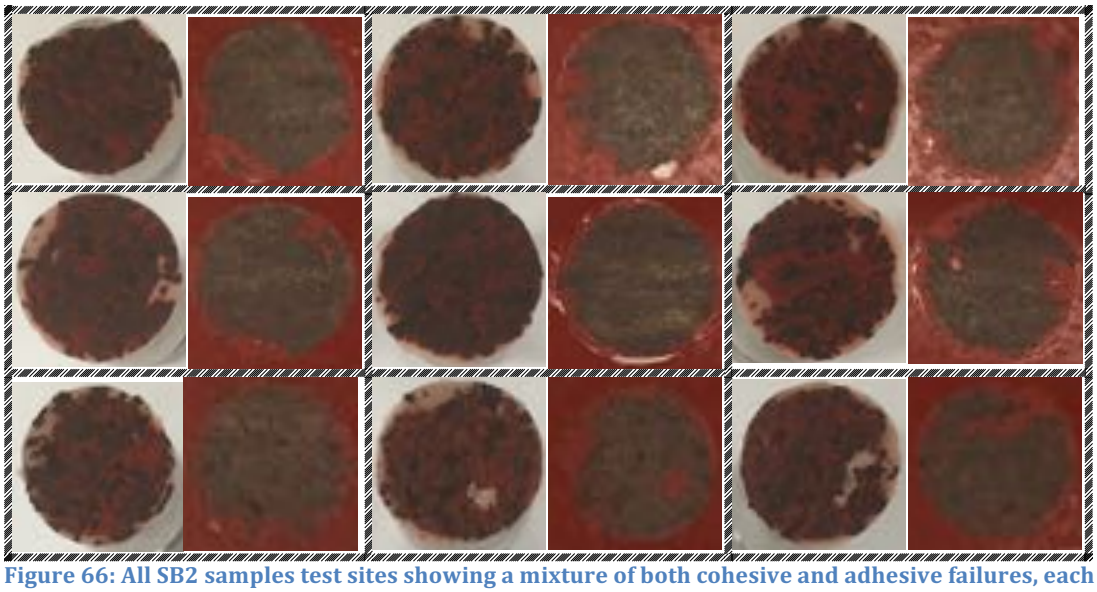

Figure 66: All SB2 samples test sites showing a mixture of both cohesive and adhesive failures, each row is a sample, and the dollies are at the left of the corresponding test sites.

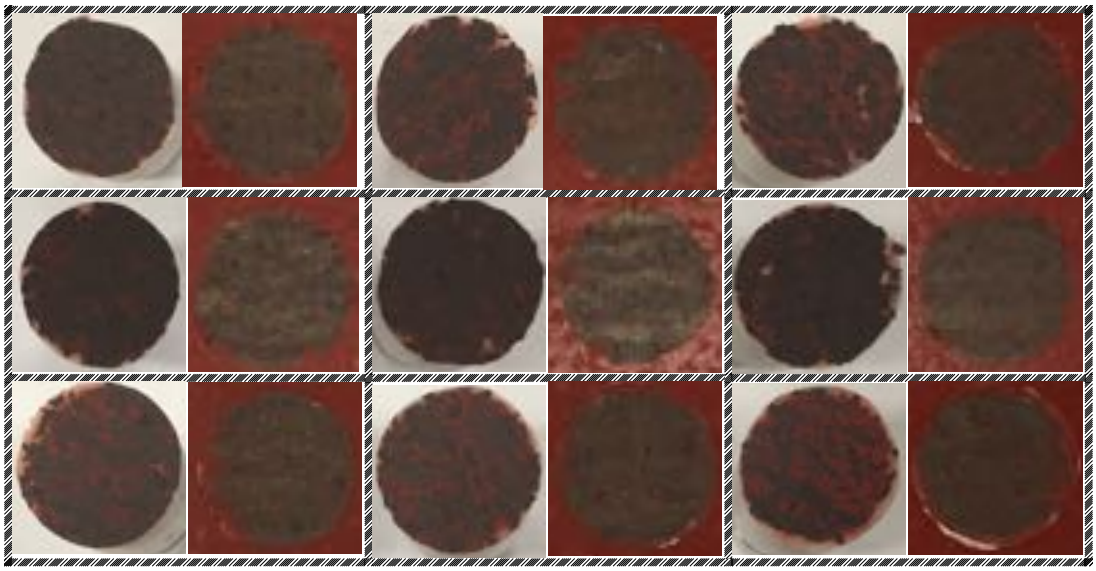

Figure 67: All NM samples test sites showing a mixture of both cohesive and adhesive failures, each row is a sample, and the dollies are at the left of the corresponding test sites.

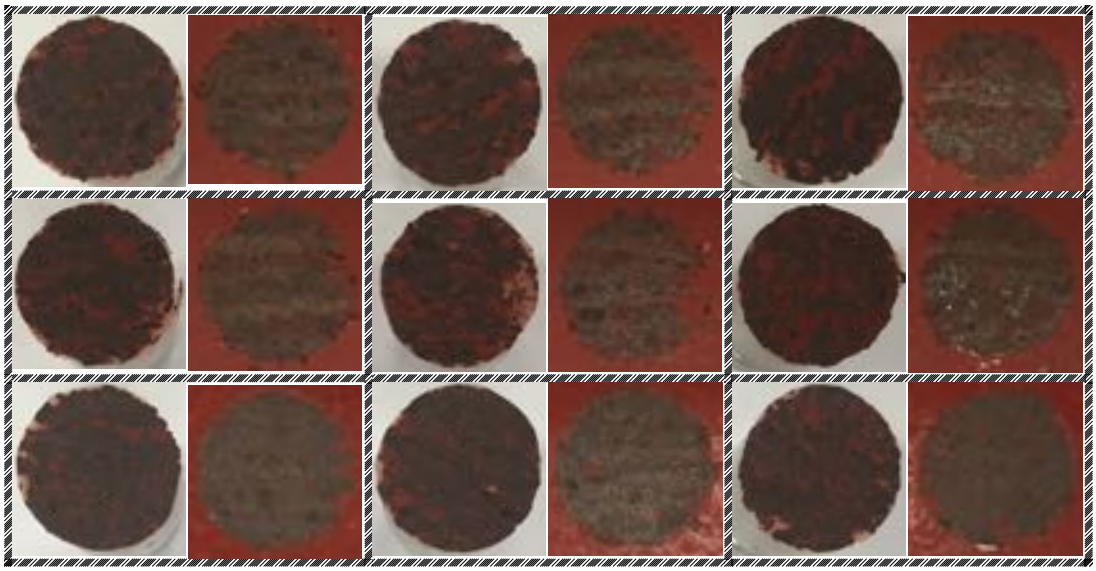

Figure 68: All SM samples test sites showing a mixture of both cohesive and adhesive failures, each row is a sample, and the dollies are at the left of the corresponding test sites.

Looking at the photographs in Figures 66 to 68, it is noted that when a rusted layer is seen both on the dolly and the test site then the failure is cohesive in nature within the rust layer on the sample plate. On the other hand, If the coating is visible on the dolly face and the test site is rusty, then the failure is an adhesive failure and occurred at the rust-to-coating interface. In addition, white spots were also observed on the dolly surface, with the corresponding location on the substrate being always the red of the coating, this indicates adhesion failure on the coating/adhesive interface.

Table 7 below shows the layers at which failure occurred and the corresponding estimation of failure percentage.

Table 7: Cohesive and adhesive failures layers and percentages for the samples with mixed failure mode

	Cohesive Failure		Adhesive Failure		Other
Test Site	Layer	%	Layers	%	%
SB2-09.1	Rust	50	Rust & Coating	45	5
SB2-09.2	Rust	48	Rust & Coating	48	4
SB2-09.3	Rust	42	Rust & Coating	52	8
SB2-10.1	Rust	55	Rust & Coating	38	7

	Cohesive Failure		Adhesive Failure		Other
Test Site	Layer	%	Layers	%	%
SB2-10.2	Rust	50	Rust & Coating	48	2
SB2-10.3	Rust	43	Rust & Coating	50	7
SB2-11.1	Rust	46	Rust & Coating	45	9
SB2-11.2	Rust	45	Rust & Coating	45	10
SB2-11.3	Rust	46	Rust & Coating	45	9
NM-09.1	Rust	89	Rust & Coating	10	1
NM-09.2	Rust	77	Rust & Coating	20	3
NM-09.3	Rust	50	Rust & Coating	45	5
NM-10.1	Rust	80	Rust & Coating	17	3
NM-10.2	Rust	80	Rust & Coating	17	3
NM-10.3	Rust	80	Rust & Coating	15	5
NM-11.1	Rust	67	Rust & Coating	30	3
NM-11.2	Rust	58	Rust & Coating	40	2
NM-11.3	Rust	47	Rust & Coating	50	3
SM-04.1	Rust	70	Rust & Coating	28	2
SM-04.2	Rust	60	Rust & Coating	39	1
SM-04.3	Rust	59	Rust & Coating	39	2
SM-08.1	Rust	67	Rust & Coating	32	1
SM-08.2	Rust	55	Rust & Coating	40	5
SM-08.3	Rust	55	Rust & Coating	44	1
SM-11.1	Rust	82	Rust & Coating	15	3
SM-11.2	Rust	85	Rust & Coating	14	1
SM-11.3	Rust	80	Rust & Coating	17	3

On Table 7, the category “other” refers to any other failures and are mostly glue failure on these samples.

5.6.4. Pull-Off Strength to Failure

The pull off strength was measured at three different sites per sample and three samples were tested per condition. Table 8 below shows the values measured per test site and the average value and sample standard deviation per sample condition.

Table 8: Table of measured pull strengths to failure with respective averages and standard deviations for each sample condition

Pull-Off Strength (MPa)									
RN	**NC1**	**NB1**	**SB1**	**SC1**	**SB2**	**NM**	**NN**	**SM**	**SN**
1,66	0,61	0,55	0,22	0,32	0,20	0,60	0,38	0,44	0,16
2,54	1,30		0,23	1,27	0,47	0,45	0,23	0,61	0,18
2,30	0,39	0,19	0,47	0,75	0,92	0,63	0,33	0,54	
2,17	0,23		0,55	0,35	0,40	0,70	0,28	0,41	0,31
1,68	0,25	0,30	0,24	0,31	0,71	0,29	0,22	0,41	
2,44	0,28	0,20	0,37	1,19	1,02	0,54	0,51	0,50	
1,23	0,79	0,47	0,39	0,55	0,43	0,24		0,70	0,16
2,04	0,63	0,63	0,56	0,73	0,34	0,97		0,57	
2,18	0,65		0,71	0,91		1,41	0,20		0,18
Mean									
2,03	**0,57**	**0,39**	**0,41**	**0,71**	**0,56**	**0,64**	**0,31**	**0,52**	**0,20**
Sample Standard Deviation									
0,43	**0,34**	**0,19**	**0,17**	**0,36**	**0,29**	**0,35**	**0,11**	**0,10**	**0,06**

The values on Table 8 above are arranged in ascending order of sample number and test site number (from top to bottom) as in the previous tables (Tables 6 and 7). The locations of the blank cells on the table indicate samples and test sites whose values were not reliable for use or were not measured at all for some reason.

5.6.5. Adhesion Strength and Coating Performance

On Figure 69 below, the samples are presented from the best to the worst performing condition. The corresponding pull strengths are plotted to show the relationship between adhesion and time to corrosion initiation.

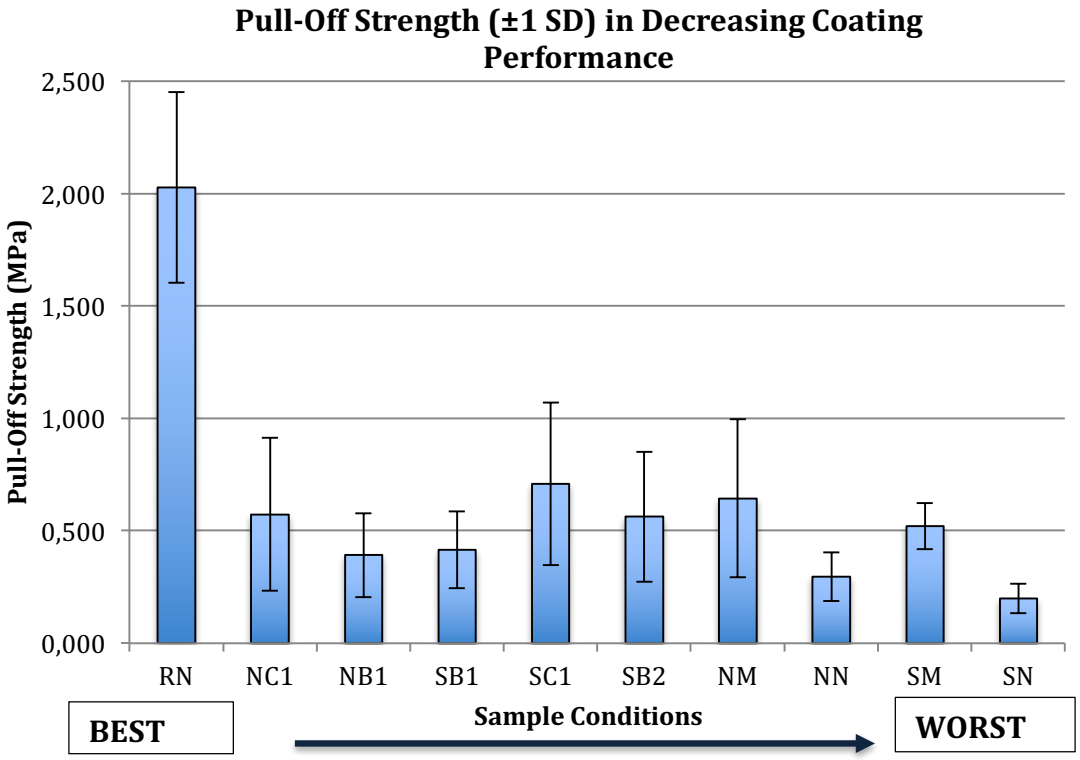

Figure 69: Pull-off strength of samples arranged in decreasing coating performance

The graph on Figure 69 above shows no particular pattern between the pull-off strength to failure and the coating performance across the studied conditions.

5.7. Electrochemical Impedance Spectroscopy (EIS) Results

There are a number of parameters from EIS measurements that can be used to determine the coating performance of organic coatings. The main advantages of EIS as a tool to determine organic coating performance are the non-destructive nature of the test and the ability to determine coating performance at the very early stages of the exposure, even before any damage is visible. Hence, the correlation between coating performance from visual inspection and the parameters from EIS measurements was investigated here. The EIS parameters studied were:

i. Phase angle at high frequency (10 kHz) and

ii. Total impedance at low frequency (1 Hz).

5.7.1. Phase Angle at High Frequency and Coating Performance

Three sample plates were tested per condition and the data for each surface condition is presented in Table 9 below.

Table 9: The phase angle at 10 kHz for each surface condition studied at various exposure periods

Mean Phase Angle (˚) at 10 kHz											
No of Cycles	Time (h)	RN	NC1	NB1	SC1	NN	SB1	SB2	SM	NM	SN
0	0	87,8	69,4	48,0	43,6	61,0	73,2	59,4	42,0	51,4	20,1
1	8	86,8	38,0	20,4	11,7	17,2	20,6	19,5	26,8	24,2	9,3
2	17	86,0	20,1	14,2	11,1	18,8	16,5	22,2	36,2	18,5	5,7
4	34	85,6	31,0	21,4	17,4	14,7	15,0	16,7	28,3	17,6	4,6
8	68	84,3	19,9	16,4	20,3	17,1	11,8	12,1	30,3	13,5	4,9
16	136	84,2	20,7	20,9	23,3	29,1	13,1	12,3	30,1	10,1	4,9
Standard Deviation											
No of Cycles	Time (h)	RN	NC1	NB1	SC1	NN	SB1	SB2	SM	NM	SN
0	0	0,11	7,03	31,76	25,81	13,62	9,87	3,13	30,41	15,14	6,18
1	8	0,22	22,83	7,79	5,33	2,44	10,41	1,31	2,43	7,10	1,06
2	17	0,59	7,02	5,78	2,65	2,00	4,32	5,64	2,11	3,08	0,28
4	34	1,25	18,51	5,22	5,24	2,69	7,98	4,40	7,49	4,27	0,24
8	68	1,74	14,57	6,27	3,34	4,51	4,48	4,17	4,48	4,12	0,43
16	136	1,9	5,50	7,93	3,67	2,36	4,89	4,50	1,53	1,61	0,33

The data in Table 9 are better visualized when represented graphically. Figure 70 shows the phase angle at 10 kHz for various exposure period plotted against the

surface conditions arranged in decreasing performance as assessed by visual inspection.

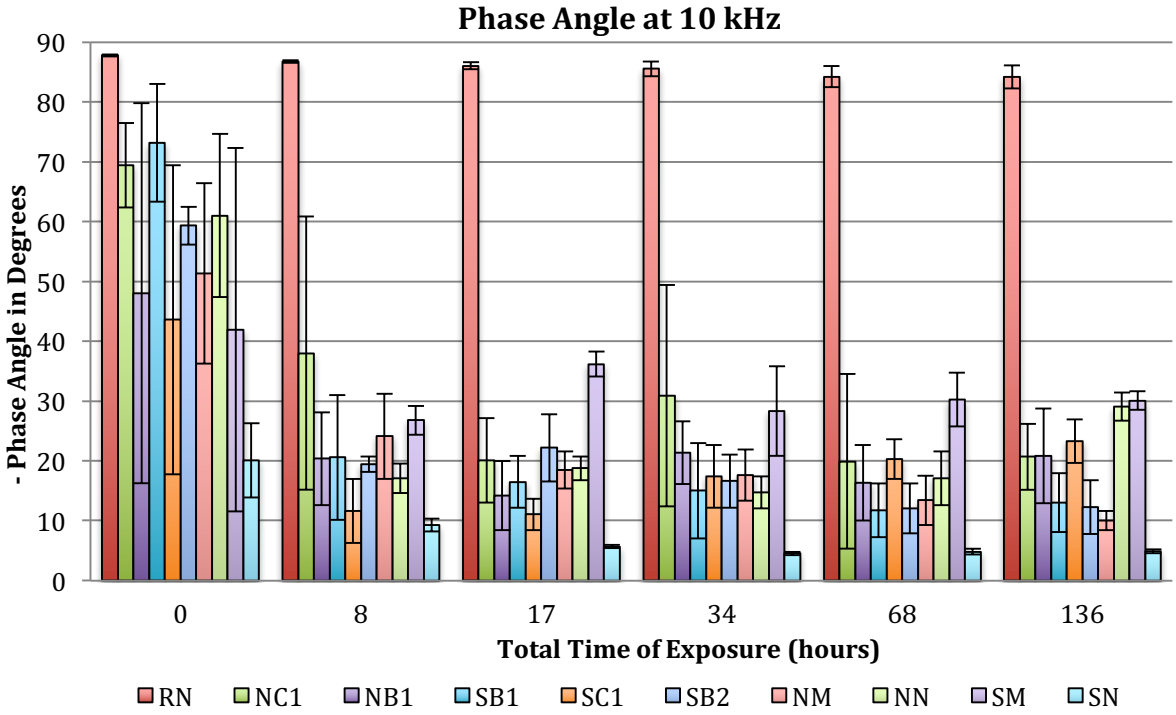

Figure 70: Phase angle at high frequency (10kHz) with surface condition arranged in decreasing coating performance

The bar chart in Figure 70 above is useful for comparing phase angle at 10 kHz among the different surface conditions for each exposure period. There is no clear pattern across the surface conditions with the only exceptions being the extremes; the reference samples (RN) having the highest phase angle values and the samples without any kind of preparation (SN) having the lowest phase angle values at every period of exposure studied.

Although the phase angle value is often used to determine coating performance, a more useful approach is to plot the change of phase angle with time of exposure. The change of phase angle for each surface condition is shown in Figure 71 below.

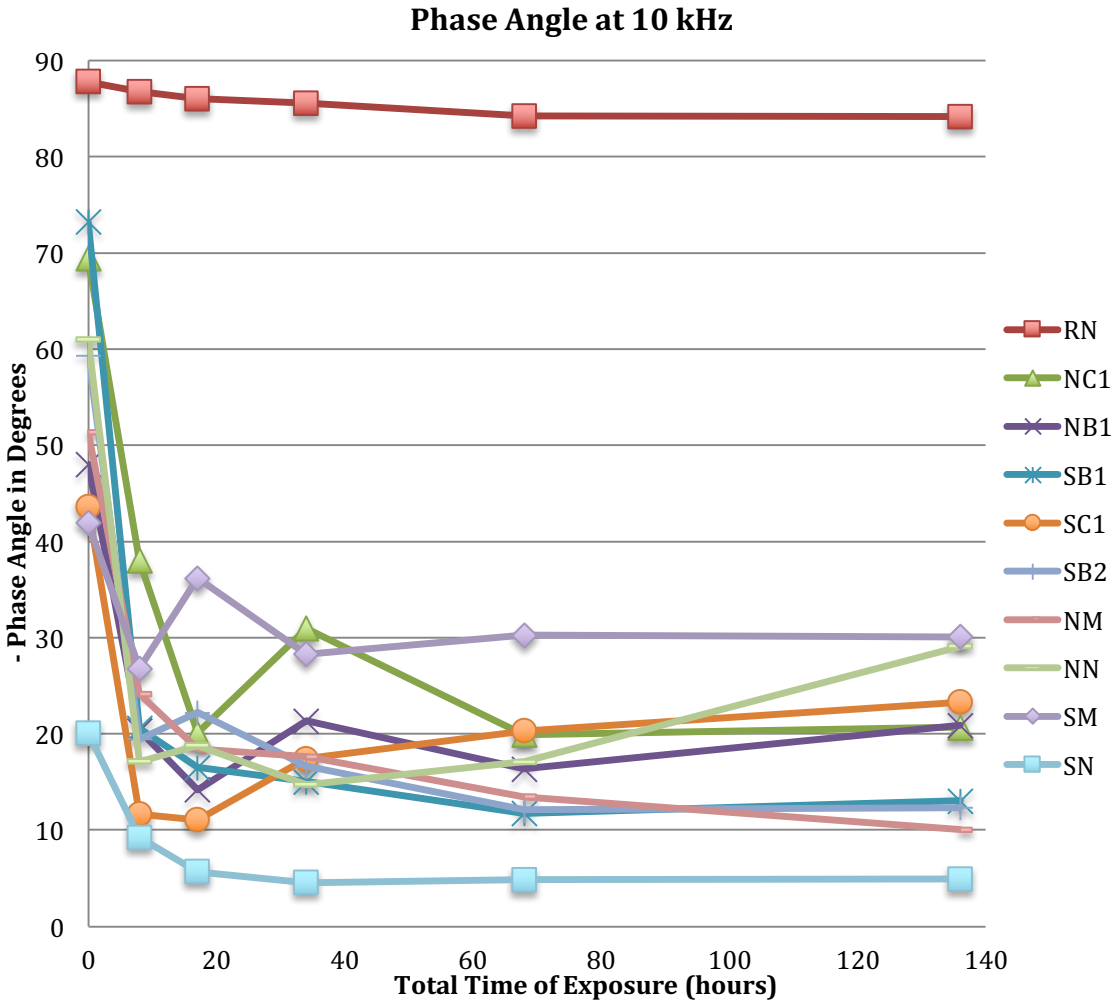

Figure 71: Change of phase angle at high frequency (10kHz) with time of exposure

Looking at the graphs in Figure 71 above, the following can be observed:

- The graph of reference new samples (RN) is above all other graphs at all times (including ±1 Standard Deviation).
- The graph of the samples with no treatment (SN) is below all other graphs (considering the average values only).
- The highest change in phase angle (a sharp decrease) occurs during the first hours of exposure. RN does not undergo as much change as the other surface conditions.
- At some point after the sharp decrease in phase angle, there is a spike up in the value of the phase angle. This is not observed on RN, SB1, NM and SN for the number of data points plotted.

- In the late stages of exposure, the graphs flatten out indicating very small changes in phase angle.
- Again, no particular pattern is observed across the sample conditions (organized in decreasing coating performance), except for the new sample (RN) on top, unprepared surface (SN) on the bottom and all the others bundled up in the middle.

5.7.2. Total Impedance at Low Frequency and Coating Performance

Another EIS parameter used for organic coating evaluation was the total impedance at low frequency. The total impedances of the tested samples are presented on Table 10 below.

Table 10: The Total impedance at 1 Hz for each condition studied at various exposure periods

Average Total Impedance at 1 Hz											
No of Cycles	Time (h)	RN ($10^7\Omega$)	NC1 ($10^4\Omega$)	NB1 ($10^3\Omega$)	SC1 ($10^3\Omega$)	NN ($10^3\Omega$)	SB1 ($10^3\Omega$)	SB2 ($10^3\Omega$)	SM ($10^3\Omega$)	NM ($10^3\Omega$)	SN ($10^1\Omega$)
0	0	9,77	20,2	443	65,4	71,8	182	44,1	14,9	31,3	304
1	8	6,56	2,92	6,86	2,62	3,85	6,59	5,31	4,53	4,26	17,8
2	17	6,00	0,74	3,76	1,78	3,68	4,57	6,03	7,88	1,85	7,94
4	34	6,26	1,55	6,99	3,44	2,65	4,23	3,22	2,24	1,74	7,29
8	68	3,68	0,73	4,20	3,56	2,52	2,18	1,83	1,39	1,27	6,61
16	136	3,51	0,70	5,57	3,71	3,07	2,23	1,34	1,33	0,71	7,44
Standard Deviation											
No of Cycles	Time (h)	RN ($10^7\Omega$)	NC1 ($10^4\Omega$)	NB1 ($10^3\Omega$)	SC1 ($10^3\Omega$)	NN ($10^3\Omega$)	SB1 ($10^3\Omega$)	SB2 ($10^3\Omega$)	SM ($10^3\Omega$)	NM ($10^3\Omega$)	SN ($10^1\Omega$)
0	0	1,15	12,7	717	61,3	82,7	115	11,8	13,1	19,4	148
1	8	1,26	3,27	3,95	2,16	1,28	4,95	0,89	0,80	2,63	7,27
2	17	1,44	0,48	2,75	0,95	0,30	1,73	2,56	3,89	0,48	1,92
4	34	2,16	1,20	3,10	2,27	0,30	3,07	1,40	2,43	1,47	2,45
8	68	2,54	0,83	2,88	1,72	0,18	1,45	1,15	0,92	0,97	1,67
16	136	3,45	0,33	3,64	0,56	0,89	1,19	8,37	0,75	0,40	1,64

The data in Table 10 is presented in Figure 72 where the total impedances across the different surface conditions are plotted in decreasing order of performance as assessed by visual examination, for each exposure period.

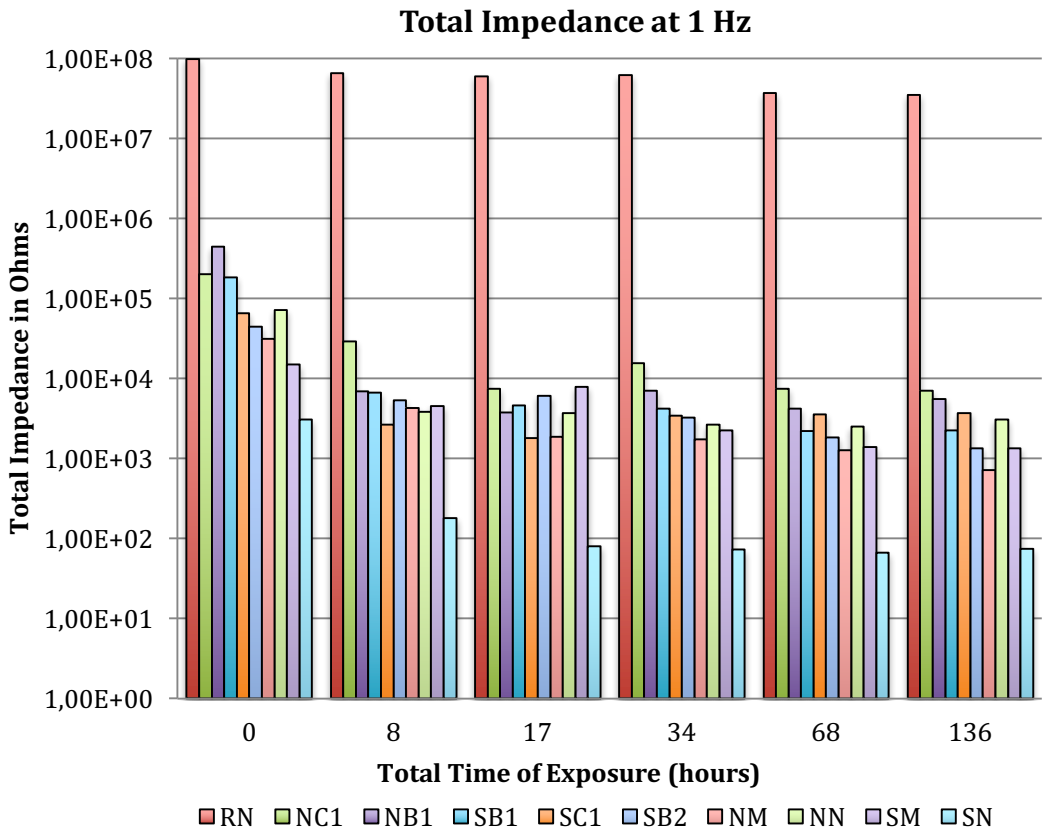

Figure 72: Total impedance at low frequency (1 Hz) with surface condition arranged in decreasing coating performance

Figure 72 shows a decreasing trend in the total impedance with decreasing performance for each exposure period, across the sample conditions. However, at 17 hours of exposure the trend is not well-defined, some unusual trends are also noted, which become clearer if one examines Figure 73.

Figure 73 below presents the data set from Table 10 for better visualization of the total impedance change with time, for each surface condition.

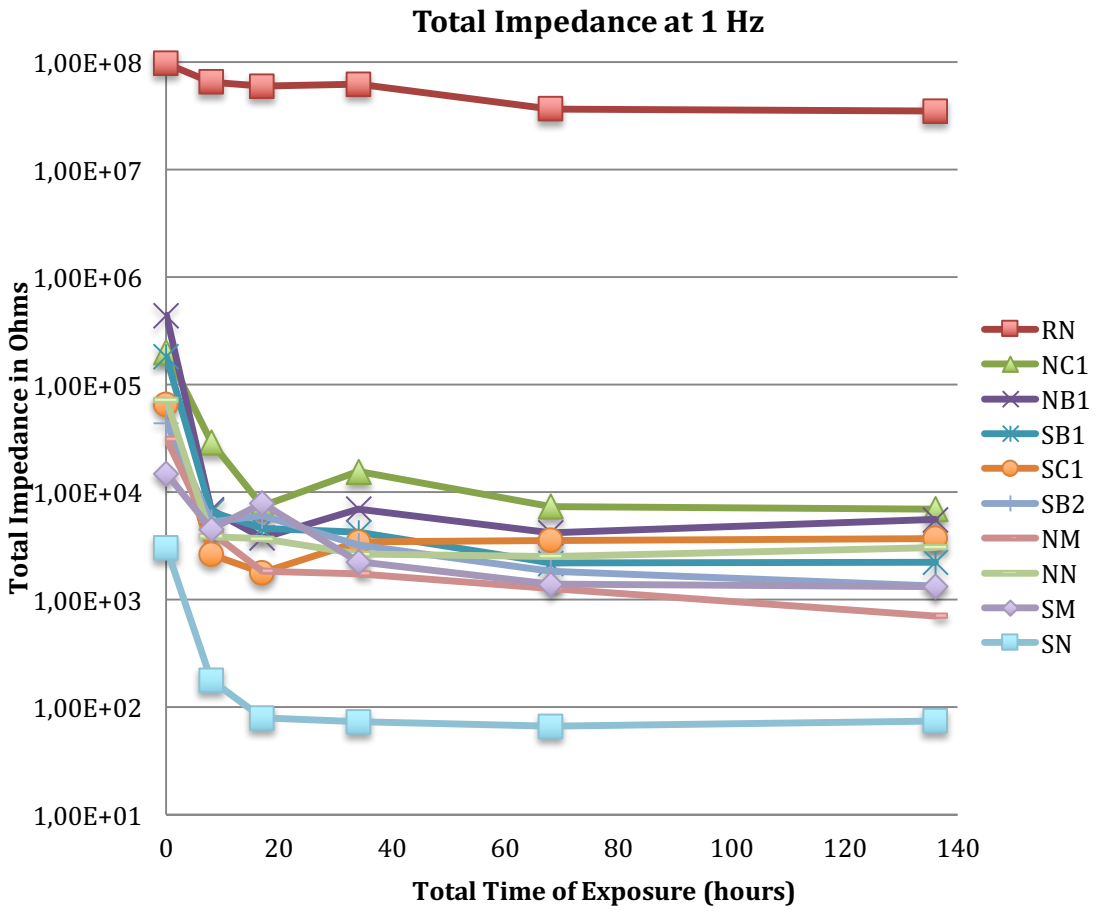

Figure 73: Change of total impedance at low frequency (1 Hz) with time of exposure

Figure 73 shows that the major changes are observed in the first hours of exposure when a sharp decrease in total impedance occurs, after that a spike up occurs, and finally it remains almost unchanged for the remainder of the test period.

Again, the two extremes (RN and SN) occupy the uppermost and the lowermost positions on the graph. And the other conditions are close to each other between the two extremes.

CHAPTER 6. DISCUSSION

6.1. Coating Performance Based on Visual Inspection

6.1.1. Types of Failure Observed on the Samples

The type of coating failure visible on the test plates varies with the surface pre-treatment applied on the metal substrate prior to coating. This is because different kinds of contamination on the surfaces and different surface treatments all have a variable impact on the coating applied to the plates. Moreover, other aspects such as substrate geometry and surface roughness also influence coating deterioration, which may trigger some types of failure and not others.

The edges of the sample plates are more prone to corrosion due to their sharpness and the chance of physical damage. A coated sample has smoother edges after coating application, which suggests a much thinner coating on the edges – see Figure 74. Hence, failure triggered by low coating thickness starts at the test plate edges where the dry film thickness is below specification.

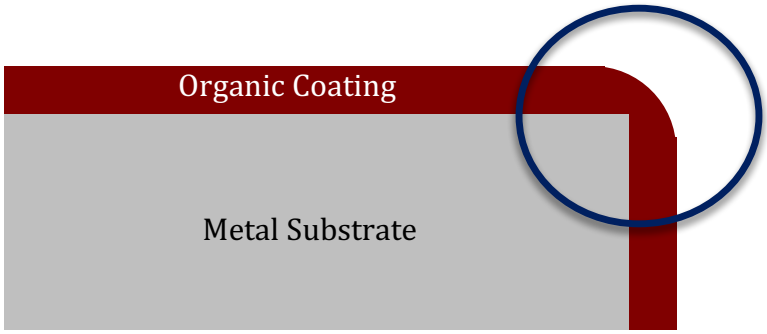

Figure 74: Cross section of a coated sample showing how the paint can be thinner on the edges (top right corner)

Rust staining was observed on samples when their top edges were damaged at the time of observation. RN samples showed rust staining (Figure 38, page 52) since the brand-new samples were likely to have had sharper edges and consequently a thinner coating at the edge. Also, rust staining is seen most clearly on RN samples, as the samples underwent no other type of failure, unlike SM samples where rust staining is more difficult to assess due to the presence of rust rashing and rust spotting (Figure 46, page 56). On the other hand, the water runoff pathways on other test samples were free of corrosion products and were not assessed as rust staining.

Blistering usually occurs when electrolyte finds its way underneath the coating. On RN samples the effects of contamination are minimal since the surface is well prepared and properly cleaned. Since it is more difficult for electrolyte to penetrate the coating on a properly cured coating, electrolyte reaches the metal substrate where the coating is damaged. Hence, blistering propagates from the edges of RN samples where coating has been damaged. (Figure 38, page 52).

The failure type observed on NC1 samples is classified as rust spotting. The observed spots are elongated, which makes them more like cracks (Figure 39, page 53). However, they do not qualify as typical cracks such as seen in checking, crazing, cracking and alligatoring/crocodiling. In fact, it is possible that the failure is similar to alligatoring where the undercoat (converted rust) is more flexible than the topcoat (paint used), but the surface did not show the characteristic alligator like texture.

Rust spotting was observed in almost every sample examined (NC1, NB1, SB1, SB2, NN and SM) regardless of the salt contamination level and rust removal approach (see Figures 39, 40, 41, 43, 45 and 46 on pages 53 to 56). Out of the known causes of rust spotting (see Table 1, page 7), the most probable on these cases are defects in steel, such as lamination (possibly of rust) and inclusions (loose corrosion products). However, there are other factors and types of failure affecting rust spotting viz.

- On NC1 samples, alligatoring was also observed.
- On NB1 samples, undercutting predominated (Figure 40, page 53)
- On SB1 and SB2 samples, rust spotting was observed so early in the testing that it was the only failure type seem (Figures 41 and 43, pages 54 and 55)
- On NN samples, rust spotting was the predominating failure mode, with the water runoff pathways being the most affected (Figure 45, page 55).
- Finally, on SM samples, rust rashing was first observed on the plates and this later changed to the more severe rust spotting (Figure 46, page 56).

The most probable cause of undercutting is application of coating on corroded substrate. Since all surface conditions studied, except the reference new (RN) samples, were pre-corroded before employing the surface pre-treatment, undercutting may be expected on all surface conditions to lesser or greater extent. However, depending on the pre-treatment, undercutting may only occur after other types of failure have manifested themselves. NB1 samples presented undercutting just after rust spotting occurred at transition time to corrosion (Figure 40, page 53), while SC1 samples presented undercutting only as the main mode of failure, at the transition time to corrosion (Figure 42, page 54). In comparison, it makes sense that NB1 samples

took much longer for coating disbonding than SC1 samples since NB1 samples had less corrosion product on the surface as they were prepared with wire brushing (grade St 2-C) before applying rust converter. Also, the larger quantity of salt on the surface of SC1 samples results in increased coating delamination as salt increase water absorption. All other samples had undergone other types of failure before undercutting was noticed.

The samples with the lower mean DFT per condition (NM, NN, SM and SN) underwent rust rashing, which is expected since rust rashing is usually caused by low film thickness on high surface profile. However, the fact that SM samples, with probably smoother surface profile than NN samples due to the wire brushing applied, experienced rust rashing earlier than NN samples may still be somewhat puzzling. Nevertheless, this may be explained by the fact that the difference in thickness is negligible when considering their standard deviations (see Figure 52, page 65) and the salt level on SM samples is much higher than on NN samples (see Figure 55, page 68).

6.1.2. Estimated Percentage Failure

Both RN and NC1 samples showed less than 25% failure for the longest period of exposure studied, 710 hours (Table 3, page 60). Although the failure percentage of NC1 samples is closer to 25% than that of RN samples, the coating degradation of NC1 samples is very slow at this stage as shown by the very small change on degradation from 506 to 710 hours of exposure (Figure 39, page 53). This slow degradation may well be thanks to the converted rust acting as primer on NC1 samples.

The NM and NN exhibited the transition to corrosion with failure percentages between 25% and 50% at exposure periods between 68 and 136 hours (Table 3, page 60). From the images (Figures 44 and 45, page 55) there is no clear difference in degradation rate despite the estimated failure of NM samples being closer to 25% and that of NN samples closer to 50%. This is to be expected considering that the only difference between the pre-treatments is the wire brushing (Figures 5 and 7, page 20). SB2 samples reached the transition to corrosion at exposure period between 68 and 136 hours as well. However, the failure percentage was between 0% and 25%, probably due to much lower amount of rust remaining after treatment with rust remover.

SB1 and SC1 both reached the transition to corrosion at the exposure period between 189 and 341 hours (Figures 41 and 42, page 54). Nevertheless, the estimated failure percentage fell between 0% and 25% for SB1, and between 50% and 75% for SC1,

which shows faster degradation of SC1 samples. This is probably due to a higher degree of salt contamination which promotes delamination and undercutting.

6.2. Effect of Dry Film Thickness on Coating Performance

Organic coatings act as a form of insulator so as to protect the substrate from a corrosive environment (electrolyte). However, a coating that contains holidays, pores or defects will offer little protection to the metal surface. Furthermore, the thinner the coating, the greater the chance of electrolyte being able to penetrate through the coating. For that reason, two sets of NC1 samples with different dry film thicknesses showed increasing coating performance with increasing coating thickness (Figures 50 and 51, pages 64 and 64).

In contrast, dry film thickness does not affect pull-off tests in a similar fashion because the failure is not through electrolyte penetration. Nevertheless, testing is still important since thicker film means increased chance of cohesive failure on the coating layer.

To minimize the effect of thickness on coating performance, constant dry film thickness was aimed for all samples in every surface condition. Despite the small differences still remaining, the effect of thickness on coating performance was negligible, showing no direct correlation between the thicknesses and the performances for such small DFT variation (Figures 49, 52, 53 and 54, pages 63 to 66), that is due to far more influential parameters such as remaining corrosion product and salt contamination present on the surface conditions studied.

6.3. Salt Contamination

Besides the Reference conditions studied (RN and SN), only the use of rust converter played a more substantial role on coating performance than the level of salt contamination. The reference new (RN) samples and the fully corroded samples with no pre-treatment prior to coating application (SN) were the best and the worst performing surface conditions respectively.

The best performance, other than RN, was obtained from samples treated with rust converter (Figure 48, page 61). This was probably due to converted rust acting as primer coating on the test plates, thus adding additional protection, while a single coating layer was used for the other surface conditions. All this is explained by the decreasing performance with increasing salt content seen on samples treated with rust

converter followed by samples treated without rust converter showing identical correlation but at comparatively lower performance (Figure 55, page 68).

Looking at the mean salt contamination values, only NC1 and NB1 samples do not seem to follow this behaviour. However, the difference in salt content between NC1 and NB1 samples is negligible as shown by their standard deviations (Figure 55, page 68) and the small difference between their mean values (Table 5, page 67). Thus, for a similar amount of salt contamination, rust converter shows improved performance on samples with more corrosion product to convert into primer coating.

Coating application on corroded surface results in poor coating performance, and the more rusted the surface is, the more poorly it performs. However, the opposite was seen for NC1 and NB1 samples on the paragraph above. Similarly, NN samples contain more corrosion product than SM samples but show better coating performance; here, the reasons align with the amount of salt contamination as NN samples have lesser salt contamination than SM samples.

6.4. Using EIS for Early Evaluation of Organic Coating Performance on Different Surface Condition

One of the advantages of EIS is the early detection of coating deterioration and possible corrosion initiation. Having ranked the surface conditions by coating performance based on visual inspection, the coating evaluation can also be performed with EIS so as to demonstrate its capability for the early detection of organic coating degradation.

Phase angle at high frequency (10 kHz) and total impedance at low frequency (1 Hz) are the EIS methods used in this research. Both methods demonstrated that the RN samples have the best surface condition and SN samples the worst, as they exhibited the highest and the lowest values of phase angle and total impedance for the entire exposure period (see Figures 70 to 73, pages 81 to 85). In general, total impedance at low frequency agreed more closely with the visual inspection results (Figure 72, page 84) than phase angle at high frequency.

6.4.1. Sudden drop in both phase angle and total impedance values

After the first 8 hours of CCT1 exposure, electrolyte found its way through the pores of the coating drastically decreasing coating resistance (Figures 71 and 73, pages 82 and 85). This is reflected in the phase angle, because with low coating resistance current flows preferably through the resistor, resulting in a more resistive than capacitive coating response, which is characterized by the phase angle value moving

towards 0˚ (Figure 71, page 82). Since total impedance comprises coating resistance and charge transfer resistance only (Mahdavian and Attar, 2006), the total impedance drops with the fast drop on the coating resistance.

6.4.2. Some increase of both phase angle and total impedance values

The sudden drop in the values of phase angle and total impedance in the first hours of exposure is followed by some increase of these values (Figures 71 and 73, pages 82 and 85). This increase is likely the result of maturing of the coating (more curing time being needed due to poor surface preparation), recovery by inhibitors in the coating and blocking of pores by corrosion products. In the coating used, polymerization reactions continue after coating application to produce a densely cross-linked film (Section 4.1.2, page 18), hence the possibility of these post-application chemical reactions and cross-linking being further enhanced (beyond the manufacturer's recommended curing time due to the unconventional surface treatment performed) by the exposure environment (mainly by temperature and humidity), and restore some of the barrier properties of the coating. Recall also that another way coatings protect the substrate is by acting as reservoir for inhibitors, which restore some of the protective properties of the coating when electrolyte permeates into the coating and corrosion initiates. Furthermore, when corrosion starts underneath the coating the resulting corrosion products may block the pores and decreases the amount of electrolyte in contact with the substrate, which contributes towards improving the barrier properties of the coatings.

6.4.3. Final drop of both phase angle and total impedance values

At some point the permeation rate of electrolyte into the organic coating overcomes the recovery rate of barrier properties mentioned above and slowly the phase angle and total impedance values start decreasing again (Figures 71 and 73, pages 82 and 85). These decreases occur after maturing of the coating, as degradation progresses and unreacted moieties (reactive sites) run out, coating resistance decreases and so does charge transfer resistance as corrosion reactions start. In addition, the decrease is promoted by the limitations of the inhibitors to boost barrier properties of the coating by either a galvanic or a passivation mechanism. Furthermore, with increasing number of pores, the blocking effect by the corrosion products becomes negligible. After this decrease, the values of both phase angle and total impedance stay essentially unchanged as permeation reaches saturation, pores are fully developed, and corrosion products have covered the reactive sites.

6.4.4. The EIS and the Visual Inspection Results

It was seen in the discussion above that the major changes in both phase angle and total impedance are related to the coating resistance, which lead to similarity in the response of phase angle and total impedance. However, the results show that total impedance values have a better agreement with the visual inspection results than the phase angle values. This is because phase angle at high frequency agrees very closely with coating capacitance and coating resistance, while impedance at low frequency depends primarily on charge transfer resistance and coating resistance as it is a near DC response of the system (Mahdavian and Attar, 2006). It is important to note that the deciding factor is the difference imposed by the coating capacitance and the charge transfer resistance onto the phase angle and total impedance responses respectively.

The results of total impedance at low frequency agree more with the visual inspection results than the results of phase angle at high frequency because of the effect of charge transfer resistance on its response as opposed to the effects of coating capacitance observed on the response of phase angle at high frequency. This is probability because visual inspection is an evaluation of the coating performance at late stages of exposure and the corrosion breakthrough was used to rank the different surface conditions. Similarly, for total impedance at low frequency, charge transfer response reflects a later stage of the degradation process since it represents the electrochemical reactions taking place on the substrate during the corrosion process. On the other hand, for phase angle at high frequency, coating capacitance evaluates the coating properties with little influence of the corrosion process underneath it.

CHAPTER 7. CONCLUSION

7.1. Effects of Geometry on Coating performance

The geometric properties studied in this research are sample size and coating thickness. The results show that small samples are more susceptible to corrosive attack than larger ones with 50% of the surface conditions following this pattern (RN, NC1, NB1, SB1 and SB2), 30% (SC1, NN and SN) showing the opposite behaviour (larger samples corroding faster) and 20% (SM and NM) remaining unclear. On the other hand, the result of the effect of thickness on coating performance is clear, namely that the higher the dry film thickness the better the coating performance provided it is kept within the recommended DFT. In conclusion, using the same size samples helped to avoid any possible influence of sample size.

7.2. Effects of Contamination on Coating performance

The contaminants studied are soluble salts and the corrosion product on the surface of the coating. The former was dealt with by washing the surface and the latter by applying different surface pre-treatment. For a similar amount of salt contamination, samples with the least corrosion product on the surface showed better coating performance (NM and NN samples). Likewise, for a similar amount of corrosion product, the coating performs best if it has the least amount of salt contamination. However, the lowest amount of salt contamination always leads to better coating performance even if the quantity of corrosion product changes. In conclusion, salt contamination has the most negative impact on the coating performance and its treatment greatly improves coating performance.

7.3. Effects of Rust Cleaning Approach on Coating performance

Chemical surface preparation is better than mechanical preparation by simple hand tool such as wire brushing. Comparing the two chemical treatment approaches used, rust converter leads to better coating performance than rust remover. However, the presence of contamination affects the coating performance across samples with same surface preparation. An increase in salt contamination always decreases coating performance, while the amount of corrosion product depends on the amount of rust

converter (NC1 and NB1). In summary, chemical surface preparation with rust converter leads to the best coating performance when compared to all other surface preparation methods studied in this project.

7.4. Effects of Adhesion on Coating performance

The adhesion between the coating and substrate is of good quality for the surface conditions studied. The system failed in the pre-treatment layer before the adhesion of the coating-to-substrate is compromised. Moreover, after exposure, no delamination failures occurred except for the converted corrosion product lifting up during undercutting. This shows that adhesion between the coating and substrate is of the least concern if the pre-treatments and salt cleaning employed are so poor as to induce pull-off failure at the pre-treatment layer.

7.5. Early Coating Evaluation with EIS

EIS measurement proved a useful tool for early evaluation of organic coating deterioration, producing results within 136 hours of exposure while visual inspection took up to 710 hours of exposure. The EIS methods used were phase angle at high frequency (10 kHz) and total impedance at low frequency (1 Hz). Although both methods show some agreement between them, total impedance at low frequency has a closer correlation with visual inspection at the late stages of plate exposure.

REFERENCES

Akbarinezhad, E., Ebrahimi, M. and Faridi, H. R. (2009) 'Corrosion inhibition of steel in sodium chloride solution by undoped polyaniline epoxy blend coating', *Progress in Organic Coatings*, 64(4), pp. 361–364.

ASM International (1987) 'Metals Handbook, Ninth Edition: Volume 13 - Corrosion', in *ASM International*, p. 1415.

ASTM (2013) 'D1141-98 Standard Practice for the Preparation of Substitute Ocean Water', *ASTM International*, 98(Reapproved 2013), pp. 1–3.

Bierwagen, G., Tallman, D., Li, J., He, L. and Jeffcoate, C. (2003) 'EIS studies of coated metals in accelerated exposure', *Progress in Organic Coatings*, 46(2), pp. 149–158.

Cabanelas, I., Collazo, A., Izquierdo, M., Nóvoa, X.R. and Pérez, C. (2007) 'Influence of galvanised surface state on the duplex systems behaviour', *Corrosion Science*, 49(4), pp. 1816–1832.

Callister, W. D. (2003) *Materials science and engineering: an introduction*, *New York*.

Collazo, A., Pérez, C., Izquierdo, M. and Merino, P. (2003) 'Evaluation of environmentally friendly paints over weathering galvanised steel', *Progress in Organic Coatings*, 46(3), pp. 197–210.

Elcometer (no date) 'Elcometer 138 Bresle Salt Kit User Guide'.

Fitzsimons, B. and Parry, T. (2016) 'Coating Failures and Defects', in *A Comprehencive Field Guide*. Corrosionpedia.com.

Gamry (2015) *Introduction to Electrochemical Impedance Spectroscopy*, *2015*. Available at: https://www.gamry.com/assets/Uploads/Basics-of-Electrochemical-Impedance-Spectroscopy.pdf.

González, S., Fox, S. and Souto, R. M. (2004) 'Laboratory evaluation of corrosion resistance at metallic substrates by an organic coating: Delamination effects', *Journal of Adhesion Science and Technology*, 18(4), pp. 455–464.

International Organization for Standardization (2011) 'STANDARD ISO 8501 Corrosion Protection of Steel Structures by Painting', 33(February), pp. 1–4.

Lasia, A. (1999) 'Electrochemical Impedance Spectroscopy and its Applications', 32, pp. 143–248.

Loveday, D., Peterson, P. and Rodgers, B. (2004) 'Evaluation of organic coatings with electrochemical impedance spectroscopy. Part 2: application of EIS to coatings',

Journal of Coatings Technology, 1(10), pp. 88–93.

Loveday, D., Peterson, P. and Rodgers, B. (2004) 'Evaluation of Organic Coatings with Electrochemical Impedance Spectroscopy. Part 1: Fundamentals of Electrochemical Impedance Spectroscopy', *Journal of Coatings Technology*, (August), pp. 88–93.

Loveday, D., Peterson, P. and Rodgers, B. (2005) 'Evaluation of Organic Coatings with Electrochemical Impedance Spectroscopy; Part 3: Protocols for Testing Coatings With EIS', *Journal of Coatings Technology*, 2(13), pp. 22–27.

Maeda, S. (1996) 'Surface chemistry of galvanized steel sheets relevant to adhesion performance', *Progress in Organic Coatings*, 28, pp. 227–238.

Mahdavian, M. and Attar, M. M. (2006) 'Another approach in analysis of paint coatings with EIS measurement: Phase angle at high frequencies', *Corrosion Science*, 48(12), pp. 4152–4157.

McCafferty, E. (2009) *Introduction to Corrosion Engineering*, New York: Springer Science+Business Media. Available at: http://scholar.google.com/scholar?hl=en&btnG=Search&q=intitle:Introduction+to+Corrosion+Engineering#1 (Accessed: 3 May 2014).

McCafferty, E. (2010) *Introduction to corrosion science*, *Introduction to Corrosion Science*.

Mittal, K. L. and Pizzi, A. (1999) *Adhesion Promotion Techniques: Technological Applications*. Edited by K. Mittal and A. Pizzi. Boca Raton, Florida: CRC Press, 1999. Available at: http://www.dekker.com.

Q-LAB (2011) 'Cyclic Corrosion Tester - Technical Manual - Q-FOG CCT Model'.

Rammelt, U. and Reinhard, G. (1992) 'Application of electrochemical impedance spectroscopy (EIS) for characterizing the corrosion-protective performance of organic coatings on metals', *Progress in Organic Coatings*, 21(2–3), pp. 205–226.

Revie, R. W. and Uhlig, H. H. (2008) *Corrosion and Corrosion Control: An introduction to corrosion science and engineering*, *British Corrosion Journal*. John Wiley & Sons, Inc.

Merten, B., Skaja, A., Tordonato, D. and Little, D. (no date) 'Re-Evaluating Electrochemical Impedance Spectroscopy (EIS) for the Field Inspector's Toolbox: A First Approach', pp. 1–13.

Skerry, B. S., Alavi, A. and Lindgren, K. I. (1988) 'Environmental and electrochemical test methods for the evaluation of protective organic coatings', *J. Coat. Technol.*, 60(765), pp. 97–106. Available at: http://www.csa.com/partners/viewrecord.php?requester=gs&collection=TRD&recid=

890236CO.

Touzain, S. (2010) 'Some comments on the use of the EIS phase angle to evaluate organic coating degradation', *Electrochimica Acta*, 55(21), pp. 6190–6194.

van Westing, E. P. M., Ferrari, G.M., Geenen, F.M. and de Wit, J.H.W. (1993) 'In situ determination of the loss of adhesion of barrier epoxy coatings using electrochemical impedance spectroscopy', *Progress in Organic Coatings*, 23, pp. 89–103.

Zuo, Y., Pang, R., Li, W., Xiong, J P and Tang, Y M. (2008) 'The evaluation of coating performance by the variations of phase angles in middle and high frequency domains of EIS', *Corrosion Science*, 50(12), pp. 3322–3328.

APPENDIX

Pull-Off Test Rig Drawings

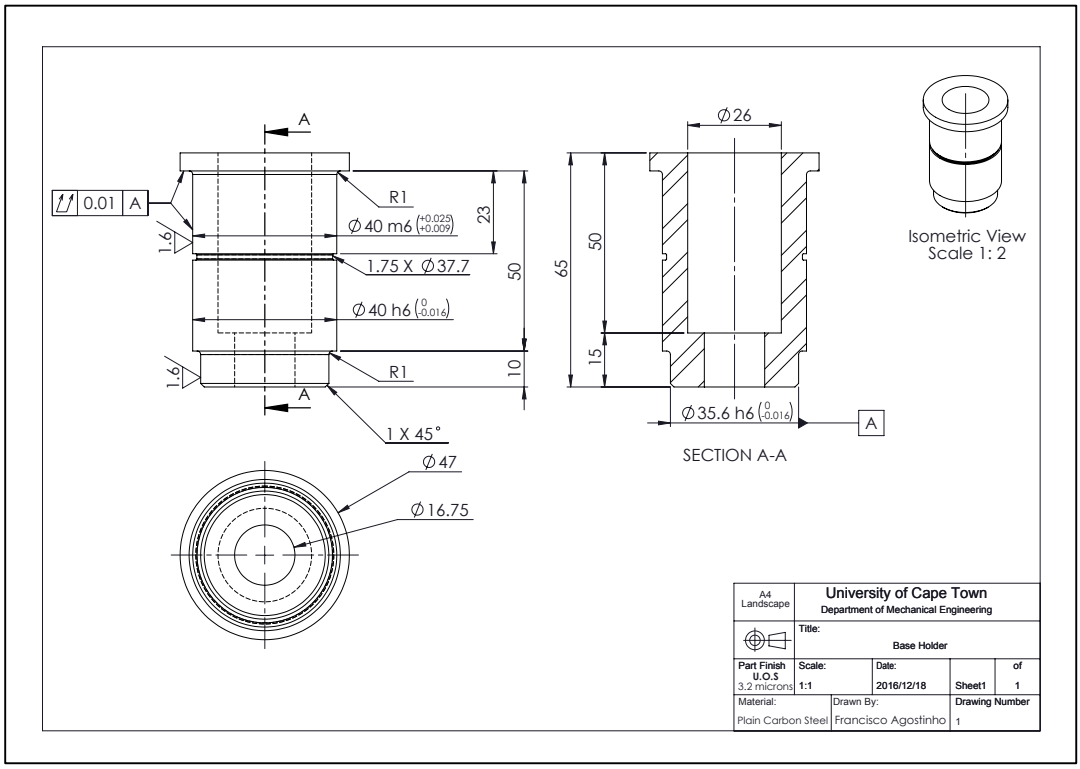

Figure 75: Base Holder drawing

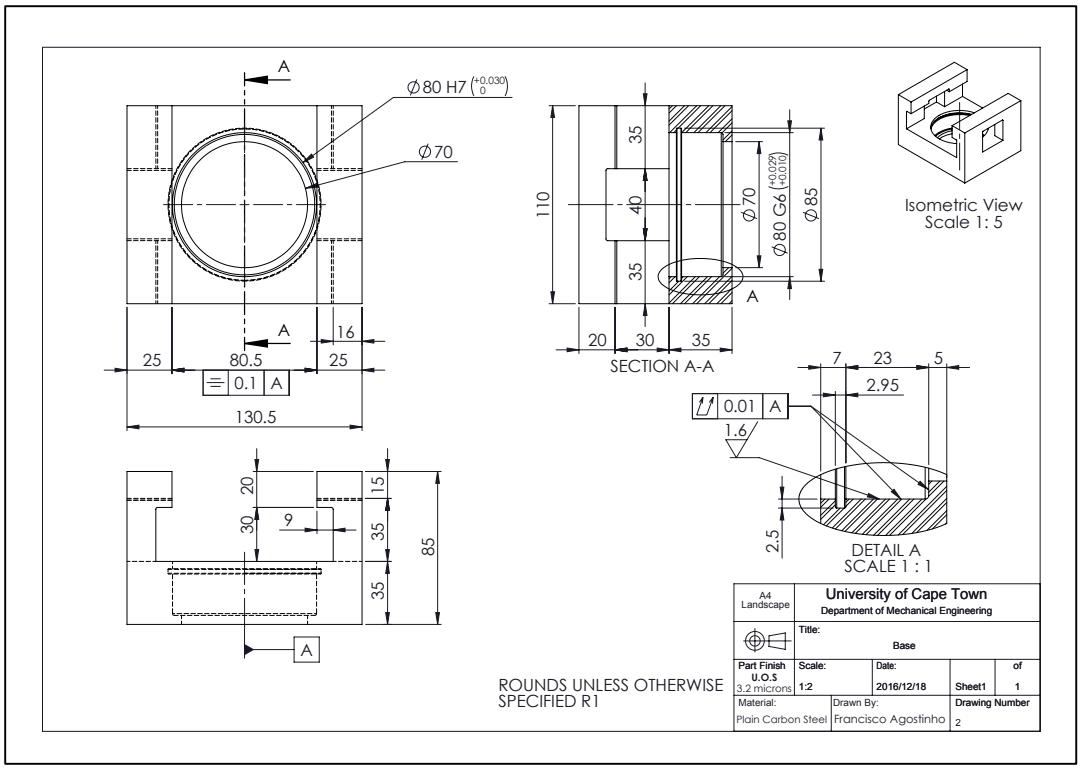

Figure 76: Base drawing

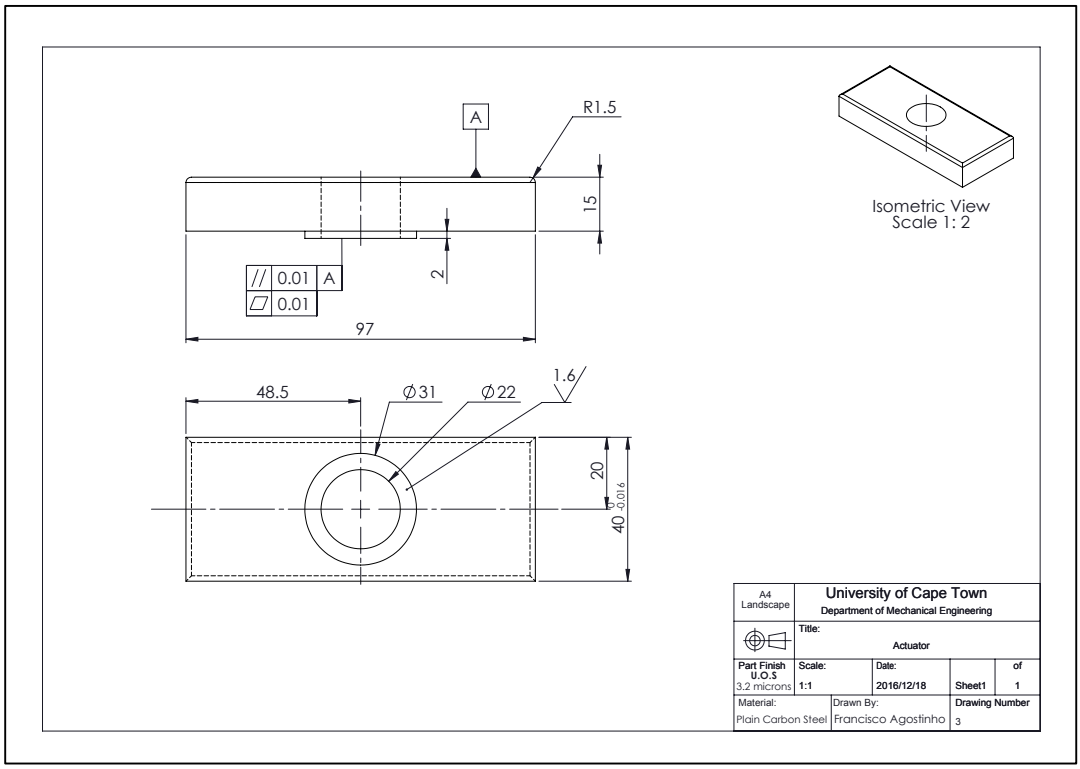

Figure 77: Actuator drawing

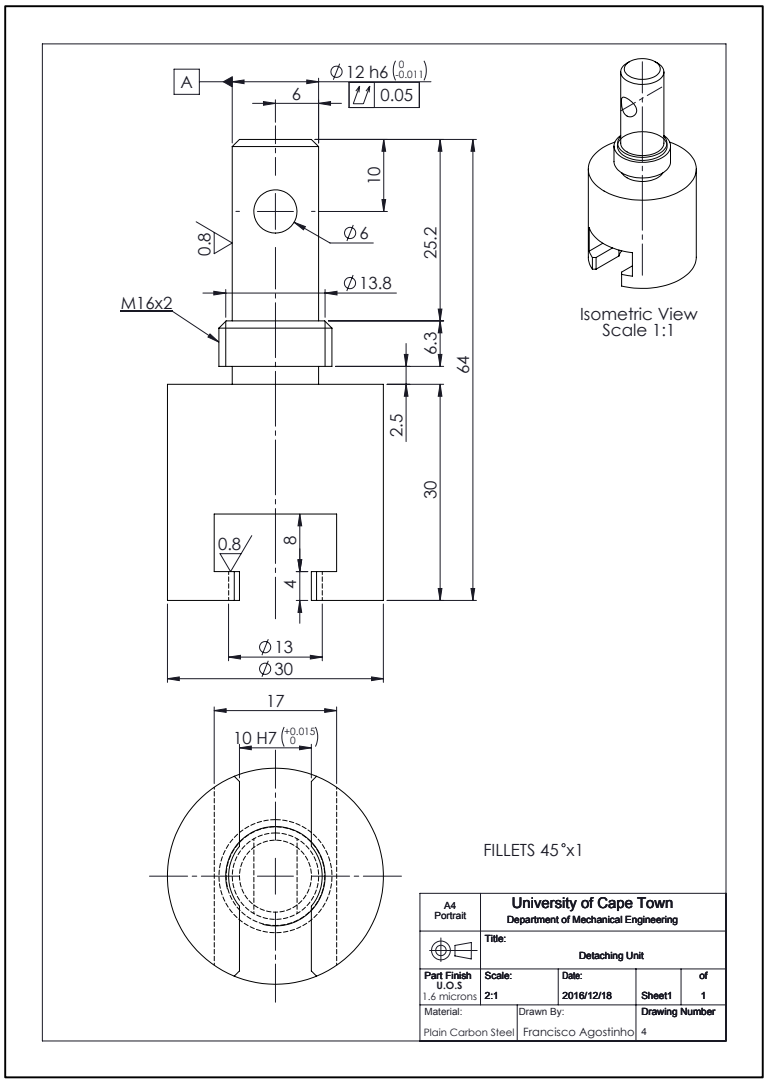

Figure 78: Detaching Unit drawing

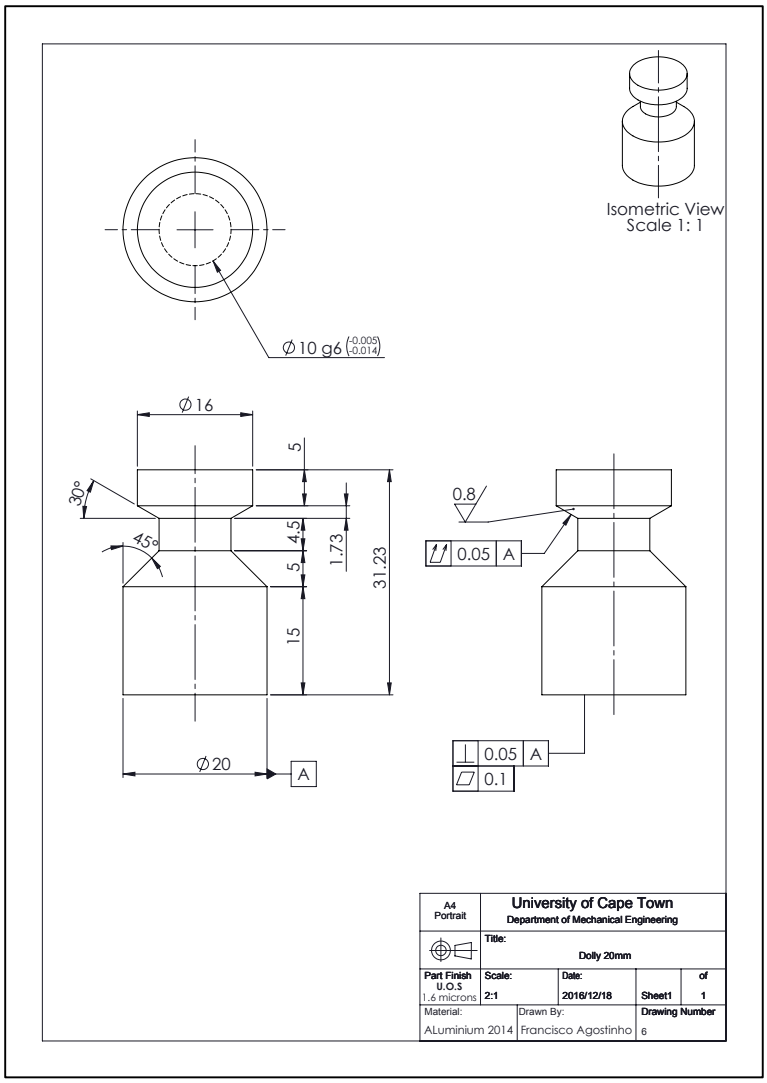

Figure 79: Dolly drawing

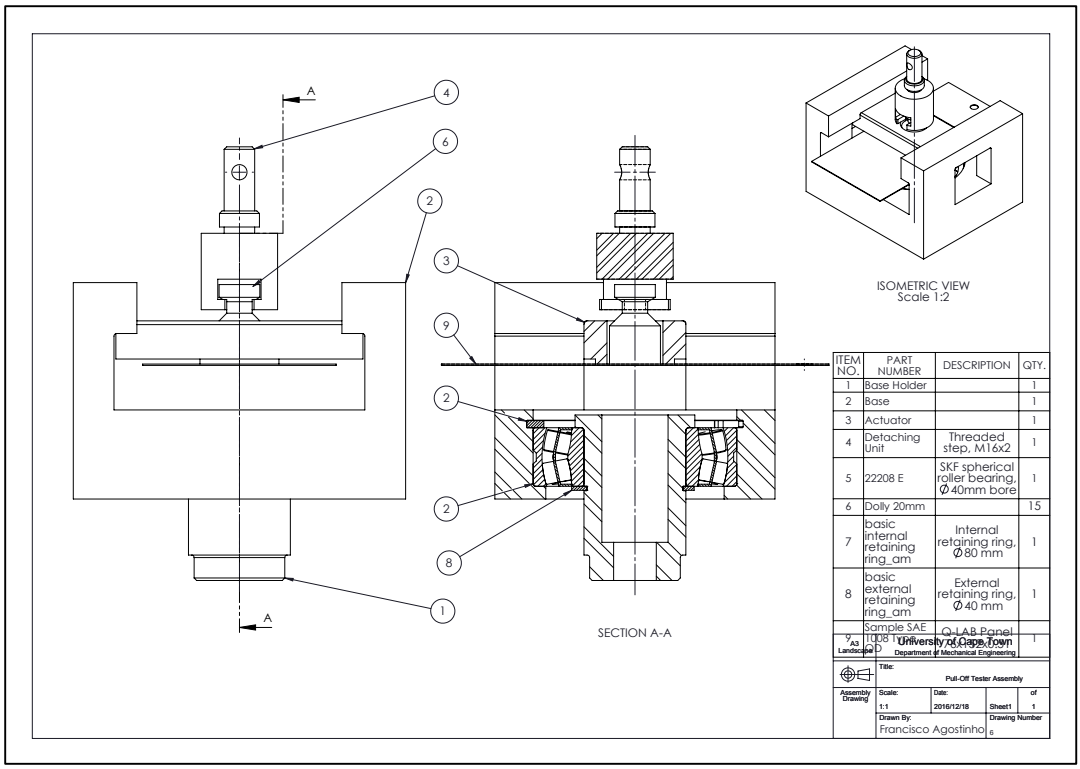

Figure 80: Pull-Off Tester assembly drawing

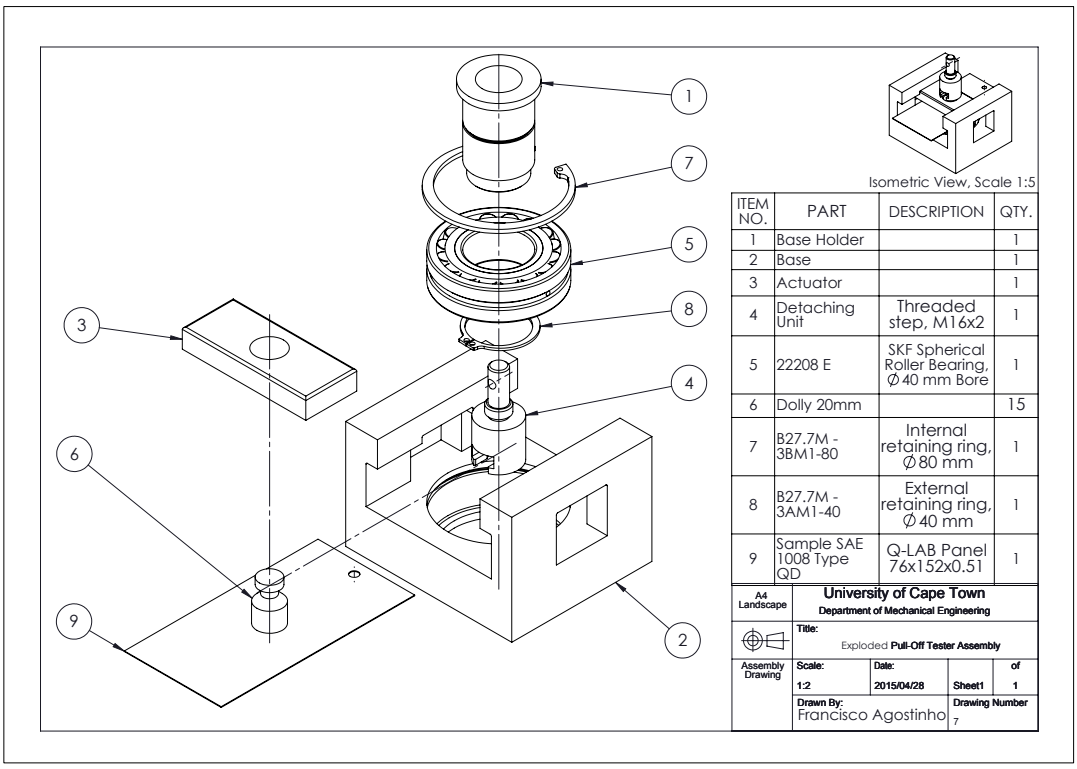

Figure 81: Pull-Off Tester exploded view